

CAPTURE OF RARE CIRCULATING TUMOR CELLS FROM BLOOD ON BIO-  
ACTIVATED OXIDE SURFACE INSIDE MICROFLUIDIC CHANNELS

A THESIS SUBMITTED TO  
THE GRADUATE SCHOOL OF NATURAL AND APPLIED SCIENCES  
OF  
MIDDLE EAST TECHNICAL UNIVERSITY

BY

HATİCE CEREN ATEŞ

IN PARTIAL FULFILLMENT OF THE REQUIREMENTS  
FOR  
THE DEGREE OF MASTER OF SCIENCE  
IN  
MICRO AND NANOTECHNOLOGY

FEBRUARY 2018



Approval of thesis:

**CAPTURE OF RARE CIRCULATING TUMOR CELLS FROM BLOOD ON  
BIO-ACTIVATED OXIDE SURFACE INSIDE MICROFLUIDIC CHANNELS**

submitted by **HATİCE CEREN ATEŞ** in partial fulfillment of the requirements for the degree of **Master of Science in Micro and Nanotechnology Department, Middle East Technical University** by,

Prof. Dr. M. Gülbin Dural Ünver  
Director, Graduate School of **Natural & Applied Sciences**

\_\_\_\_\_

Prof. Dr. Burcu Akata Kurç  
Head of Department, **Micro and Nanotechnology, METU**

\_\_\_\_\_

Prof. Dr. Haluk Külâh  
Supervisor, **Electrical and Electronics Eng. Dept., METU**

\_\_\_\_\_

Assoc. Prof Dr. Ebru Özgür  
Co-Supervisor, **Mikro Biyosistemler Inc.**

\_\_\_\_\_

**Examining Committee Members:**

Prof. Dr. Tayfun Akın  
Electrical and Electronics Eng. Dept., METU

\_\_\_\_\_

Prof. Dr. Haluk Külâh  
Electrical and Electronics Eng. Dept., METU

\_\_\_\_\_

Prof. Dr. Rengül Ç. Atalay  
Graduate School of Informatics, METU

\_\_\_\_\_

Prof. Dr. Uğur Tamer  
Analytical Chemistry Dept., Gazi University

\_\_\_\_\_

Asst. Prof Dr. Erhan Bat  
Chemical Engineering Dept., METU

\_\_\_\_\_

**Date:** 07.02.2018

**I hereby declare that all information in this document has been obtained and presented in accordance with academic rules and ethical conduct. I also declare that, as required by these rules and conduct, I have fully cited and referenced all material and results that are not original to this work.**

Name, Last name: Hatice Ceren Ateş

Signature:

## **ABSTRACT**

### **CAPTURE OF RARE CIRCULATING TUMOR CELLS FROM BLOOD ON BIO-ACTIVATED OXIDE SURFACE INSIDE MICROFLUIDIC CHANNELS**

Ateş, Hatice Ceren

M.S., Department of Micro and Nanotechnology

Supervisor: Prof. Dr. Haluk Kùlah

Co-supervisor: Assoc. Prof. Dr. Ebru Özgür

February 2018, 95 pages

Isolation and characterization of circulating tumor cells (CTCs) have important clinical significance in terms of prognosis and early detection of response to treatment. Moreover, downstream characterization of CTCs may help better patient stratification and therapy guidance. However, CTCs are extremely rare ( $\sim 10$  CTCs/ $10^{10}$  peripheral blood cells) and highly sensitive, and specific technology is required for their isolation. Rapidly developing microfluidic technologies offer variety of advantages in rare cell isolation including rapid, low-cost and automated sample processing, and higher sensitivity and specificity due to their similar physical dimensions to biological cells. Many of these technologies utilize immuno-affinity based CTC capture, where anti-EpCAM antibody against epithelial cell surface biomarker is widely utilized for CTC-specific cell capture. In such applications, a proper antibody immobilization plays a crucial role for high

efficiency cell capture. In this study, development and evaluation of four different surface modification approaches to immobilize anti-EpCAM on the silicon oxide surfaces was presented and the selected modification method is implemented in microfluidic channels. Cell capture efficiency and capture specificity were determined using different breast cancer cell lines as a CTC model. Selective CTC capture was demonstrated using breast cancer cells (MCF-7) spiked in buffer containing background leukocytes with cell concentration ratio of 1:10<sup>4</sup>. Cell capture efficiency and specificity of 90% and 87% have been achieved, respectively, with MCF7 cells. Besides, protocols for in-channel immunofluorescent cell staining and viable cell release have been developed. Shelf life of the functionalized surfaces was also determined by inspecting the capture efficiency of microchannels weekly.

**Keywords:** CTC, EpCAM, Covalent immobilization, Bio-affinity immobilization, Microfluidic channel, SiO<sub>2</sub>

## ÖZ

### **KANDAKİ ENDER TÜMÖR HÜCRELERİNİN MİKROAKIŞKAN KANAL İÇİ BİYO-AKTİF OKSİT YÜZEYDE YAKALANMASI**

Ateş, Hatice Ceren

Yüksek Lisans, Mikro ve Nanoteknoloji Bölümü

Tez Yöneticisi: Prof. Dr. Haluk Külah

Ortak-Tez Yöneticisi: Assoc. Prof. Dr. Ebru Özgür

Şubat 2018, 95 sayfa

Kanda dolaşan tümör hücrelerinin tespiti ve karakterizasyonu hastalığın prognozunu belirleme ve ilaç tedavisine verilen cevabı ölçme gibi biyomedikal uygulamalar için bir hayli önemlidir. Buna ek olarak, hücrelerin karakterizasyonu, metastaz riski, hastalığın ilerlemesi ve/veya tedaviye yanıtı öngörmede yararlı olabilecektir. Fakat kanda oldukça nadir olmaları sebebiyle (~10 tümör hücresi/  $10^{10}$  periferik kan hücreleri), kanda dolaşan tümör hücrelerin tespiti için hassas ve spesifik bir teknoloji kullanılması gerekmektedir. Hızla gelişmekte olan mikroakışkan teknolojiler, ender hücre izolasyonu için hızlı, düşük maliyetli ve otomatize edilmiş örnek hazırlama gibi avantajların yanısıra, hücre boyutuna benzer boyutlara sahip olması sayesinde yüksek duyarlılık ve özgünlük sağlamaktadır. Bu teknolojilerin bir çoğu, ender hücrelerin immunolojik markeri olan EpCAM antikor ekspresyonunun kullanıldığı affinite tabanlı ender hücre yakalamaya dayanmaktadır. Bu

teknolojilerde kritik nokta, hücrelerin izolasyonu için kullanılan antikorların, yüzeylere doğru bir şekilde immobilize edilmesidir. Bu çalışmada kandan ender hücre tespiti için, dört farklı silisyum oksit yüzey aktifleştirme yöntemi geliştirilip değerlendirilerek, seçilen bir yöntem mikroakışkan kanallara uygulanmaktadır. Önerilen yöntemin hücre yakalama başarısı ve hücre seçiciliği, farklı meme kanseri hücre hatlarının kanda dolaşan tümör hücresi modeli olarak kullanılması ile belirlenmiştir. Geliştirilen yüzey aktifleştirme protokolünün hücre yakalama seçiciliği, beyaz kan hücresi içeren solüsyona 1:10<sup>4</sup> oranında MCF-7 hücresi atılarak tespit edilmiştir. Hücre yakalama başarısı ve özgülüğü MCF-7 meme kanseri hücre hattı ile test edilmiş ve sırasıyla %89.6 ve %90 olarak elde edilmiştir. Yakalanan hücrelerin çip-üstü tespiti ve canlı bir şekilde kanaldan koparılmaları için yöntemler geliştirilmiştir. Son olarak, aktifleştirilmiş yüzeylerin raf ömrü, bir haftalık aralıklarla yapılan hücre tutundurma testleri ile belirlenmiştir.

**Anahtar Kelimeler:** Dolaşımdaki tümör hücreleri, epitel hücre adezyon molekülü (EpCAM), kovalent immobilizasyon, biyo affinite immobilizasyonu, mikroakışkan kanal, SiO<sub>2</sub>.

to Cihan  
&  
to life  
we will live  
to the fullest  
together

## ACKNOWLEDGMENTS

My deepest gratitude is to my supervisor, Prof. Dr. Haluk Klah, who gave me a chance to get in this topic and let me become a member of Mikro Biyosistemler family. Without him, not only this thesis, many of the things in my life would not have happened. I would like to give my deepest heartfelt thanks to my co-advisor, Assoc. Prof. Dr. Ebru zgr, for her never ending motivation, patience and unbounded tolerance. I am grateful for the times of intense discussions and all the knowledge she shared with me.

I would like to express my heartfelt appreciation to Prof. Dr. Nevin Seluk who supported me not only academically but also emotionally through this rough and let me beware of ethics and honesty.

I am deeply grateful to Mikro Biyosistemler family since I have been blessed with a friendly and cheerful work environment. I would like to express my gratitude to Dr. zge Zorlu, he has provided good arguments about my topic and helped me gain different aspects of it. Grhan zkayar, thank you first for serpentine channel design but more importantly keeping us entertained with your stories and endless appetite. Taylan Tral, thank you for carrying extremely heavy nitrogen tank every time I needed and fabricating the serpentine microfluidic channel. Yağmur Demircan Yalm, thank you for always cheering me up with your endless positive energy and let me feel happy even during crises in the laboratory. Special thanks to Selin Varol for fulfilling chats about new books, exhibitions or movies; Duygu Ulak for always keeping me fresh with coffee, Murat Aktrk for kindly donating his blood for experiments.

I would like to show my greatest appreciation to Begm Ően Doğan “abla”. It has been my pleasure to work with you and learned so much from you. I will always remember our good times, tea-breaks and all the fun we have had during experiments.

I owe my deepest gratitude to Dr. Nilüfer Afşar Erkal. Thank you for always supporting me during my hardest times from the very beginning in the Mikro Biyosistemler. It is indeed my good fortune to have not only such a good mentor, but also someone who loves me like a sister.

I am especially thankful to my BioMEMS research group: Didem Çetin, Furkan Gökçe, Eren Aydın, Mustafa Kangül, Metin Dünder Özkan, Alper Kaan Soydan, Mahmut Kamil Aslan, Bedirhan İlik, Kaan Sel, Hasan Uluşan, Parinaz Ashrafi Özkayar, Aziz Koyuncuoğlu, Zeynep Çağlayan, Ali Can Atik, and Salar Chamanian for being good friends and creating such an entertaining research group.

My dearest design team from Chemical Engineering Department, Özge Batır, Fatma Genç and Merve Sarıyer. Thank you for keeping me updated about latest gossips and changing my depressed mood with our little talks. Your friendship was irreplaceable.

Coollest food engineers in the world, you are the best! Nilay Tam, Seren Oğuz (ikiz) and Bahar Ustaoglu, who made me feel special, boosted my motivation and made me smile all the time whenever we met or talked. I am more than very happy to have a friend like you, thank you!

Celal Dudak, you have always been a role model to me and you are the main reason for me being a METU student in the first place by burying my “göbek bağı”.

My dad Ahmet Servet Özcan, my mom Müzeyyen Özcan and my sister İlayda Özcan; your support has been unconditional all these years, you have supported me whenever I need and cherished me. Still, I’m only able to say a mere thank you for the limitless love you give.

Cihan, my significant other, my love, my husband. I feel very lucky and grateful for the day I meet you. I cannot recall a single moment, in which you are not by my side and I feel truly happy for being able to walk this path together, where seeing your smiling face encourages me to step forward with such ease with your hand in mine. Thank you for always being there for me, for us.

## TABLE OF CONTENTS

ABSTRACT .....	v
ÖZ .....	vii
ACKNOWLEDGMENTS .....	x
TABLE OF CONTENTS .....	xiii
LIST OF TABLES.....	xvii
LIST OF FIGURES.....	xix
CHAPTERS	
1 INTRODUCTION.....	1
1.1 Cancer Diagnosis: Traditional Biopsy vs. Liquid Biopsy.....	2
1.2 CTC Isolation.....	4
1.2.1 Use of Microfluidics in CTC isolation.....	4
1.2.2 Label Free Isolation.....	8
1.2.3 Affinity-Based CTC Isolation.....	15
1.3 Research Objectives .....	25
2 METHODS AND MATERIALS .....	27
2.1 Device Fabrication .....	28
2.2 CTC Model.....	30
2.3 Surface Functionalization.....	31
2.3.1 Materials.....	31
2.3.2 Silanization of Oxide Surfaces.....	31
2.3.3 Antibody Immobilization.....	31
2.4 Surface Characterization .....	35
2.4.1 Contact Angle.....	35
2.4.2 Spectroscopic Ellipsometry.....	35

2.4.3	X-ray Photoelectron Spectroscopy.....	36
2.4.4	Fluorescence Microscopy.....	36
2.5	Cell Capture.....	36
2.5.1	Plain Surfaces.....	36
2.5.2	In Channel.....	37
2.5.2.1	Cell Capture Efficiency Determination .....	39
2.5.2.2	Selective Cell Capture from Blood.....	40
2.5.2.3	Cell Capture Based on EpCAM Expression Level.....	42
2.5.2.4	Viable Cell Release.....	43
2.6	Statistical Analysis .....	44
3	RESULTS .....	45
3.1	Characterization of Functionalized Surfaces.....	45
3.2	Comparison of Antibody Immobilization Protocols on Plain Surfaces .....	51
3.3	Cell Capture Efficiency in Microfluidic Channels.....	56
3.4	Cell Capture Specificity in Microfluidic Channels .....	57
3.5	Cell Capture Sensitivity.....	59
3.6	Viable Cell Release .....	66
3.7	Shelf-Life of Bio-functionalized Surfaces.....	69
4	CONCLUSIONS .....	71
5	REFERENCES .....	75
APPENDICIES		
A.	XPS ANALYSIS .....	91

## LIST OF TABLES

Table 1:1 Comparison of mass transfer coefficient in micro and macro domain [9].....	6
Table 1:2 Summary of Label-Free CTC Isolation Technologies.....	14
Table 1:3 Summary of Affinity Based CTC Isolation Technologies.....	19
Table 3:1 Atomic compositions of the surfaces modified with P1-4 at each step of functionalization.....	51
Table 3:2 Comparison of protocols with respect to cost and modification time.....	55
Table 3:3 Summary of protocol comparison.....	55
Table 3:4 Cell Capture Efficiency Determination.....	57
Table 3:5 Selective Cell Capture from Blood.....	58
Table 3:6 Binding efficiency of CAMA-1 cells.....	64
Table 3:7 Binding efficiency of MDA-MB-231 cells.....	64
Table 3:8 Binding efficiency of MDA-MB-468 cells.....	64
Table 3:9 Binding efficiency of SKBR-3 cells.....	65
Table 3:10 Cell Release Efficiency.....	67
Table 3:11 Shelf-Life Determination.....	70

## LIST OF FIGURES

Figure 1:1 Circulating tumor cells (CTCs), circulating tumor DNA (ctDNA) and exosomes as blood based biomarkers [3].....	3
Figure 1:2 Velocity profile for a laminar flow.....	6
Figure 1:3 Schematic representation of CTC isolation methods in microfluidic channels.....	8
Figure 1:4 Schematic representation of microfluidic ratchet device (adapted from [21]).....	10
Figure 1:5 Forces acting on the cells in a microchannel for laminar flow regime.....	11
Figure 1:6 Separation of cells in acoustophoresis.....	13
Figure 1:7 (a) Schematic representation of antibody, (b) Antibody immobilization on solid surfaces (adapted from [80]).....	22
Figure 1:8 CTC release strategies after affinity-based capture (adapted from [97]).....	25
Figure 2:1 Fabrication steps of microfluidic channel.....	29
Figure 2:2 Schematic representation of antibody immobilization in P1 (a), P2 (b), P3(c) and P4(d).....	33
Figure 2:3 (a) Surfaces incubated in six well plates, (b) surfaces prepared for fluorescence microscopy imaging.....	37
Figure 2:4 Microfluidic Test Setup.....	39
Figure 2:5 Preparing Blood Sample; (a) whole blood in EDTA tube, (b) whole blood lysis solution mixture, (c) mixture become transparent red after successful lysis, (d) after centrifuge WBCs in the bottom of the tube as pellet, (e) WBCs are resuspended in PBS.....	41
Figure 2:6 Schematic representation of EpCAM sensitive cell capture experiments.....	43

Figure 2:7 Schematic representation of viable cell release experiments.....	44
Figure 2:8 Re-culture of released cells and proliferation check.....	44
Figure 3:1 Contact angle measurements: (a) P1, (b) P2, (c) P3, (d) P4.....	46
Figure 3:2 Ellipsometric film thickness of each layer: (a) P1, (b) P2, (c) P3, (d) P4.....	49
Figure 3:3 Fluorescence microscopy images of surfaces (5x) incubated in MCF-7 cell solution.....	52
Figure 3:4 Number of cells captured on the surfaces functionalized with protocols P1-P4.....	52
Figure 3:5 Fluorescent microscopy images of surfaces (5x) incubated in CCRF-CEM cell solution.....	54
Figure 3:6 Images of whole channels showing the cells before (top) and after (bottom) high flow rate washing (5x).....	56
Figure 3:7 (a) WBC: CTC mixture in channel before (top) and after washing (bottom) step (5x), (b) CTC:WBC in channel (20x).....	58
Figure 3:8 Fluorescent microscopy images of stained MCF-7 and leukocytes (40x).....	59
Figure 3:9 Morphology of breast cancer cell lines (20x).....	61
Figure 3:10 Flow cytometry measurements of unstained control and EpCAM (PE) for (a) MCF-7, (b) MDA-MB-231, (c) CAMA-1, (d) MDA-MB-468, (e) SKBR-3.....	62
Figure 3:11 EpCAM expression of cell lines compared with MCF-7 (a) MDA-MB-231, (b) SKBR-3, (c) MDA-MB-468, (d) CAMA-1, (e) all cell lines.....	63
Figure 3:12 Normalized binding efficiencies of cell lines.....	65
Figure 3:13 Fluorescence images of MCF-7 cells inside antibody-free microchannel before (top) and after (bottom) washing step (5x).....	66
Figure 3:14 Fluorescence images of CTCs captured (top) and released (bottom) (5x)...	67
Figure 3:15 Observation of re-cultured cells (Day 1-4).....	68
Figure 3:16 Observation of re-cultured cells (Day 6-8).....	69





# CHAPTER 1

## INTRODUCTION

Cancer is the second leading cause of death after heart diseases and strokes and number of cancer cases is expected to increase by 70 % in the upcoming 20 years [1]. Cancer is not a recent disease, in fact, paleopathologic findings reveal that prehistoric animals had tumor long before humans been on earth. The oldest definition of cancer is presented in the Edwin Smith Papyrus that was written circa 3000 BC. The writer described the breast tumor as bulging form and concluded that “there is no treatment for it”. After a while, Hippocrates used the word “carcinom” a Greek word referring crab to define tumors since the finger-like spreading of cancer reminded him to the movement of a crab. He believed that body contains four humors (body fluids) and their imbalance can cause cancer. Humoral theory was replaced by lymph theory in the 17<sup>th</sup> century, which suggested that tumors are created by Lymph. Later, Johannes Muller, a German pathologist, proved that cells rather than lymph cause cancer and proposed that tumor cells developed from blastema. Metastasis was first described in the 1860s by Karl Thiersch, a German surgeon, and he demonstrated that malignant cells can be spread to other body parts and metastasize. Trauma was believed to be main cause of cancer between the 1800 and 1920, due to the observation that experimental animals will have cancer when a failure of injury arises. Cancer was considered as contagious till 1800s and it was suggested that cancer patients should keep in quarantine to prevent the spread of disease. In the 19<sup>th</sup> century, usage of modern microscopes enabled scientists to study on diseased tissues and

pathology of cancer. Despite their missing points and misguided ideas, all made contribute to cancer treatment, diagnosis and detection [2].

## **1.1 Cancer Diagnosis: Traditional Biopsy vs. Liquid Biopsy**

Sample from cancer tissue traditionally has been obtained only by tumor biopsy. Biopsies taken from suspected areas allow detection of mutations in cancer cells and guide treatment. Different biopsy types are available like incisional biopsy, which includes removal of a small part of the suspected area that is enough for diagnosis, or excisional biopsy, which is based on removal of an entire tumor. However, such an invasive procedure may be uncomfortable for patients and they may not always be in healthy conditions to undergo surgery. Furthermore, tumors are highly heterogeneous in their nature and their properties show some alterations at different stage of the disease. Therefore, tumor biopsy may only provide a snapshot of a specific portion of a tumor at a given time. An alternative for traditional biopsy is liquid biopsy, which is detection of cancer cells or traces of these cells like DNA or RNA in patient blood that are originated from primary tumor sites. Liquid biopsy provides a wide range of information about the tumor and can be used for deciding when / how to start the treatment or assessing the treatment success. Since this technique is minimally invasive, taking regular samples of blood is possible, which gives insights about the alterations taking place in the tumor cells.

Blood sample contains three types of tumor-derived materials that can be used for further molecular analysis: circulating tumor cells (CTC), cell free circulating tumor DNA (ctDNA) and exosomes. Exosomes found in almost all body fluids are secreted membrane vesicles and provide intracellular communication. They carry various molecules like RNA, DNA or protein and elevated exosome level is observed in cancer patients, which makes them a candidate for non-invasive cancer marker. Cell free circulating tumor DNA is small DNA pieces of apoptotic or necrotic cells released to the blood stream when they are dying. Circulating tumor cells, unlike exosomes or ctDNAs that are only fragments of

cells, are intact tumor cells exfoliated from primary or secondary tumor sites into the blood circulation [3].

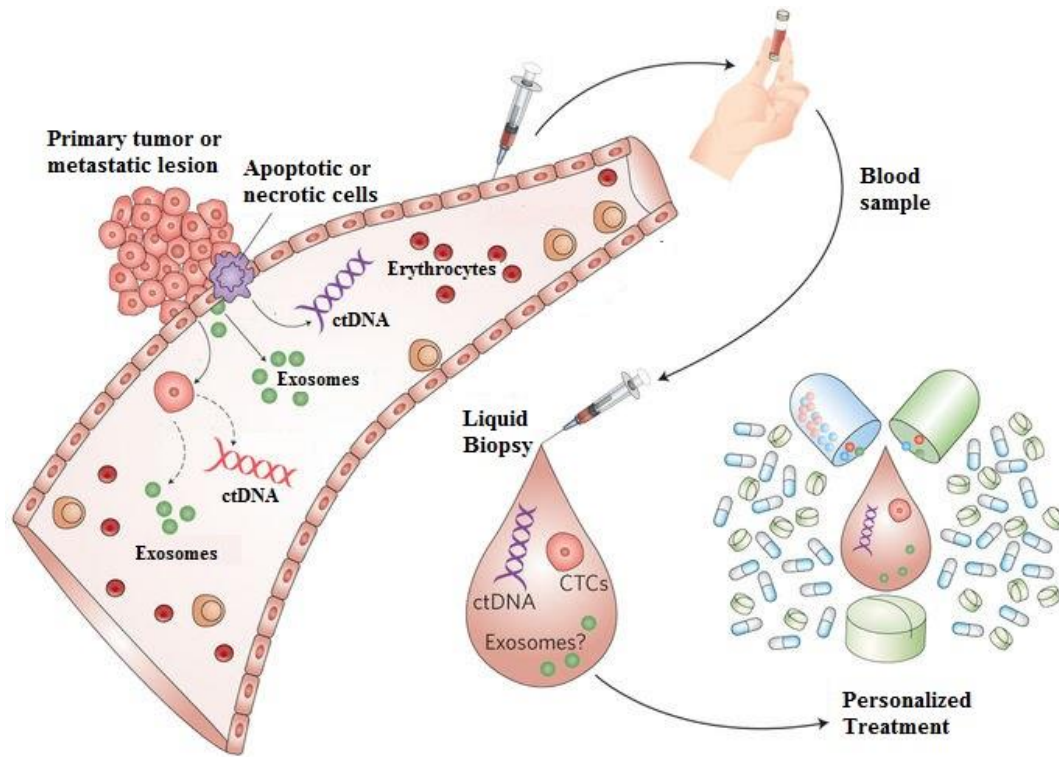


Figure 1:1 Circulating tumor cells (CTCs), circulating tumor DNA (ctDNA) and exosomes as blood based biomarkers (Reprinted by permission from [Springer Nature]: [Springer/Nature] [Nature Biomedical Engineering] ( [3] Clinical prospects of liquid biopsies, Catherine Alix-Panabieres, Klaus Pantel), [Copyright 2018 Springer] (2017))

Long before the discovery of tumor-derived materials in blood, Thomas Ashworth noticed the similarities between the morphologies of the tumor cells from the blood and from various lesions of a patient with metastatic cancer [4]. His conclusion was:

*“One thing is certain, that if they came from an existing cancer structure, that must have passed through the greater part of the circulatory system to have arrived at the internals saphena vein of the sound leg.”*

His observation and deduction was spot-on. 140 years of ongoing research in cancer has indeed demonstrated that circulating tumor cells play a significant role in metastasis [5]. Their use in clinic as prognostic biomarker has been approved by Food and Drug Administration (FDA) in breast, colorectal and prostate cancers. However, there are numerous clinical studies going on collecting clinical evidence for their utility as predictive and diagnostic biomarkers in variety of cancers, as well. Number of CTCs in blood is shown to change during the treatment and this change is correlated with the progress of the disease. Furthermore, CTCs also have the potential to be utilized for monitoring mutations or telomerase activity and developing better treatments through downstream analysis [6].

CTCs are, however, extremely rare (10 CTCs / $10^9$  blood cells) [7] making their capture quite a challenge. These cells have individual identities, which creates a variation in biophysical and biochemical properties. This variation itself is another challenge since there is no unique marker which represents such a heterogeneous mixture. Nevertheless, any CTC isolation technology must offer high recovery rate and selectivity to ensure sufficient number of viable CTCs to be utilized in downstream analysis.

## **1.2 CTC Isolation**

### **1.2.1 Use of Microfluidics in CTC isolation**

Microfluidic devices have introduced many new opportunities in applied sciences including biological studies, which has also influenced the research being carried out in CTC field. The idea of miniaturization dates back to 1960. In his paper, Feynman discussed the advantages of the “very small” scales for heat transfer, which eventually evolves to a new vision, Miniaturized Total Chemical Analysis System. In 1990s, developments in the manufacturing methods and introduction of new substrates such as polydimethylsiloxane (PDMS) brought with it ingenious biological applications. With the ability to create various structures by, researchers now have the necessary tools to use and

test various aspects of a controlled geometry in which the designer has the control over the fluid flow precisely.

The reasons behind the popularity of microfluidic devices in biological sciences can be listed as follows:

- Microchannels enable precise control over the fluid flow and mass transfer,
- They reduce the required sample amount,
- Microfluidic devices speed up and increase the quality of observations
- They can be integrated with other components necessary for the analysis such as sensors, controllers, automated systems etc.,
- They are portable as volume of the entire system can be reduced up to 1000 folds.

Fluid flow in microscale is much simpler than in macroscale. In fluid mechanics, one of the key parameters describing the flow behavior is the Reynolds number, which gives ratio of inertial forces to viscous forces:

$$Re = \frac{v_{ch}L_{ch}}{\nu}$$

where  $v_{ch}$  is the characteristic velocity,  $L_{ch}$  is the characteristic length and  $\nu$  is the kinematic viscosity. Re number for flows in microchannels is typically smaller than unity, leading to laminar flow (Figure 1:2). In this flow regime, velocity field is quite simple and there is no lateral mixing. Hence, fluid flow in micro domain gives predictive streamlines, which are easy to control and repeatable.

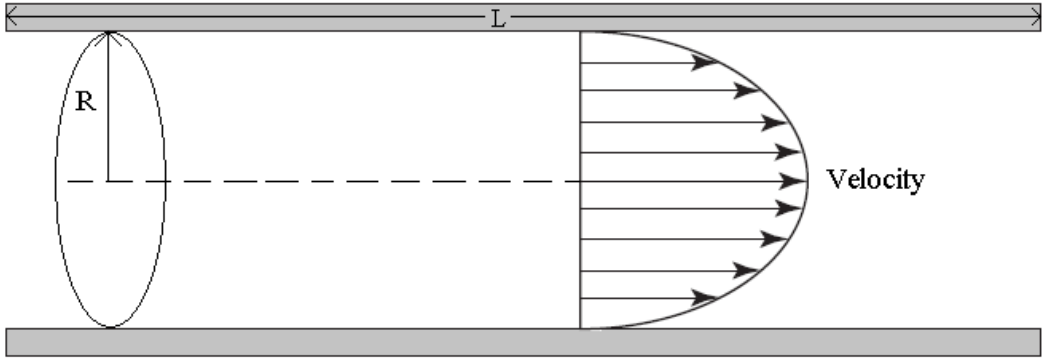


Figure 1:2 Velocity profile for a laminar flow

Mass transfer in the micro scale is diffusion controlled and small characteristic lengths of microchannels enable very fast mass transfer rates from the solution to the channel walls, which is of considerable importance for the success of chemical binding reactions occurring on the immobilized bio-molecules on channel walls. Considering the fact that time scale for diffusion within a channel is proportional to the square of its characteristic length ( $t_{ch} \sim L_{ch}^2/D_{AB}$ ) [8], mass transfer rate significantly increases in the micro domain. To further illustrate the enhanced mass transfer in microchannels, typical mass transfer rates for macro and micro scale systems are tabulated below. As can be seen from the table, reducing the scale to micro domain leads to two orders of magnitude increase in the mass transfer rate, which speeds up the overall process significantly.

Table 1:1 Comparison of mass transfer coefficient in micro and macro domain [9]

	Total mass transfer coefficient x 1000 (1/s)
Stirred tank	3-40
Tubular reactor	0.5-70
Packed columns	0.04-7
Spray column	1.2-2.2
Bubble column	0.5-24
Taylor-Couette Flow	3-21
Microchannel	30-2100

Another important advantage of microchannels is reduced sample consumption. Volumetric flow rate (Q) of steady laminar flow for a Newtonian fluid under a pressure gradient ( $\Delta P$ ) is given by Hagen-Poiseuille Equation:

$$Q(R) = \frac{\Delta P \pi}{8\mu L} R^4$$

where the volumetric flow rate is a strong function of the channel diameter, R. Therefore, in microscale, sample consumption is significantly reduced under the same flow conditions. This is very critical for biological applications as the sample amount is usually very limited, for instance blood taken from a patient.

Microfluidic devices integrated with sensors, filters, valves, pumps, mixers, flow controllers enable controlling experimental conditions with high precision. With the improvements in automated experimental practice in both isolation and characterization of cells, number of studies have been increasingly continued in biological studies. Small characteristic lengths and the precise control offered by microfluidics make it a very charming alternative for CTC isolation. With this motivation, new technologies are being developed depending on microfluidics, which either use the intrinsic (size, density, charge) / extrinsic (response to external acoustic, electric or magnetic fields) properties of cell or take advantage of the differences in affinity of cells to specific molecules. These methods are schematically shown in Figure 1:3 and details of these approaches are given in the following sections.

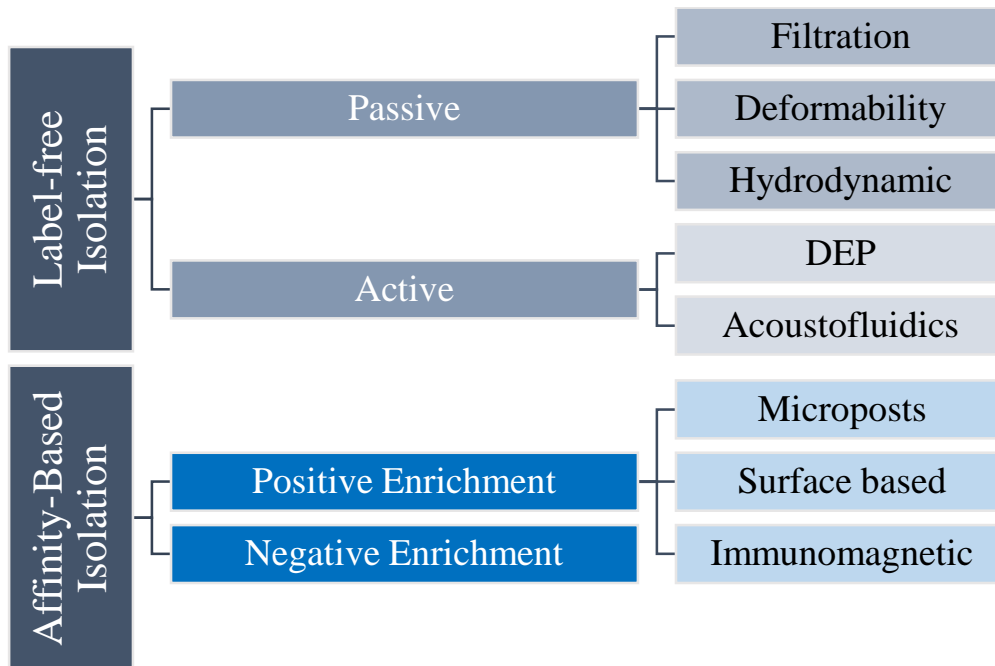


Figure 1:3 Schematic representation of CTC isolation methods in microfluidic channels

### 1.2.2 Label Free Isolation

CTC capture strategies can be classified according to their use of biophysical or biochemical properties. Utilization of physical properties for the isolation of CTCs from surrounding blood cells is called “label-free isolation” as it eliminates the need for a biological marker, “the label”. Methods utilizing only the intrinsic properties are called passive separation techniques and exploit the size and/or deformability differences among the cells in blood [10–12].

Passive label-free isolation methods can be divided into three major groups:

- Filtration
- Deformability-based separation
- Separation by using inertial forces

Filtration is the most straight-forward and cheapest approach among the alternatives. Membranes with specific pore sizes are utilized for separation, which is based on the fact

that a typical CTC diameter (12-25  $\mu\text{m}$ ) is much larger than those of blood cells (leukocytes 8-11  $\mu\text{m}$ , red blood cells 5-9  $\mu\text{m}$ ) [10].

Membranes developed for CTC filtration are initially made from polycarbonate by using track-etching. This approach yields randomly distributed pores with a high fusion probability, which in turn leads to low CTC capture efficiency. In order to alleviate such problems, polyethylene based microfilters have been developed with oxygen plasma etching giving uniform pore distribution [13]. This type of membranes has been shown to provide a high cell capture efficiency for a variety of cancer types. Nevertheless, viability of the captured CTCs is found to be very low with these membranes, which is due to the utilization of formalin in the process [14]. The stress induced with this approach is overcome via employing a 3-D membrane, where spiked CTCs in blood were captured and maintained successfully [15].

Although, CTC filtration leads to high throughput, there are still some issues to be solved. First of all, significant overlap in the sizes of CTCs and leukocytes leads to low purity [16]. Secondly, CTCs which are similar in size with leukocytes (or smaller) are lost during separation. Lastly, filter based approaches are usually prone to clogging, which leads to decreases in capture efficiency.

Deformability is another physical property used to isolate CTCs from the surrounding blood cells. Erythrocytes do not have a nucleus hence they are quite deformable, which enables them to travel freely through microvessel within tissues. Leukocytes have a nucleus and physically similar to epithelial cells. CTCs, on the other hand, usually have larger nuclei compared to healthy epithelial cells due to chromosomal abnormalities. Hence ratio of the nucleus to cytoplasm for CTCs becomes much greater than leukocytes [17,18]. It has been shown that nuclei and nucleoplasm is significantly more viscous (4 to 10 times) and stiffer than the cell cytoplasm [19,20]. Therefore, CTCs are expected to be more rigid than leukocytes and less likely to deform under stress and this difference is being exploited to isolate CTCs.

Deformability based separation is a relatively new concept. In one of the pioneering works, [21] a microfluidic ratchet mechanism in which cells flow through tapered throats were developed. In the case where the entrance is smaller than the diameter of the cell,

their shape is forced to deform and whether cells will cross or not depends on their deformability, shape and force applied. In their design, [21] applied an oscillating pressure so that cells that cannot pass the throats but not clog the channel (Figure 1:4). More recently, [22] further extended the concept and designed 3-D conical shape microstructures for deformability based separation.

However, CTCs are known to change continuously with respect to their cytoplasmic content and cytoskeleton, which will create a variation in the ratio of nucleus to cytoplasm. More importantly, cluster of CTCs was shown to have higher deformability compared to an individual CTC and able to pass through vessel walls [23]. Therefore, further studies are necessary to establish a base between deformability and CTCs.

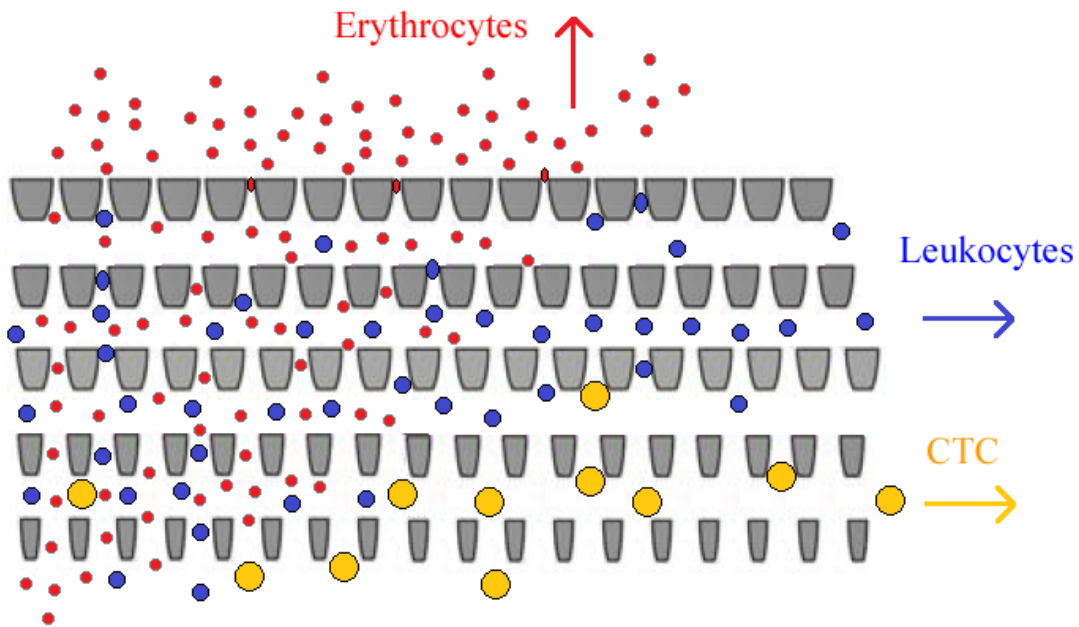


Figure 1:4 Schematic representation of microfluidic ratchet device (adapted from [21])

Hydrodynamic separation makes use of hydrodynamic forces to steer cells as if they are “solid particles” into specific streamlines based on cell property differences. As described in Section 1.2.1, laminar flow regime in microchannels results in well-behaved streamlines with a parabolic velocity profile. In such a flow field, cells travelling with the fluid are exposed to a velocity gradient, which creates lift force towards to the wall due to

shear stress. In the vicinity wall, on the other hand, cells are pushed away due to the pressure build-up, which will create equilibrium positions between the two competing forces acting on the body (Figure 1:5). Position of these equilibrium streamlines shown in Figure 1:5 depends on the shape of the channel (straight / curve) and the cross-sectional area (circular, duct).

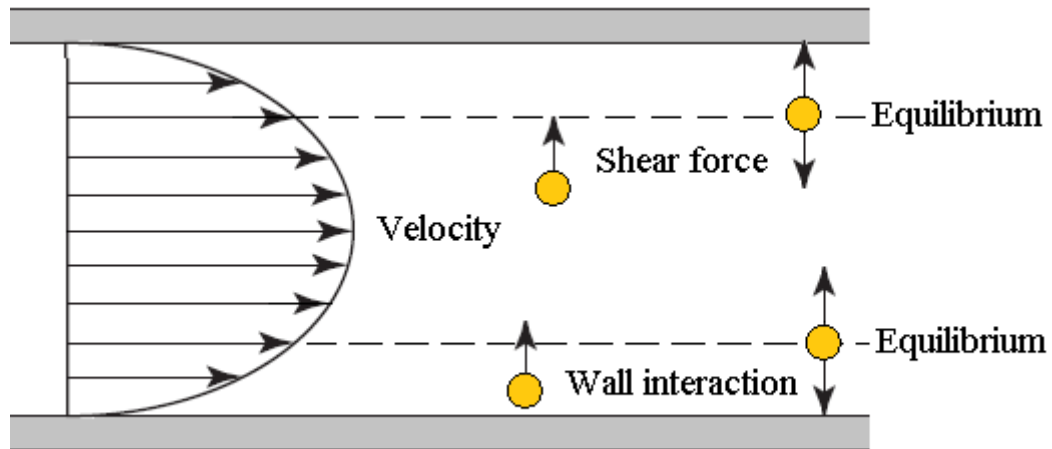


Figure 1:5 Forces acting on the cells in a microchannel for laminar flow regime

There are several successful applications of CTC isolation utilizing hydrodynamic forces. MARC proposed by [24] uses two consecutive rectangular microchannels with reversed aspect ratios, in which authors separated 10  $\mu\text{m}$  particles from 20  $\mu\text{m}$  particles with a high efficiency (90 %). Authors observed that MARC performs well over a wide range of flow conditions ( $30 < \text{Re} < 80$ ) for particles and it can be used to separate rare cells from whole blood successfully [25]. Another inspiring example is developed by [26]. Their design uses centrifugal forces to separate large CTCs from the blood cells, which has been shown to yield a high recovery rate (85 %). Deterministic later displacement (DLD) is another inertia based method, first proposed by [27], where cells are categorized depending on their size while they are drifting under laminar flow conditions through arrays of obstacles. In the initial design, major disadvantages of this approach were its low throughput due to the induced resistances to flow and clogging. Recently, these problems

have been alleviated as demonstrated in [28], where a high throughput is maintained with a high efficiency (85 %) without losing cell viability.

Methods utilizing extrinsic properties, that is the response of the cells to external acoustic, electric or magnetic fields are called active separation techniques and mainly exploit charge differences among the cells in blood.

Most widely used active label-free isolation methods can be classified into two major groups with respect to the external field they utilize:

- Dielectrophoresis (DEP)
- Acoustophoresis

DEP method uses another physical property, polarizability of the cells, to separate CTCs from the surrounding blood cells by creating non-uniform electric fields. In this field, each cell experiences a different force so that target cells can be directed into specific zones. This movement can follow the gradient itself (positive DEP) or be against the field (negative DEP) depending on its dielectric properties. Responses of the cells to the applied electric field, in fact, depends on individual cell size, conductivity, morphology, membrane potential and phenotype as well as the properties of the surrounding cells and dielectric medium [29–31]. First DEP study dates back to 1950 [32] where the polarized particle movement in an electric field was described. In mid 1990s, dielectric properties of tumor cells were distinguished from the erythrocytes and lymphocytes and DEP was used to isolate CTCs from the blood [33]. A major milestone was achieved in 2005 by [34]. They successfully applied DEP on a chip, where carcinoma cells are separated from erythrocytes. In 2011, [35] presented a method for continuous isolation of CTC and first commercialized CTC isolation device based on DEP become available in 2012, ApoStream™ [36]. The major disadvantage of ApoStream is its low selectivity (70 %), which is the bottleneck of DEP based applications today.

Knowledge on the nature of sound dates back to ancient Greece, yet it took almost 2300 years before Kundth describes the motion of particles in standing sound waves. At the beginning of the 21<sup>st</sup> century, [37] utilized ultrasound in micro domain, which brings about new opportunities for cell isolation in microchannels.

Sound is simply a mechanical wave hence needs a medium to propagate. If the medium is fluid, this movement is observed as continuous compression and refraction. In microchannels, cells are exposed to this force field, which convey the cells to the zones with minimum pressure gradients. Velocity of this movement is a function of cell size, density and its relative compressibility. A schematic representation of CTC isolation within a channel, in which an acoustic standing wave is applied, is shown below. The term *standing wave* corresponds to the case where incident and reflecting waves with same amplitude and frequency coincide in opposite directions. As can be seen from the figure, larger CTCs are carried towards the centerline of the channel from an initial position near the walls as they are subject to a stronger acoustophoretic force. In general, success of separation in acoustophoresis depends how much acoustic properties and size differs in the cell mixture.

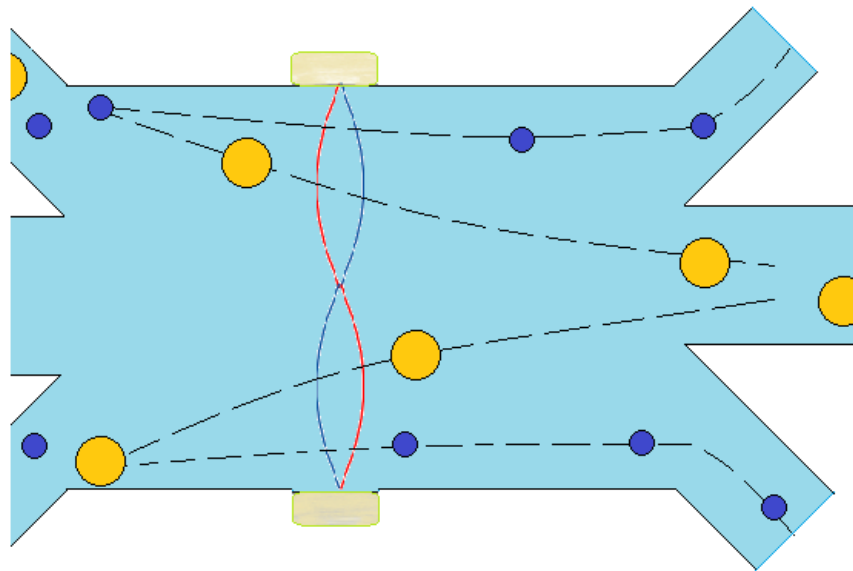


Figure 1:6 Separation of cells in acoustophoresis

It has been shown that it is possible to separate red blood cells, white blood cells and CTC in the recent literature [38–42] with a very high purity and recovery rate. Nevertheless,

throughput of acoustophoresis in those studies is very limited and prone to clogging problems, especially at high cell concentrations.

In summary, isolation of CTCs based on physical properties makes it possible to capture cells with different surface markers. Label-free approaches also enable high cell viability [10,11,43]. However, there are certain disadvantages. First of all, significant overlap in the sizes of CTCs and leukocytes leads to low purity [16]. Secondly, CTCs which are similar in size with leukocytes (or smaller) are lost during separation. Lastly, filter based approaches are usually prone to clogging, which leads to decreases in capture efficiency. In Table 1:2, studies utilizing label-free CTC isolation methods from the last two years are summarized. It should be noted that some of those studies are limited to cell lines while the others use clinical samples. As can be seen from the table, recovery rates of all studies are significantly high while none of the studies using clinical samples reports purity which is the Achilles' heel of these approaches. Nevertheless, studies with cell lines gives promising results in terms of purity.

Table 1:2 Summary of Label-Free CTC Isolation Technologies

Platform	Capture method	Test sample	Recovery rate (%)	Purity (%)	Viability (%)	Ref.
<b>Membrane microfilter</b>	Size based (filter-pore type)	In lysed whole blood: MCF-7, MDA-MB-231	93 to 95	-	-	[44]
		Patient: prostate, breast, colon, bladder	51 of 57	-	-	
<b>Microsieve</b>	Size based (filter-pore type)	In diluted blood: LNCaP	90	-	-	[45]
		Diluted patient blood: breast, colon, prostate, cervix	All 8 patients	-	-	
		In whole blood: HepG2/GFP MCF-7	> 80	-	-	

Table 1:2 Summary of Label-Free CTC Isolation Technologies (cont'd)

		Patient: breast	19 of 24	-	-	
<b>p-MOFF</b>	Size based (hydrodynamic)	In whole blood: MCF-7	93.73	-	-	[46]
		In whole blood: MDA-MB-231	91.60	-	-	
<b>MS-MOFF</b>	Size based (hydrodynamic)	In whole blood: MCF-7	>98.9	-	-	[47]
<b>DLD</b>	Size based (hydrodynamic)	In growth medium: MCF10A, MDA-MB-231	91	>95	-	[28]
		Diluted whole blood: MCF10A, MDA-MB-231	86	>95	-	
<b>DEP</b>	Size based (DEP)	In normal cells: MDA-231	>95	-	-	[48]
<b>DEP-FFF</b>	Size based (DEP)	In T-lymphocytes: MDA-436	70	99.2	-	[49]

### 1.2.3 Affinity-Based CTC Isolation

Affinity-based approaches employ antibodies against cell surface markers. This technique has been utilized by the only FDA approved CTC isolation system, CellSearch®. The major challenge in affinity-based CTC isolation is the heterogeneity of surface markers, which makes it difficult to establish a single universal antigen.

In general, bio-affinity based cell isolation strategies can be grouped in two main categories:

- Positive enrichment where CTCs are targeted via surface markers such as EpCAM

- Negative enrichment where leukocytes are targeted by using markers such as CD45

Majority of positive enrichment studies reported to date has been developed to isolate CTCs originated from epithelial tumors, for which the most common surface marker is the epithelial cell adhesion molecule (EpCAM). This transmembrane protein is highly expressed on most non-hematologic cancers such as breast, lung, brain, prostate and colon [50,51]. One of the earliest works using EpCAM antibody for positive enrichment is the work of [52], which has eventually evolved into CellSearch® and their work set the standards of the CTC isolation. Since then cells with EpCAM<sup>+</sup>/CK<sup>+</sup>/CD45<sup>-</sup> marker is accepted to be the CTC and several technologies have been developed by using this marker to capture and isolate CTCs.

One of the earliest emerged approaches using microfluidics for CTC enrichment from whole blood was developed by [53]. On their microchip, they assembled 78800 microposts with anti-EpCAM antibody with an optimized geometric distribution to maximize advantages offered by laminar flow conditions in the channel, which enables their microchip (CTC-chip) to isolate CTCs from patients' whole blood with CTC numbers varying between 5 and 1000 CTCs/mL while achieving 50 % purity. It should be noted that this was not possible with the CellSearch® [53]. With this significant accomplishment, several other devices have been developed following the same principle. Geometrically enhanced differential immunocapture (GEDI) is one of these approaches, which introduced hydrodynamic enrichment exploiting size differences into micropost arrays with anti-EpCAM antibody to reduce impurities such as leukocytes. It was utilized to capture CTCs from whole blood of prostate cancer patients, where GEDI provides up to 400-fold increase in CTC enrichment compared to CellSearch® [54]. OncoCEE technology developed by Biocept further extends the micropost array approach by using more than one antibodies to functionalize the microchannel (EpCAM, HER2, MUC-1, EGFR, TROP2, N-Cadherin) and applying in-situ fluorescent staining, which enables OncoCEE to identify 53 % of the patients with metastatic breast cancer with CK<sup>+</sup>/CD45<sup>-</sup> CTCs. Despite the success of CTC enrichment, CTC isolation via microposts is quite a

challenge due the difficulties in its fabrication and its high flow resistance, which allows only low throughput rates (~1 mL/h).

This low throughput problem was somewhat alleviated by incorporating surface based isolation as in [55], where herringbone channels are deployed within microchannels instead of micropost arrays. In their design HB-Chip [55], Stott et al. achieved a CTC capture efficiency (14/15 patients) by processing whole blood with a flowrate of 4.8 mL/h. Similarly, GEM chip presented in [56] and GO developed by [57] yielded higher flowrates by deploying geometric manipulations in the channel, giving 3.6 mL/h and 2 mL/h, respectively, while offering a high capture efficiency. Another surfaced based application is the CTC isolation on sinusoidal channels with high aspect ratio (1:5) called BioFluidica [58]. In this design, it has been shown that CTCs can be captured with a relatively high volumetric flow rate (about 10 mL/h), high purity (86 %) and sensitivity (11 CTCs/mL can be detected). Furthermore, the device has been combined with several modules in which CTCs can be counted, stained, imaged and indexed.

One of the major issues on surface based CTC isolation is the reversibility of the functionalized surfaces. Captured cells can be released for further analysis via trypsinization [56], though this process may harm the surface receptors, which may be critical in the downstream analysis. Immunomagnetic methods offer a solution for this problem. Ephesia®, which is essentially a magnetic beads based array chip utilize antibody linked posts for CTC isolation within a microchannel with a flow rate of 3 mL/h or more [59]. The key difference in Ephesia is the ability to self-assemble these magnetic microposts. These posts are also sufficiently small (4.5 µm) that they do not create any problem during imaging process. Validity of Ephesia for CTC isolation has also been carried and its performance has been shown to exceed the performance of CellSearch® in 10/13 samples [59]. Magnetic Sifter is another application of immunomagnetic methods, in which flow is oriented vertically through magnetic pores. This design enables a very high CTC recovery (6/6 patients) at significantly high flow rates (10 mL/h) [60]. IsoFlux™ and LiquidBiopsy are other two of the recently emerged technologies using immunomagnetic isolation [61]. They are both used under continuous flow and consist of multiple zones. CTC-i Chip, another immunomagnetic technology processing whole

blood, combines the advantages of DLD, inertia based and immunomagnetic separation in a single device with a high processing rate, 8 mL/h [62,63]. They tested the validity of CTC-i Chip with clinical samples from several cancer types and showed that CTCs with a concentration higher than 1cell / 2 mL can be detected in 90 % of the samples and CTC-i Chip is more sensitive than CellSearch® [63].

Negative enrichment is also under the affinity based capture technologies' umbrella where background cells are targeted and removed with specific antibodies like anti-CD45. While negative enrichment is advantageous for isolation of cells with low /none EpCAM expression and leave target cells intact for downstream analysis; purity is generally lower than the positive enrichment. There are two negative enrichment platform reported for CTC isolation from clinical samples EasySep™ (STEMCELL Technologies, Canada) [64] and Quadrupole Magnetic Separator (QMS) [65,66]. EasySep™ is a commercialized system that employs magnetic nanoparticles coated with anti-CD45 antibodies to capture labelled leukocytes with a magnet that creates magnetic field. Unlike EasySep™ in which the process is batch type, QMS system is magnetic cell separator utilizing microfluidics for cell sorting. Additionally, some positive enrichment platforms discussed above can be used for negative enrichment by only replacing the capture antibody with anti-CD45. Example platforms that isolate CTCs via both depletion and enrichment are MACS [67] and CTC-iChip [62,63].

Table 1:3 Summary of Affinity Based CTC Isolation Technologies

Platform	Capture method	Test sample	Recovery rate (%)	Purity (%)	Viability (%)	Ref.
<b>CTC-chip</b>	Positive affinity (EpCAM)	Patient prostate, pancreatic, breast, colon	23 of 36	50	98.5	
		In whole blood: NCI-H1650	>60	50	-	[53]
		In PBS: NCI-H1650, SKBr-3, PC3-9, T-24	65	-	-	
<b>HB-chip</b>	Positive affinity (EpCAM)	Patient: prostate	14 of 15	-	-	
		In whole blood: PC3	92	-	-	[55]
<b>Graphene oxide nanosheets</b>	Positive affinity (EpCAM)	Patient: breast, lung, pancreatic	23 CTCs	-	-	
		In buffer: MCF-7	>82.3	-	-	
		In buffer: Hs-578T 21	<10	-	-	[68]
<b>HTMSU</b>	Positive affinity (EpCAM)	In whole blood: MCF-7	73-94	-	-	
		In citrated whole rabbit blood: MCF-7	97	-	-	[69]
<b>Microchip-based immunomagnetic EpCAM</b>	Positive affinity (EpCAM antibody)	In centrifuged whole blood: COLO205	90	-	-	[70]
<b>Magnetic array</b>	Positive affinity (EpCAM)	In endothelial cells: MCF-7	80 ±20	-	-	[71]

Table 1:3 Summary of Affinity Based CTC Isolation Technologies (cont'd)

<b>Magnetic micropillar EpCAM</b>	Positive affinity (EpCAM)	In DMEM: HCT116	>70	-	78	[72]
		In whole blood: HCT116	>40	-	-	
<b>GEDI</b>	Positive affinity (PSMA)	Patient: prostate	-	62±2	-	[73]
		In PBS: LNCaP	97±3	-	-	
		In whole blood: LNCaP	85±5	68±6	-	
<b>Aptamer microchip</b>	Positive affinity (DNA-aptamer)	In RPMI: CCRF-CEM, NB-4	>80	97	-	[74]
<b>Aptamer nanosubstrates</b>	Positive affinity (DNA-aptamer)	In artificial blood: A549	>80	99	79-83	[75]
<b>3D SiNP array</b>	Positive affinity (EpCAM)	In culture medium: MCF-7	45-65	-	84-91	[76]
<b>Nanowire substrate</b>	Positive affinity (EpCAM)	In culture medium: A549	65±25	-	-	[77]
		In whole blood: A549	67±15	-	-	
<b>Negative immunomagnetic</b>	Negative affinity (CD45)	Lysed patient blood: head, neck	2.32 CTC/ml	-	-	[78]
		In buffy coats: SCC-4	83	-	-	
		In buffy coats: Melanoma	84	-	-	

Table 1:3 Summary of Affinity Based CTC Isolation Technologies (cont'd)

<b>PosCTC-ichip</b>	Positive affinity (EpCAM)	Patient: prostate, breast, pancreas, colorectal, lung	37 of 41	-	-	[62]
		In whole blood: SKBR3	98.6 ±4.3	-	-	
		In whole blood: PC3-9	89.7 ±4.5	-	-	
		In whole blood: MDA-MB-231	77.8 ±7.8	-	-	
<b>NegCTC-ichip</b>	Negative affinity (CD45)	In whole blood: MCF10A	96.7 ±1.9	-	-	[62]

- **Antibody Immobilization Strategies for Affinity-Based CTC Isolation**

Immunoaffinity based approach offers high purity and sensitivity [6] although its success depends on orientation, homogeneity and stability of immobilized antibodies [79–81]. A wide range of antibody immobilization approaches is available in the literature with different degrees of complexity. The selection of appropriate immobilization strategy is made by considering the physical and chemical properties of both surface and molecule to be immobilized. For successful immobilization, it is important to have proteins face away from the surface so that their active sites are accessible (Figure 1:7). Furthermore, the protein structure should be intact for success and repeatability of the immobilization. Several immobilization approaches have been developed which can be grouped into three categories: physical, covalent and bio-affinity immobilization.

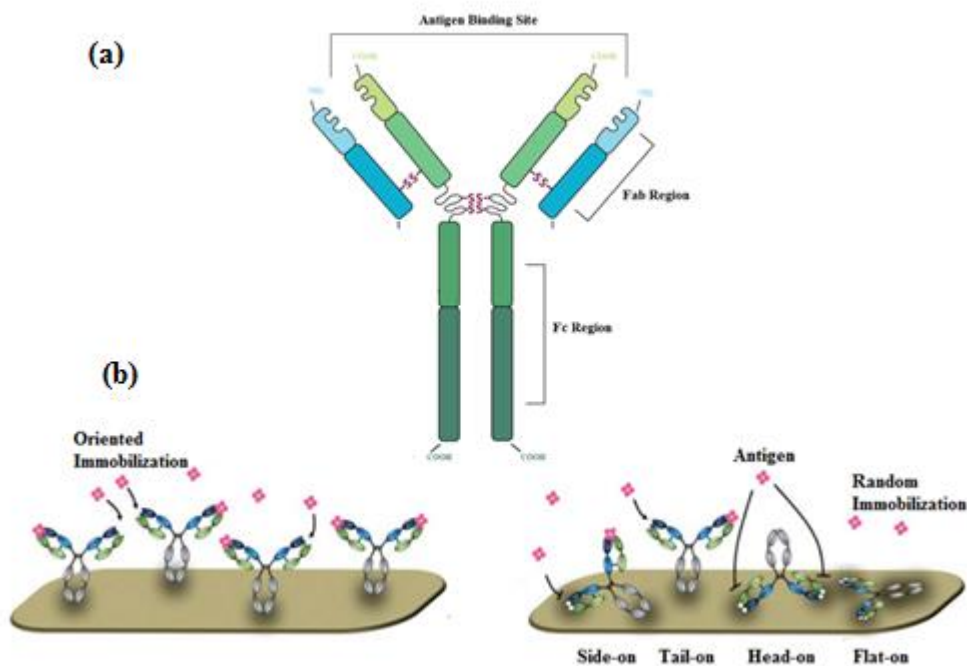


Figure 1:7 (a) Schematic representation of antibody, (b) Antibody immobilization on solid surfaces (adapted from [80])

Physical adsorption is the easiest and most straightforward strategy and frequently utilized for protein immobilization. Proteins are simply adsorbed by the surfaces by intermolecular forces like hydrophobic, hydrogen bond, electrostatic, van der Waals via incubation of surface with protein solution without sophisticated chemistry or chemicals. Nevertheless, physically adsorbed antibodies are unstable and prone to significant loss of functionality due to random immobilization [58,59]. Furthermore, environmental effects like temperature, pH of the solution and type of the surface can affect the strength of the intermolecular forces which inhibit reproducible protein immobilization.

Covalent bonding, on the other hand, forms stable and irreversible bonds with a high immobilization density between the functional groups of surface marker and antibody [82–84]. This approach has been utilized extensively and applied for CTC capture via EpCAM immobilization [11,85–89]. However, covalent based antibody immobilization may result in randomly oriented antibodies since covalent immobilization utilizes the

residues that typically found on the exterior of the protein. Random orientation may decrease the density and accessibility of active sites and create heterogeneity [80,90]. This can be overcome with well-defined immobilization strategies which enables reproducible, oriented protein immobilization with diminished denaturation.

To increase the number of functional antibodies on the surface, oriented immobilization can be introduced by bio-affinity immobilization. Bio-affinity immobilization enables homogeneous protein immobilization with oriented and reproducible manner. While there are several bio-affinity based techniques available like usage of antibody binding proteins (Protein A/G) and DNA linkers, avidin-biotin interaction is a widely used bio-affinity immobilization approach [81] and successfully implemented for EpCAM based CTC isolation [91–95]. This technique however requires multiple steps for surface functionalization and each step increases the complexity, production time, and cost of the technique.

- **CTC Release Strategies After Affinity-Based Capture for Downstream Applications**

Although CTC enumeration have a proven clinical utility, the main power of CTCs in cancer management reside in the downstream analysis of isolated cells, which includes their molecular characterization via genomic, transcriptomic and proteomic analyses, as well as their proliferation in culture media for further cancer research and drug development studies. For this reason, issues related to release of the isolated CTCs in viable form must be considered. Release technologies should ensure (i) efficient release of CTCs, (ii) non-destructive recovery of CTCs, (iii) compatibility with wide range of downstream applications following the release, and (iv) simplicity. Generally, three methods have been utilized to release captured CTCs: enzymatic digestion, cleavage of the link between surface and the affinity agent and degradable polymeric coatings.

Enzymatic digestion of the affinity agent technique is based on cleaving of cell surface proteins to release bound cells. Most commonly used enzymatic digestion reagent is

trypsin. In normal adherent cell culture applications, cells are detached from the surface with trypsin solution (0.25% in 0.02 % EDTA) for 3-5 minutes at 37 °C. In microfluidics, it has been demonstrated that 0.05% to 0.25% trypsin can successfully detach captured cells with almost 100% efficiency [69,88,96].

When CTC capture is achieved by utilization of aptamers, exonucleases or the anti-sense oligonucleotide sequence can disrupt the aptamer's antigen binding and release the cells [97]. This technique is implemented in bio-affinity functionalized silicon nanowire to release captured non-small cell lung cancer (NSCLC) cells with 85% release efficiency and 80% viability [75].

Another strategy to release CTCs is usage of specifically designed linkers that can cleave the linkage between affinity agent and surface. One of the example is USER (Uracil Specific Excision Reagent); it digests the oligonucleotide linkers that helps the immobilization of antibodies to the surface with uracil specific enzymes. It was reported that cell release efficiency is 90% with 85% cell viability [98].

Additionally, polymer coatings, having varying capture characteristics with respect to external changes like temperature, pH, electric field, can be used for cell release. Hou et al. constructed silicon nanowires with temperature responsive polymer brushes. These brushes are hydrophobic at 37° C and suitable for cell capture whereas they are hydrophilic at 4° C and enable cell release with 95% efficiency [99]. Similarly, gelatin nano-films functionalized with avidin- biotin interactions that melt with temperature or degrade with mechanical influences can be used for cell release. Finally, biotin doped polypyrrole system is developed that release captured cells with electrical stimulation [94].

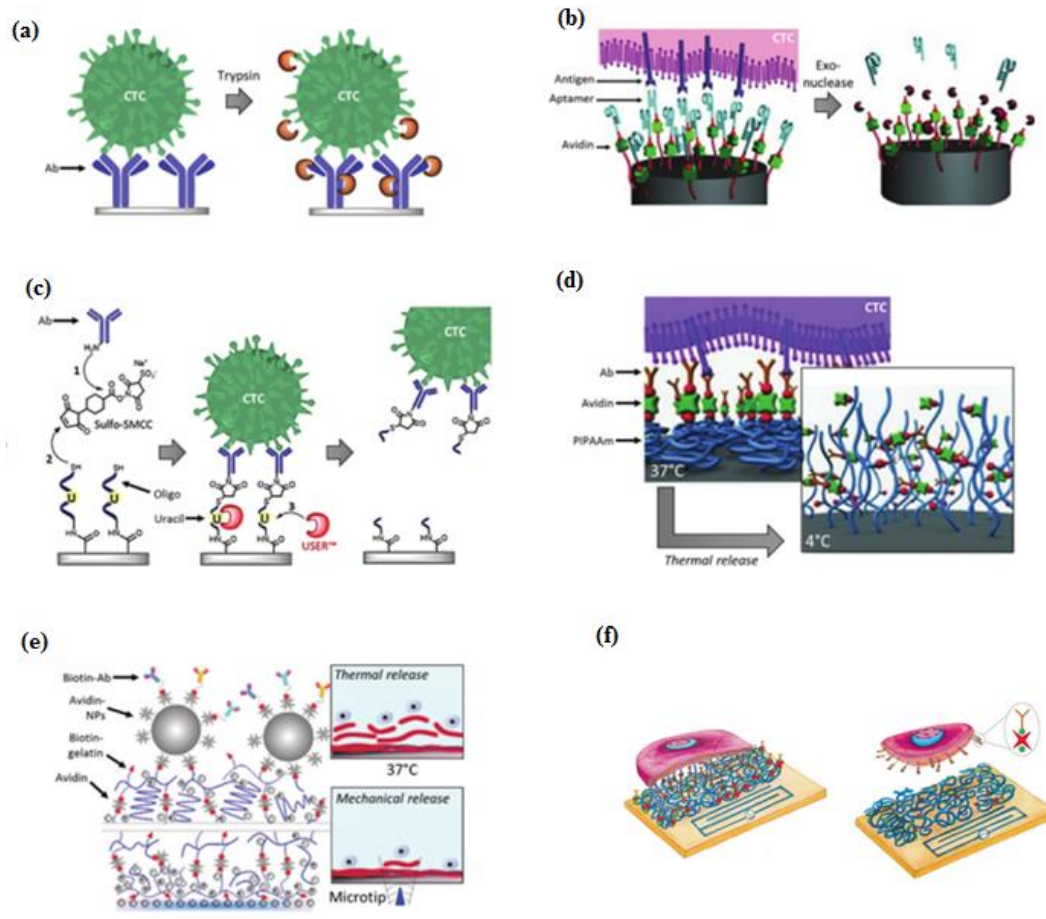


Figure 1:8 CTC release strategies after affinity-based capture (adapted from [97])

### 1.3 Research Objectives

The number of circulating tumor cells (CTCs) in blood is highly associated with prognosis in several types of cancer like breast, prostate, lung and colorectal cancer. Consequently, isolation and characterization of CTCs have important clinical significance in terms of prognosis and early detection of response to drug treatment. However, CTCs are extremely rare (as low as 1 in a billion of blood cells) and a highly sensitive and specific technology is required to isolate CTCs from blood cells. Immunoaffinity based approaches have been shown to provide sufficiently high CTC capture efficiency in a number of studies. However, it is not possible to comment on the relative CTC capture

efficiencies of antibody immobilization methods utilized in these studies. Therefore, available methods are needed to be compared in one comprehensive study with respect to CTC capture efficiency and selectivity.

Objective of this study is to investigate alternative antibody immobilization methods for efficient CTC isolation on plain surfaces and propose an efficient surface functionalization strategy that can be applied in microchannels.

To achieve these objectives, following studies should be carried out systematically:

- Development of oxide surface functionalization strategies
- Physical and chemical characterization of surfaces to ensure success of functionalization
- Comparison of strategies with respect to capture efficiency, selectivity, time and cost
- Implementation of selected strategy in microchannel configuration
- Determination of cell capture efficiency with MCF-7 cell line as CTC model
- Determination of selective cell capture from blood and non-specific cell capture rate
- On-chip detection of captured cells with immunostaining
- Investigation of cell capture behavior of CTCs with different EpCAM expression levels
- Viable CTC release from capture zone and re-culture of released CTCs for downstream applications
- Shelf-life analysis of functionalized surfaces

## CHAPTER 2

### METHODS AND MATERIALS

Following strategy was applied to fulfill the combined objectives of the study; that is, developing an efficient surface functionalization strategy for selective CTC capture and viable cell release for downstream applications:

- i. Two covalent and two bio-affinity antibody immobilization methods were proposed, inspired from most commonly used approaches in the literature, and applied on plain SiO<sub>2</sub> surfaces.
- ii. Surfaces were physically and chemically characterized at each step of functionalization via contact angle, spectroscopic ellipsometry and XPS measurements.
- iii. After confirming the success of surface functionalization for each protocol, developed immobilization methods were compared with respect to cell capture efficiency, specificity, cost and time on plain SiO<sub>2</sub> surfaces. This was achieved by using target breast cancer cell line, MCF-7, and non-target acute lymphoblastic leukemia cell line CCRF-CEM, as CTC model.
- iv. Following the determination of the most efficient protocol with respect to cell capture efficiency, specificity, cost and time, selected protocol was implemented to serpentine microfluidic channels, following the same concentrations of reagents and incubation periods applied on the plain SiO<sub>2</sub>

surfaces, to determine the cell capture efficiency, cell capture selectivity, viable cell release ability and shelf life of functionalized microchannels. Specificity studies were performed by using MCF-7 cells spiked in buffer containing background leukocytes while the sensitivity studies were carried out by using five different breast cancer cell lines with varying EpCAM expression levels, namely MDA-MB-231, MDA-MB-468, SKBR3, MCF-7 and CAMA-1 to investigate the significance of EpCAM expression in cell capture. Viability of the released cells was investigated by collecting the cells from the channel outlet and re-culturing those cell in a vial containing cell growth media to test proliferation ability. Finally, shelf-life of bio-functionalized microchannels was tested with respect to cell capture efficiency for a period of two weeks.

Background and preliminary work done for those work steps are presented in the following sections.

## **2.1 Device Fabrication**

Plain SiO<sub>2</sub> surfaces and microfluidic channels were fabricated in METU-MEMS Center (Ankara, Turkey). Silicon substrates (1cm x1cm) with 300-nm thick thermal oxide layer were used for both surface characterization and cell capture experiments. For in-channel tests, serpentine microfluidic channels (80x200 μm (height x width)) were fabricated via DRIE process, coated with 300 nm thermal oxide and bonded to glass wafer via anodic bonding.

The first step for microfluidic channel fabrication is to clean Si wafer with standard piranha/HF process. After the cleaning, lithography step was performed for channel openings. Photoresist was stripped with oxygen plasma and oxide layers with a thickness of 2 μm for active surface and 1 μm for back side were deposited on Si wafer by using plasma enhanced chemical vapor deposition (PCVD). SiO<sub>2</sub> etching was performed with lithography followed by reactive ion etching (RIE). Channel inlet and outlet were opened

with deep reactive ion etching (DRIE). Photoresist was stripped with oxygen plasma and thermal oxide layer with a thickness of 300 nm was deposited with chemical vapor deposition (CVD). Piranha cleaned glass wafer was anodically bonded to Si wafer to obtain channel configuration (Figure 2:1).

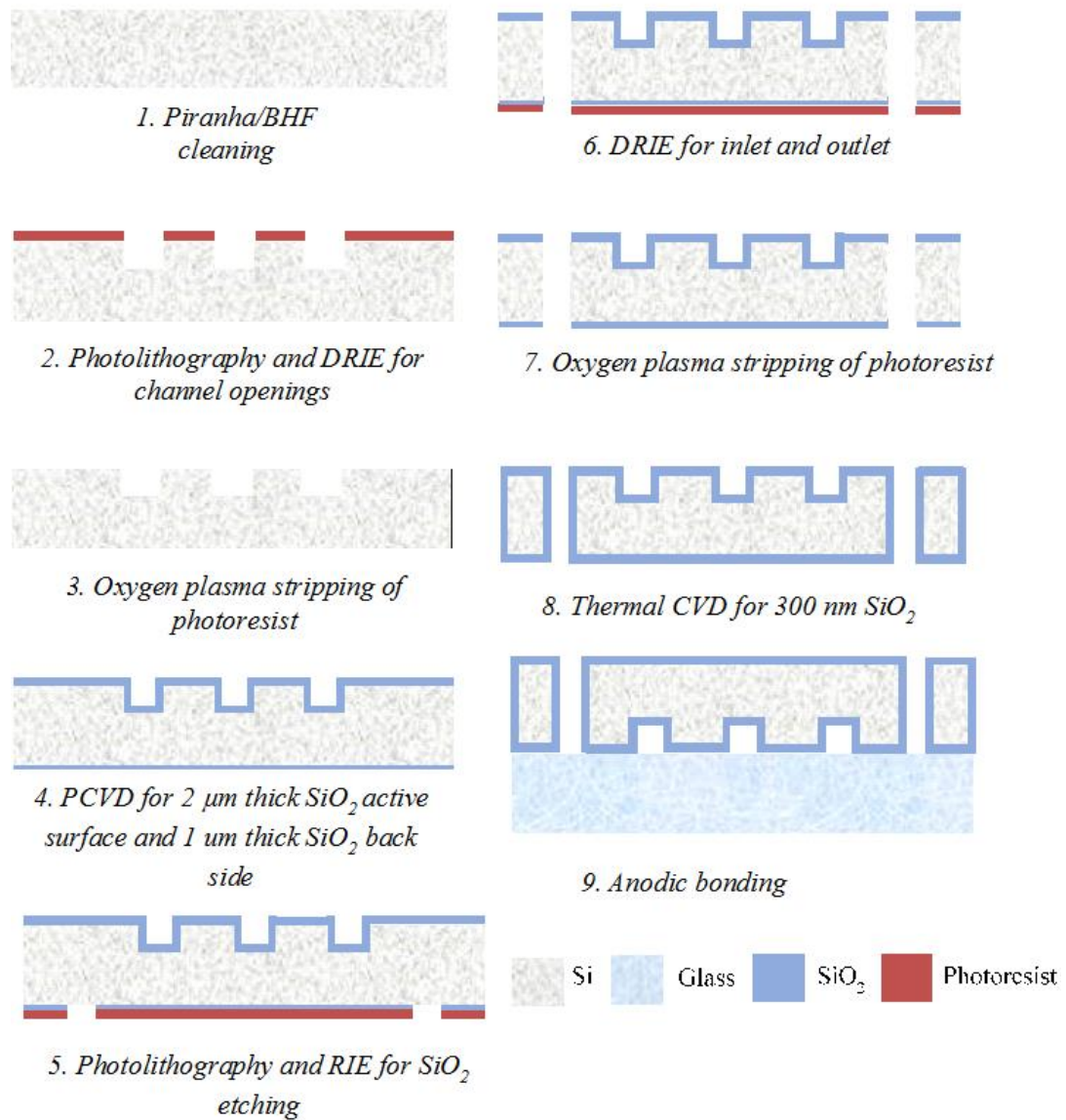


Figure 2:1 Fabrication steps of microfluidic channel

## 2.2 CTC Model

MCF-7 cells, a well-established breast carcinoma cell line known for its high EpCAM expression level, were used as the CTC model [100] to determine the cell capture efficiency of antibody immobilization methods. In order to investigate the selectivity of the functionalized surfaces, acute lymphoblastic leukemia cell line (CCRF-CEM) was utilized as the EpCAM negative CTC model [101]. Both MCF-7 and CCRF-CEM cell lines were purchased from Deutsche Sammlung von Mikroorganismen und Zellkulturen (DSMZ) (cat ACC 317) and received as frozen vials. Breast cancer cell lines with varying EpCAM expression levels were kindly donated by Dr. Rengül Atalay (MDA-MB-231, MDA-MB-468 and CAMA-1) and Dr. Özgür Şahin (SKBR-3) and used for sensitivity determination of the developed surface functionalization techniques. Breast cancer cell lines were cultured in DMEM high glucose medium (Gibco) supplemented with 10% fetal bovine serum (Capricorn Scientific), 1% Sodium pyruvate (Capricorn Scientific), 1% MEM non-essential amino acids (Gibco, cat # 11140050), and 1% penicillin–streptomycin (Sigma Aldrich) and 0.01 mg/ml Insulin human recombinant (Sigma Aldrich). CCRF-CEM cell line was cultured in RPMI 1640 medium (Thermo Fisher) supplemented with 10% fetal bovine serum (Capricorn Scientific), 1% Sodium pyruvate (Capricorn Scientific), 1% MEM non-essential amino acids (Gibco, cat # 11140050), and 1% penicillin–streptomycin (Sigma Aldrich). All were incubated in a 37 °C CO<sub>2</sub> incubator upon confluency and dislodged with cell dissociation solution (Biological Industries). For fluorescence microscopy imaging, MCF-7 cells were stained with cell tracker red dye while MDA-MB-231, MDA-MB-468, CAMA-1, SKBR-3 and CCRF-CEM cells were stained with fluorescein diacetate dye according to the manufacturer's instruction (Thermo Fisher).

## **2.3 Surface Functionalization**

### **2.3.1 Materials**

3-Aminopropyl (triethoxysilane) (APTES), Glutaraldehyde (Glu, 25% (w/v)), Streptavidin from *Streptomyces avidinii* (Str), N-(3-Dimethylaminopropyl)-N'-ethylcarbodiimide hydrochloride (EDC), N-Hydroxysuccinimide (NHS), MES monohydrate, (+)-Biotin N-hydroxysuccinimide ester (BNHS), bovine serum albumin (BSA) and phosphate buffered saline (PBS, pH:7.4) were purchased from Sigma Aldrich. Biotinylated Anti- EpCAM antibody [VU-1D9], Anti-EpCAM antibody [VU-1D9], Anti-pan Cytokeratin antibody [C-11] and Anti-CD45 antibody [f10-89-4] were purchased from Abcam. DAPI (4',6-Diamidino-2-Phenylindole, Dihydrochloride) was purchased from Thermo Fisher Scientific.

### **2.3.2 Silanization of Oxide Surfaces**

For all protocols, oxide surfaces were cleaned with standard acetone, isopropyl alcohol and ethanol treatment followed by rinsing thoroughly with ddH<sub>2</sub>O, drying with nitrogen stream and curing at 71 °C on hot plate for 30 minutes. Oxide surfaces were then incubated in a solution of 2% APTES prepared with pre-heated toluene (100-120 °C) for 45 minutes in nitrogen environment and rinsed with toluene.

### **2.3.3 Antibody Immobilization**

In this study, two covalent and two bio-affinity antibody immobilization methods were proposed, inspired from most commonly used approaches in the literature, and applied on plain SiO<sub>2</sub> surfaces (they will be referred as protocol P1- P4 hereafter). Details of those protocols are presented below.

**Protocol 1 (P1):** Immediately after the silanization step, surfaces were incubated in 2.5% (v/v) glutaraldehyde solution for 2 hours at room temperature. Then, anti EpCAM antibodies were immobilized on the surface from their amine group via glutaraldehyde linker as shown in Figure 2:2(a). This was achieved by covering the surfaces with anti EpCAM antibody solution (15 µg/ml) for 1 hour at room temperature.

**Protocol 2 (P2):** Immediately after the silanization step, anti EpCAM antibodies were directly immobilized on the surface from their carboxyl group via EDC/NHS coupling reaction (Figure 2:2(b)). This was achieved by covering the surfaces with EDC/NHS solution (250 mM :100 mM in 50 mM MES Buffer ph:6.34) containing 15 µg/ml anti EpCAM for 1 hour at room temperature.

**Protocol 3 (P3):** Immediately after the silanization step, surfaces were incubated in 2.5% (v/v) glutaraldehyde solution for 2 hours at room temperature. Next, surfaces were covered with streptavidin solution (100 µg/ml PBS) and incubated for 1 hour at room temperature. Then, anti EpCAM antibodies were immobilized on the surface via bio-affinity based interaction by covering the surfaces with anti EpCAM antibody solution (15 µg/ml) for 1 hour at room temperature (Figure 2:2(c)).

**Protocol 4 (P4):** Immediately after the silanization step, surfaces were functionalized with NHS-Biotin solution (2 mg/ml in PBS) for 1 hour at room temperature. Surfaces were then covered with streptavidin solution (100 µg/ml PBS) and incubated for 1 hour at room temperature. Finally, anti EpCAM antibodies were immobilized on the surface via bio-affinity based interaction by covering the surfaces with anti EpCAM antibody solution (15 µg/ml) for 1 hour at room temperature (Figure 2:2(d)).

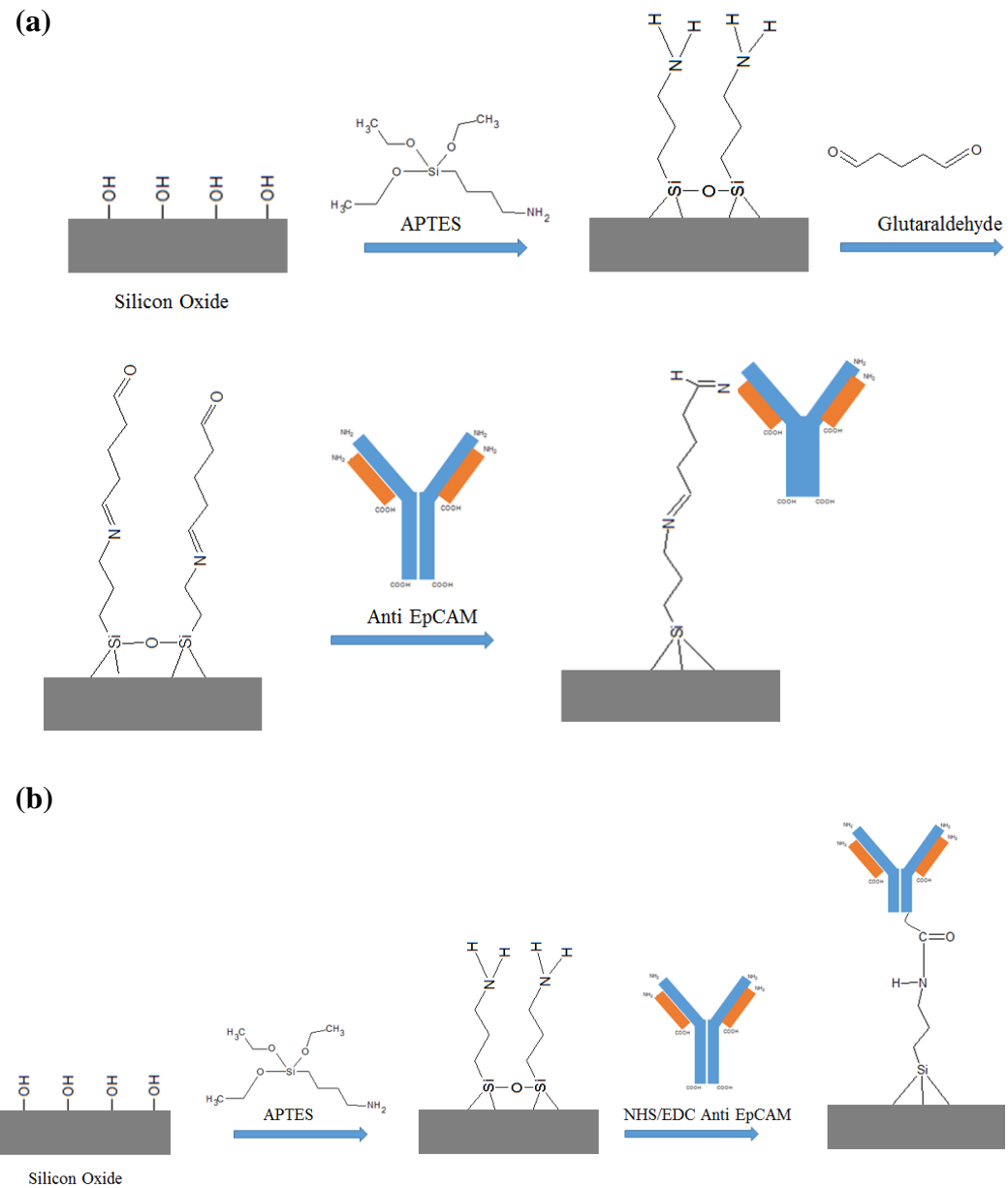
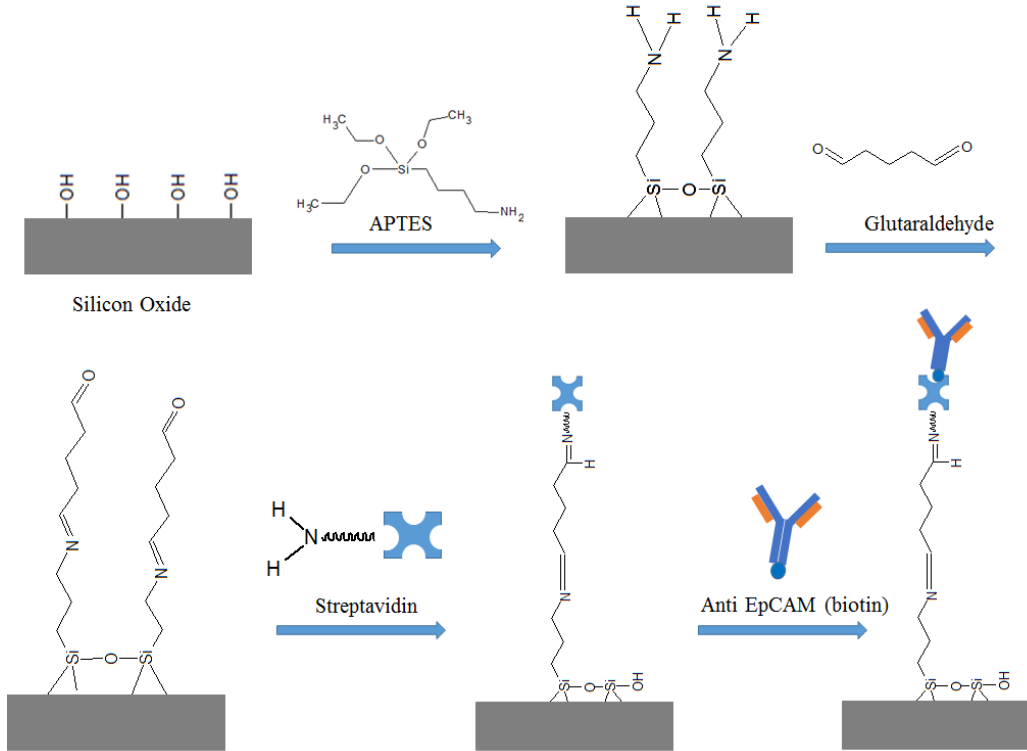


Figure 2:2 Schematic representation of antibody immobilization in P1 (a), P2 (b), P3(c) and P4(d)

(c)



(d)

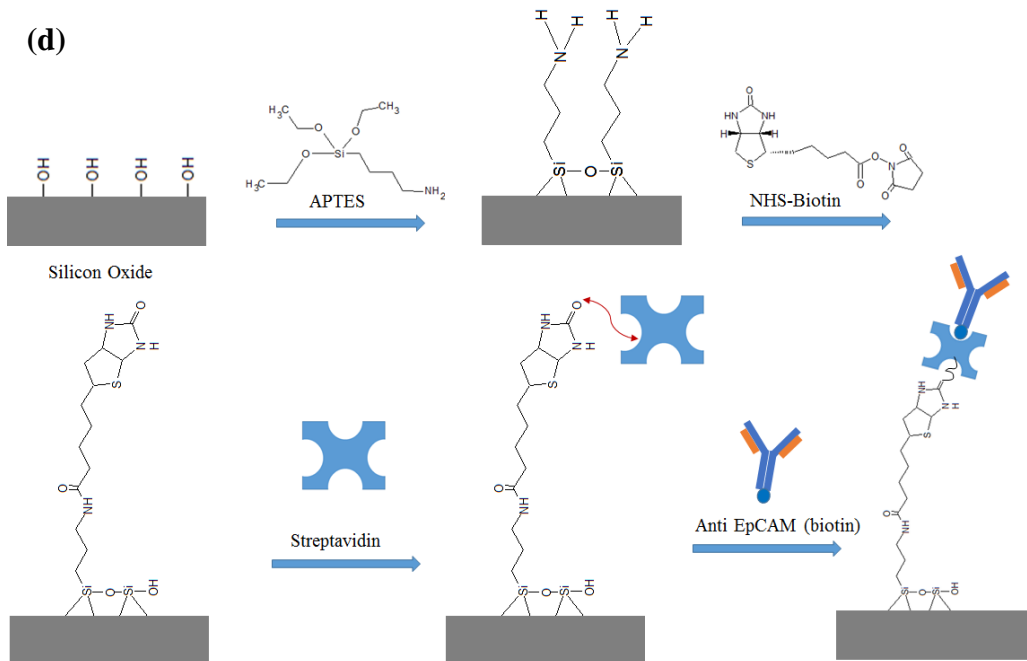


Figure 2:2 Schematic representation of antibody immobilization in P1 (a), P2 (b), P3(c) and P4(d) (cont'd)

## **2.4 Surface Characterization**

### **2.4.1 Contact Angle**

After each step of surface functionalization, contact angle was measured using Attension Theta (Biolin Scientific, Sweden) to observe the change in the surface energy. The static water contact angle was measured at room temperature using sessile drop method followed by the image analysis of the drop profile. The volume of water used was 5  $\mu$ l and the contact angle was measured 5 seconds after the deposition of drop. For each surface layer, contact angle was measured at five different locations and reported as an arithmetic average.

### **2.4.2 Spectroscopic Ellipsometry**

Spectroscopic ellipsometry (V-VASE J.A Woollam Co. Inc., USA) was used to measure surface thickness after each step of surface functionalization. All measurements were taken at an incidence angle of  $74^\circ$  and with the wavelength range varying between 210 nm and 920 nm. Data was processed via WVASE® software (J.A Woollam Co. Inc., USA) and ellipsometric parameters were fitted using the Cauchy Law. The best agreement between the experimental data and theoretical model was obtained by using refractive indices of 1.33, 1.19 and 1.45 for silane, glutaraldehyde and antibody respectively. For streptavidin and NHS-Biotin layers, best fitting was achieved for a refractive index value of 1.77. Measurements were repeated twice, and mean values and standard deviations are calculated accordingly.

### **2.4.3 X-ray Photoelectron Spectroscopy**

XPS measurements were performed by using Thermo K-Alpha Monochromated XPS spectrometer (Thermo Scientific, USA). AugerScan program was used for determination of relative atomic concentration by subtracted spectrum backgrounds with Shirley method. The neutral (C-C) carbon C1s peak at 284.6 eV was used as charge reference for XPS spectra.

### **2.4.4 Fluorescence Microscopy**

A fully automated bright field and/or fluorescence inverted microscope (Leica DMI Led 2000, Leica Microsystems Inc., Germany) was used for capturing the images of fluorescent signals emitted by fluorescent labelled cells immobilized on the surfaces.

## **2.5 Cell Capture**

### **2.5.1 Plain Surfaces**

In standard modification, each functionalization step was performed consecutively from APTES treatment to cell incubation. Protocols presented in Section 2.3 necessitate different durations for different steps of surface functionalization. Therefore, it is important to arrange a time schedule in such a way that none of the surfaces of different protocols experience a “latency time”, which they do not normally experience with the standard modification process, and experiments were performed without any “latency time” in this study.

After surface functionalization, two surfaces prepared with each protocol (totally 8 plain surfaces) were incubated in BSA (0.5mg/ml PBS pH: 6.4) solution for 15 minutes at room

temperature to block free surface sites. Surfaces were then incubated in six-well plates containing infinite number of fluorescent tagged MCF-7 cells (800,000 cells/ml) in the dark, long enough (30 minutes) to ensure maximum cell capture. In order to prevent cell agglomeration or accumulation on a specific area and provide uniform cell distribution, well plates were shaken during the cell incubation period. Surfaces were washed thoroughly with the buffer solution to remove unbound cells. For each surface, ten images were taken in order to scan the entire area. The images were then processed with a MATLAB code to determine the total number of captured cells. The same procedure was applied for non-target CCRF-CEM (800,000 cells/ml) cells while testing the selectivity of functionalized surfaces. All experiments were repeated three times with duplicate samples.

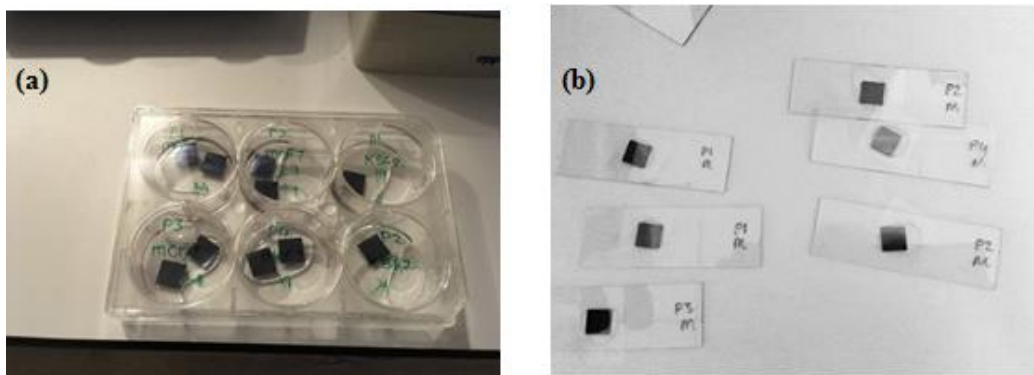


Figure 2:3 (a) Surfaces incubated in six well plates, (b) surfaces prepared for fluorescence microscopy imaging

### 2.5.2 In Channel

Serpentine microfluidic channels were functionalized with Protocol 2 following the same concentrations of reagents and incubation periods applied for the plain surfaces. Experimental procedure is given below.

- Microfluidic chip was conditioned by pumping pure ethanol for 10 minutes at 2000 mbar (45 $\mu$ l/min).
- Chip was washed with preheated toluene for 10 minutes at 2000 mbar.
- APTES solution was pumped through the microfluidic channel for 10 minutes at 1000 mbar and chips were incubated in APTES for 45 minutes at room temperature.
- After APTES incubation, channel was thoroughly washed with preheated toluene for 10 minutes at 2000 mbar.
- MES buffer (50mM pH:6.4) was pumped through the channel to make channel surface wet enough before antibody immobilization step at 2000 mbar. This process may take 15-20 minutes depending the amount of bubble formed during MES buffer washing
- When bubbles were disappeared, EDC/NHS solution (250 mM :100 mM in 50 mM MES Buffer pH:6.34) containing 15  $\mu$ g/ml anti EpCAM was flowed through the channel for 20 minutes at 500 mbar and channel incubated in this solution for 1 hour at room temperature.
- After incubation, channel was washed with MES buffer for 10 minutes at 500 mbar.
- BSA solution (0.5% w/v in MES) was flowed through the channel for 10 minutes at 500 mbar and channel incubated in this solution for 15 minutes and microchannel become ready for cell capture experiments.

Fluid flow was realized via microfluidic pressure controller system (Elveflow, France) and interconnects and a custom designed holder for fluidic interfacing (Figure 2:4).

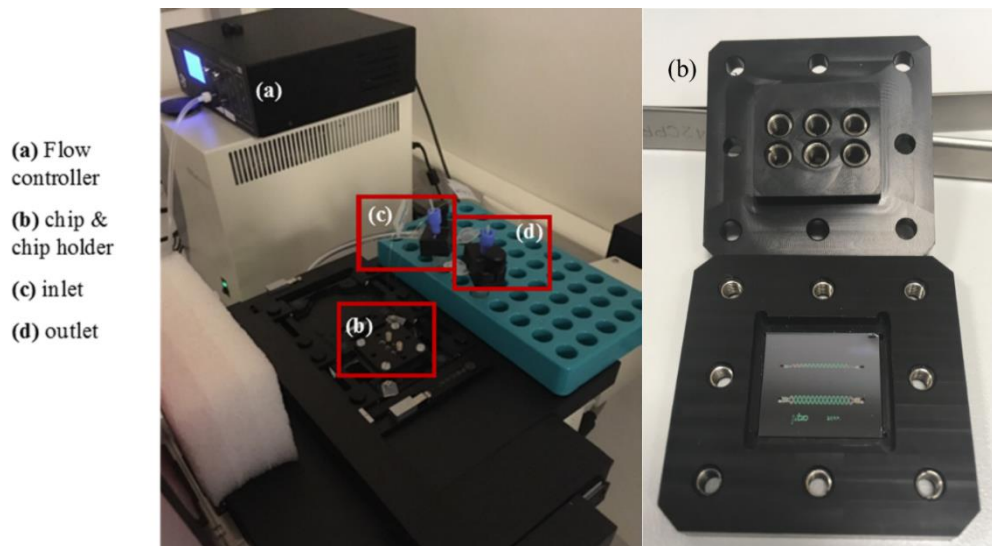


Figure 2:4 Microfluidic Test Setup

### 2.5.2.1 Cell Capture Efficiency Determination

For cell capture efficiency determination, cell suspension containing  $10^4$  MCF-7 cells/ml PBS was pumped through the bio-functionalized microfluidic channel with pressure controller. Once the channel was loaded, the flow was stopped and cells were incubated in the channel for 30 minutes to provide cell-surface interaction. After incubation period, the channel was washed with PBS (2 bars) to remove unbound cells. Washing flow rate was arranged to be adequately high for removal of unbound cells meanwhile low enough to protect captured cells from excess shear stress. Capture efficiency was determined from the images taken along the entire microfluidic channel by counting the number of cells inside the microfluidic channel before and after washing step and calculated using the following formula:

$$\text{cell capture efficiency(\%)} = \frac{\# \text{ of target cells inside the channel after washing step}}{\# \text{ of target cells inside the channel before washing step}} \times 100$$

### 2.5.2.2 Selective Cell Capture from Blood

Blood samples were taken in tubes containing anticoagulant EDTA from healthy donors as approved by the Institutional Review Board of METU Medical Center (Approval ID:28620816/398) with the informed consent from all donors of the blood samples. Whole blood (1 mL) was processed immediately and lysed with red blood cell lysis solution according to the manufacturer's instructions. Red blood cell lysis solution (10 X) was diluted to 1 X with double distilled water. 10 volume of dilute red blood cell lysis solution was mixed with 1 volume of whole blood, vortexed 5 seconds and incubated 10-12 minutes at room temperature at dark. After observing the sample becomes transparent red indicating the lysis is successful, sample was centrifuged at 300g for 10 minutes. Then, supernatant was aspirated and pellet was resuspended in PBS buffer (Figure 2:5).

MCF-7 cells were spiked in the lysed blood solution with a ratio of 1:10<sup>4</sup>. Cell concentration was arranged as 5000 MCF-7 cells and 5x10<sup>7</sup> WBC/ml by counting the cells with TC20 Automated Cell Counter (Bio-Rad, United States) and serial dilution.

Cell suspension was pumped through the bio-functionalized microfluidic channel with pressure controller. Once the channel was loaded, the flow was stopped and cells were incubated in the channel for 30 minutes to provide cell-surface interaction. After incubation period, Capture selectivity was determined by dividing the number of non-target cells inside the channel before and after the washing step.

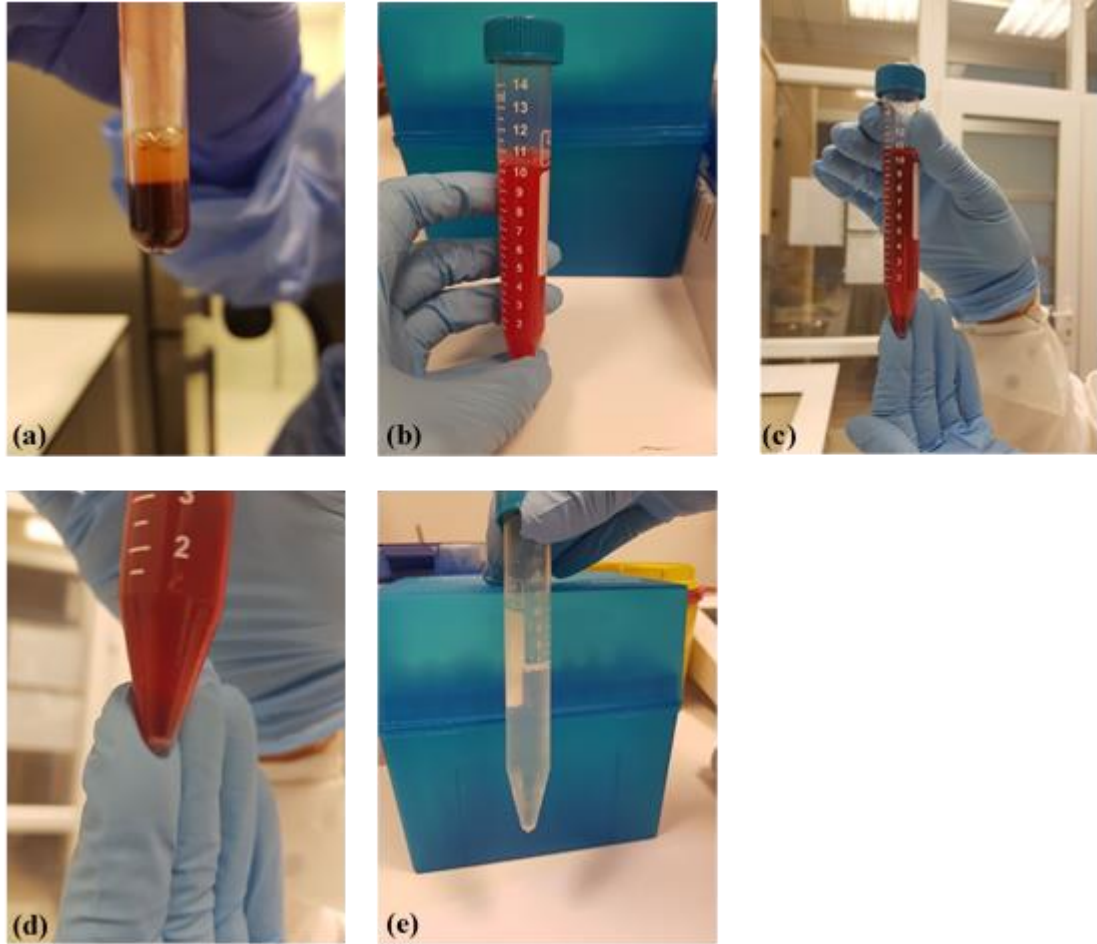


Figure 2:5 Preparing Blood Sample; **(a)** whole blood in EDTA tube, **(b)** whole blood lysis solution mixture, **(c)** mixture become transparent red after successful lysis, **(d)** after centrifuge WBCs in the bottom of the tube as pellet, **(e)** WBCs are resuspended in PBS

For on-chip detection of captured cells, a CTC: WBC cell suspension with a ratio of 1:100 was prepared and fed through the functionalized channel. After incubation and high flow rate washing, remaining cells were stained with fluorescence conjugated antibodies for CTC identification. CTCs are identified by positive expression of cytokeratin, negative expression of the leukocyte specific antigen (CD45), and nuclear staining with DAPI. The staining process enables not only visual identification of captured cells but also helps counting and morphology observation. For immunostaining, cells were fixed with 4% formaldehyde and permeabilized with 0.2% Triton X-100, for 10 minutes, each. Free

surface sites were blocked with 1% BSA solution (15 min) and cells were immunostained with anti-pan cytokeratin (panCK) (1 $\mu$ g/ml) and anti-CD45 (5 $\mu$ g/ml) antibodies for 1 hour, in dark. Finally, nucleus of cells was stained with DAPI (0.5 $\mu$ g/ml) for 1 minute and channel was washed with PBS (2 bars).

### **2.5.2.3 Cell Capture Based on EpCAM Expression Level**

Serpentine microfluidic channels were functionalized with Protocol 2 as described in Section 2.5.2. EpCAM sensitivity of the functionalized microchannel was tested with human breast adenocarcinoma cell lines MDA-MB-231, MDA-MB-468, CAMA-1, SKBR-3 and MCF-7 with different EpCAM protein expression and cell lines were prepared by following the procedure described in Section 2.2. Cell lines being analyzed were fed together with the MCF-7 cells with a ratio of 1:1. The total number of MCF-7 cells captured in functionalized microchannel after washing step was set to 100 % and binding efficiency of other cells were normalized based on the one's of MCF-7 cells.

EpCAM protein expression at the cell surface was determined with flow cytometry analysis by using phycoerythrin tagged anti-EpCAM antibody. For antibody tagging, cells reaching 85% confluency were dislodged with cell dissociation solution, washed and resuspended in ice cold phosphate buffer saline (PBS) containing 10 % fetal bovine serum (FBS) with a concentration of 10<sup>6</sup> cells/ml PBS. 20  $\mu$ l antibody was added to the cell solution and cells were incubated at dark for 60 minutes at 4 °C. After incubation, cells were washed three times by centrifugation at 300 g for 5 minutes, resuspended in PBS with 10% FBS and flow cytometry analysis were immediately performed.

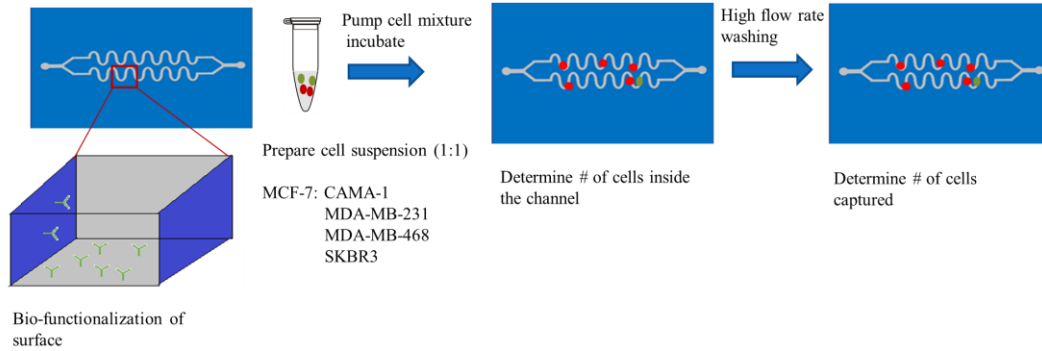


Figure 2:6 Schematic representation of EpCAM sensitive cell capture experiments

#### 2.5.2.4 Viable Cell Release

Release efficiency was calculated as the ratio of the number of captured cells in channel before to that of after enzymatic treatment.

Captured cells were released from the microfluidic channels by following the steps given below (Figure 2:7):

- Wash channel with one of the cell detachment buffers; Trypsin/EDTA, accutase or cell dissociation solution for 3 minutes at 500 mbar
- Incubate channel in cell detachment buffer for 3 minutes for release
- After incubation, wash channel with complete growth medium to inhibit the enzymatic activity for 6 minutes at 2000 mbar.
- Collect released cells from channel outlet and immediately transfer to a 96 well-plate for re-culture
- After 24 hours, gently aspirate the old medium and add fresh medium to the wells
- Take pictures of cells during the culture period to observe proliferation (Figure 2:8)

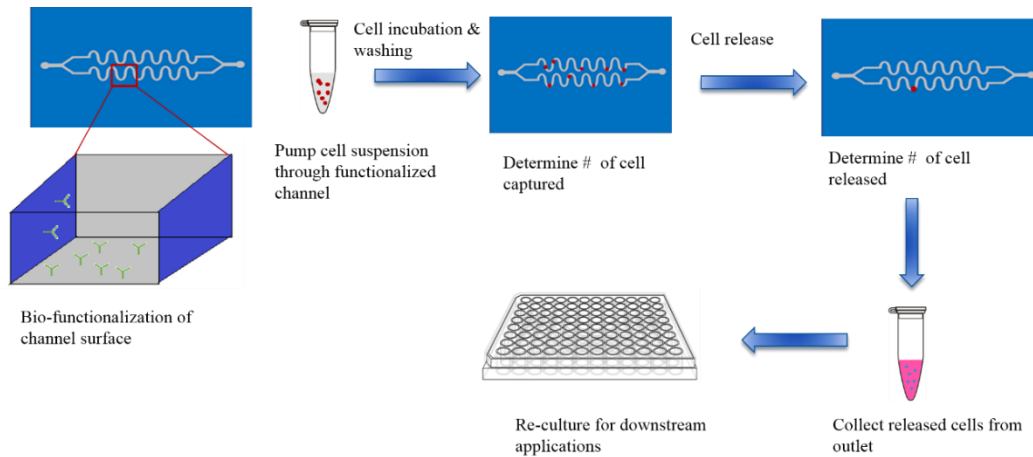


Figure 2:7 Schematic representation of viable cell release experiments

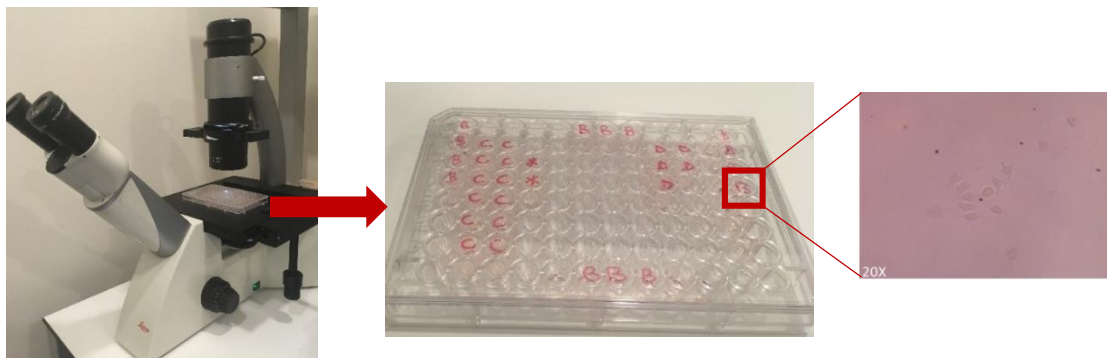


Figure 2:8 Re-culture of released cells and proliferation check

## 2.6 Statistical Analysis

All measurements were reported as the mean  $\pm$  the standard deviation. To examine the difference in cell capture efficiency obtained with different protocols, one-way analysis of variance (ANOVA) was used. Differences were considered to be significant when p value was  $< 0.05$ .

## CHAPTER 3

### RESULTS

#### 3.1 Characterization of Functionalized Surfaces

Surfaces prepared with P1-P4 were characterized by using contact angle measurement, spectroscopic ellipsometry and XPS after each step of functionalization.

Change in surface energy after each step of functionalization was determined with the contact angle measurements as shown in Figure 3:1. As can be seen from the figure, surfaces become more hydrophobic after the silanization where the contact angle increases from  $64.82^\circ \pm 0.61^\circ$  to  $82.17^\circ \pm 1.80^\circ$ . This is attributed to the fact that hydrophilic OH groups on the oxide surface is replaced by more hydrophobic amine groups [102]. Measured value is also in agreement with previously reported values for uniform silanization [102,103]. After glutaraldehyde treatment in P1 and P3, contact angle value was measured as  $62.39^\circ \pm 1.18^\circ$  indicating that surface becomes more hydrophilic, which has been confirmed by several other studies [102,104]. NHS-Biotin addition on the surface was found to decrease contact angle from  $82.17^\circ \pm 1.80^\circ$  to  $56.81^\circ \pm 1.20^\circ$  in P4, which is considered to be due to polar ureido-tetrahydrothiophene rings of biotin [105].

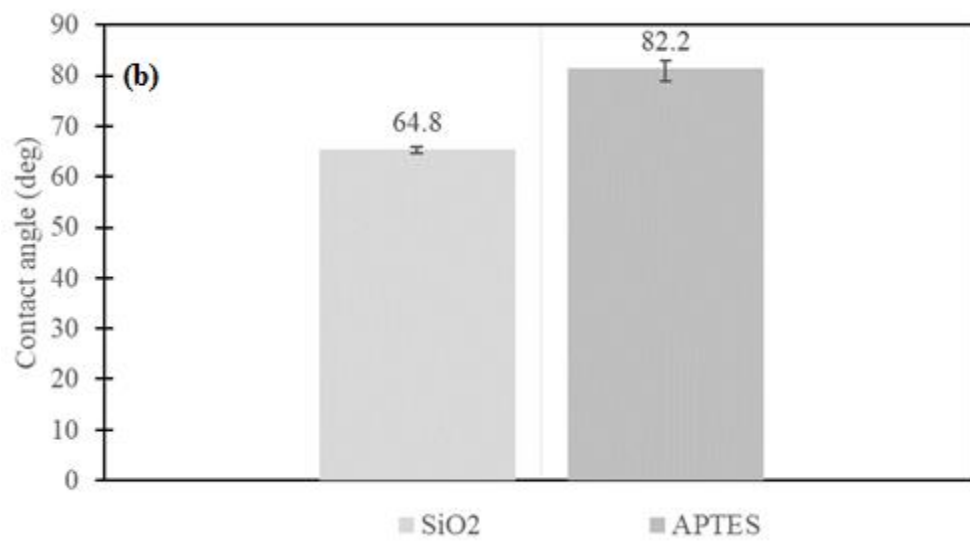
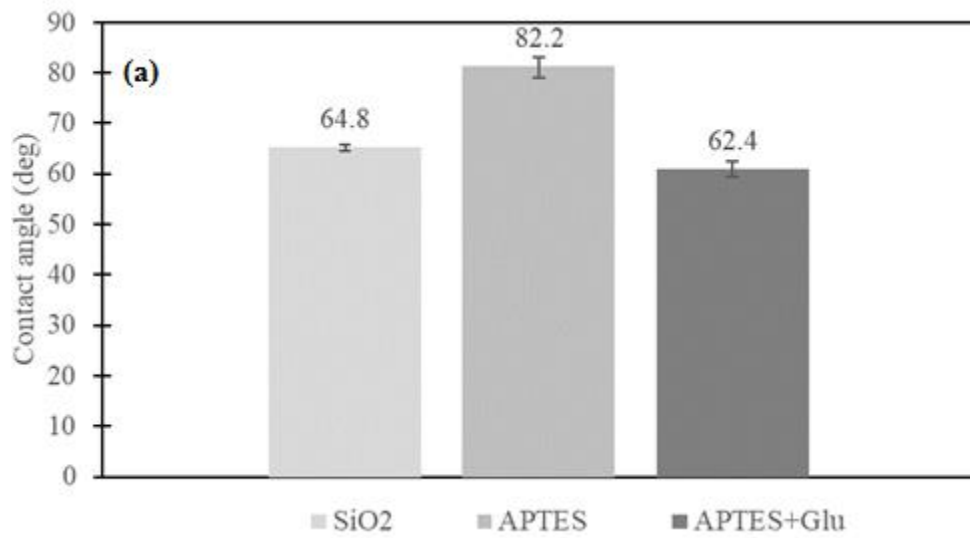


Figure 3:1 Contact angle measurements: (a) P1, (b) P2, (c) P3, (d) P4

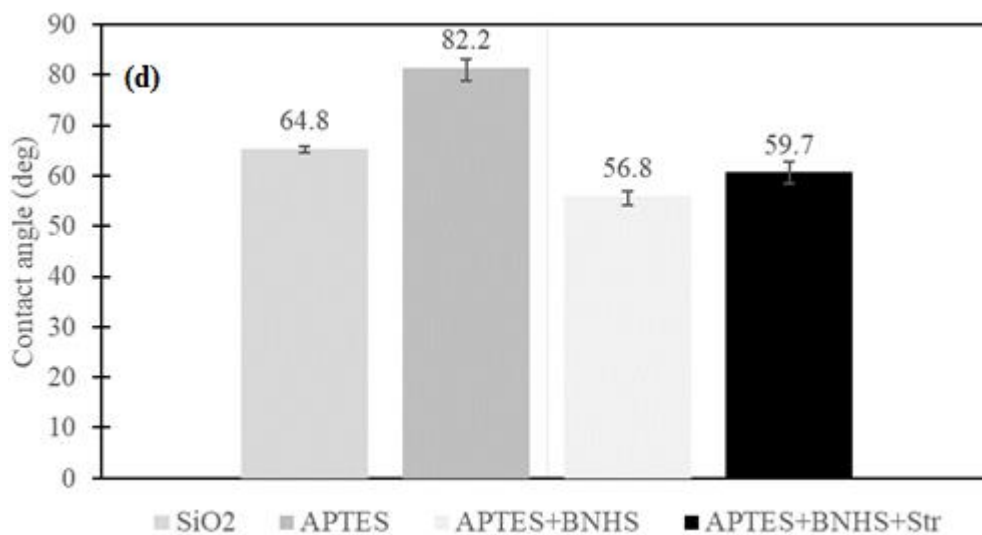
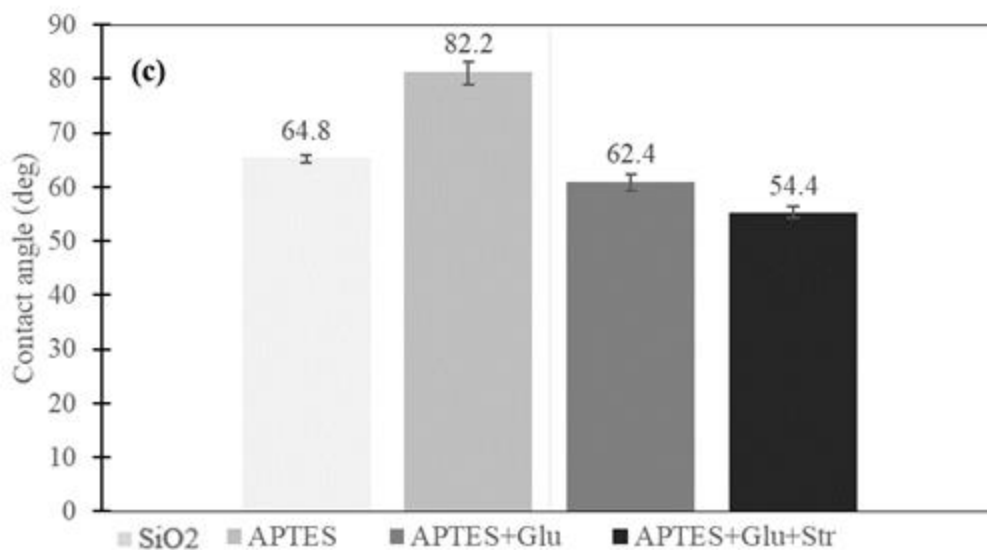


Figure 4:1 Contact angle measurements: (a) P1, (b) P2, (c) P3, (d) P4 (cont'd)

When streptavidin was immobilized on glutaraldehyde layer in P3, contact angle was further decreased as streptavidin increases the water solubility with its hydrophilic exterior. On the other hand, streptavidin addition on NHS-Biotin layer did not change surface wettability significantly.

Ellipsometric thicknesses of each layer during the surface functionalization were measured for all protocols and those measurements are illustrated in Figure 3:2. Increase in thickness after the silanization step was found to be  $3.81 \pm 0.21$  nm which corresponds to about 1.5 silane monolayers [102,106]. The thickness of the glutaraldehyde in P1 and P3 was measured as  $0.85 \pm 0.03$  nm similar to the measurements reported before [102]. Surface thickness with NHS-Biotin addition in P4 was  $0.68 \pm 0.11$  nm where the monolayer thickness is reported to be 1.10 nm [105]. When streptavidin was immobilized on glutaraldehyde layer in P3, thickness increased by  $1.16 \pm 0.07$  nm, while streptavidin addition on NHS-Biotin layer gave an increase of  $2.51 \pm 0.50$  nm in surface thickness. These values are similar to those reported in [105,107]. After surface functionalization was completed, antibodies were immobilized onto the surfaces and antibody layer thicknesses were measured as  $2.74 \pm 0.21$ ,  $3.27 \pm 0.04$ ,  $2.37 \pm 0.03$  and  $2.74 \pm 0.21$  nm for P1-P4 respectively. Gradual thickness increase at each step suggests that surfaces were modified with the molecule of interest at each step successfully.

Change in the atomic composition of surfaces after each successive functionalization step was determined by XPS analysis. Survey scans (Fig. S1-9 in Supporting information) revealed that N1s nitrogen peak near 400 eV and C1 carbon peak near 287 eV become noticeable after APTES treatment, which indicates successful silanization. Furthermore, intensity of N1s peak increased with biotin/streptavidin addition and reached its highest value with antibody immobilization. This is considered to be due to the presence of amide/peptide linkages in the proteins. It was also seen that Si2p intensity decreases steadily after each successive step of immobilization. Atomic composition analysis of the surfaces (Table 3:1) shows that silica content of the surface decreases at each successive step while the nitrogen content increases after protein immobilization indicating that surfaces were modified with the molecule of interest at each step successfully.

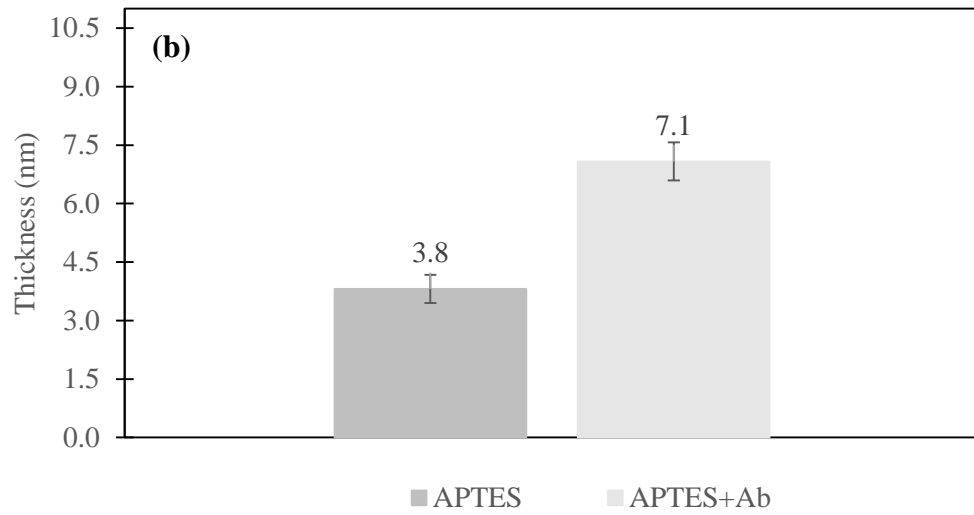
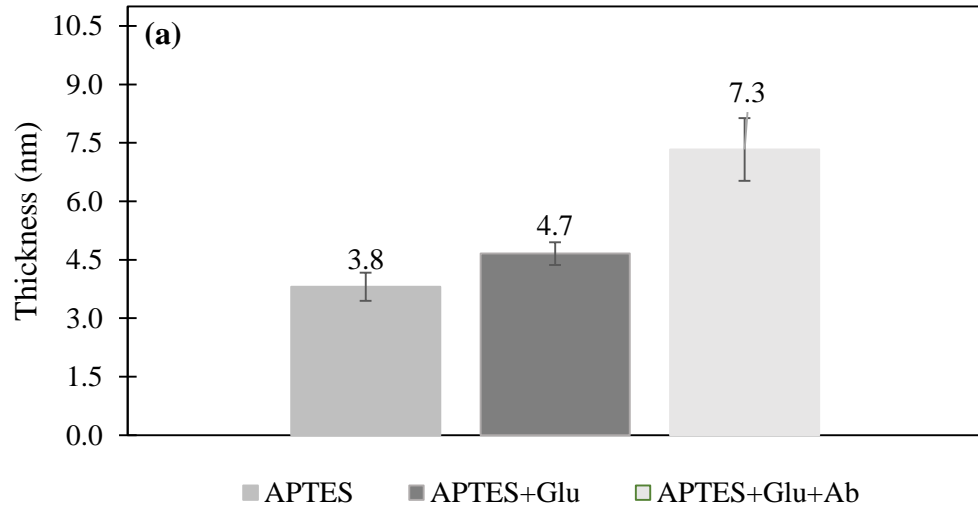


Figure 3:2 Ellipsometric film thickness of each layer: (a) P1, (b) P2, (c) P3, (d) P4

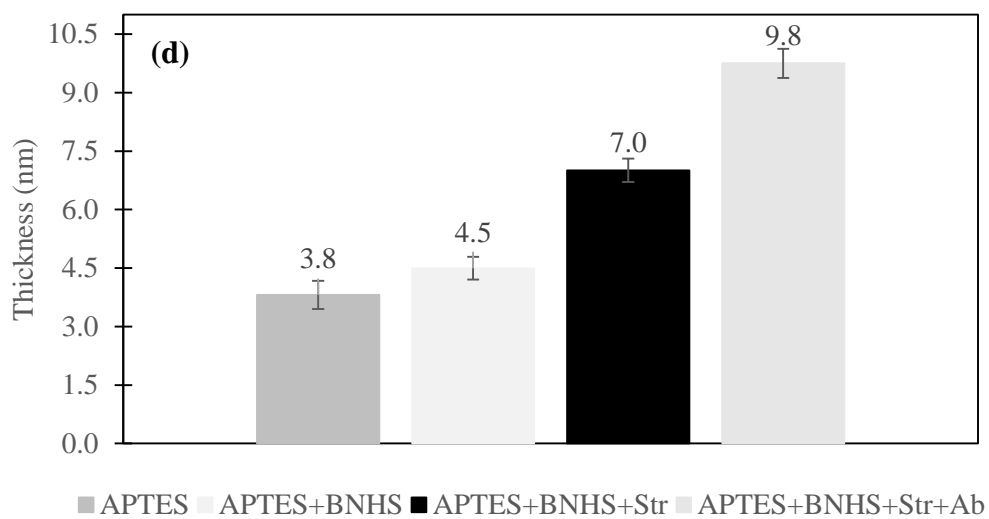
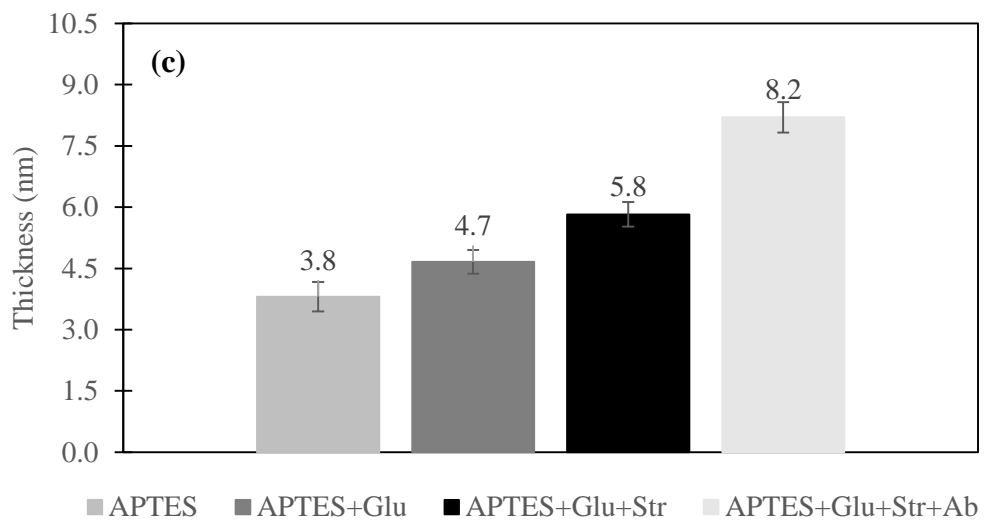


Figure 3:2 Ellipsometric film thickness of each layer: (a) P1, (b) P2, (c) P3, (d) P4  
(cont'd)

Table 3:1 Atomic compositions of the surfaces modified with P1-4 at each step of functionalization.

<b>P1 &amp; P2</b>	<b>Atomic %</b>	<b>APTES</b>	<b>APTES+Glu</b>	<b>APTES+Glu+Ab</b>	<b>APTES+EDC/NHS/Ab</b>
	<b>Si 2p</b>	23.2	21.6	18.4	16.6
	<b>C 1s</b>	39.3	41.9	42.8	43.6
	<b>N 1s</b>	2.5	1.9	6.7	8.5
	<b>O1s</b>	35.1	34.6	32.1	31.4

<b>P3</b>	<b>Atomic %</b>	<b>APTES</b>	<b>APTES+Glu</b>	<b>APTES+Glu+Str</b>	<b>APTES+Glu+Str+Ab</b>
	<b>Si 2p</b>	23.2	21.6	17.0	14.3
	<b>C 1s</b>	39.3	41.9	50.3	50.2
	<b>N 1s</b>	2.5	1.9	4.3	8.8
	<b>O1s</b>	35.1	34.6	28.5	26.8

<b>P4</b>	<b>Atomic %</b>	<b>APTES</b>	<b>APTES+BNHS</b>	<b>APTES+BNHS+Str</b>	<b>APTES+BNHS+Str+Ab</b>
	<b>Si 2p</b>	23.2	23.7	16.9	18.5
	<b>C 1s</b>	39.3	35.1	43.2	37.9
	<b>N 1s</b>	2.5	3.4	8.7	9.4
	<b>O1s</b>	35.1	37.8	31.2	34.4

### 3.2 Comparison of Antibody Immobilization Protocols on Plain Surfaces

Confirming the success of surface functionalization for each protocol via contact angle, spectroscopic ellipsometry and XPS measurements, cell capture efficiencies of the antibody immobilized surfaces were tested. Representative images from one of the experiments after the washing step are presented in Figure 3:3 and number of cells captured on the functionalized surfaces are given for P1-P4 in Figure 3:4. These numbers are the mean values obtained from the experiments repeated three times and derived from

60 images for each protocol. As can be seen from Figure 5, cell capture efficiency of P1 was significantly lower ( $p < 0.0001$ ) than those of P2-4.

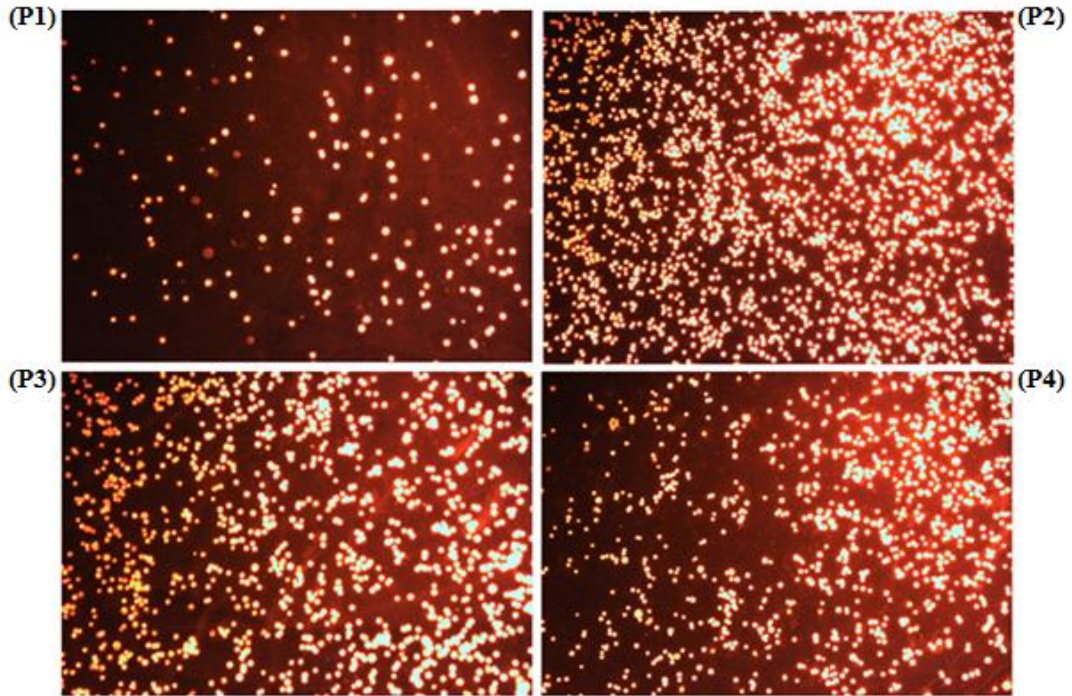


Figure 3:3 Fluorescence microscopy images of surfaces (5x) incubated in MCF-7 cell solution.

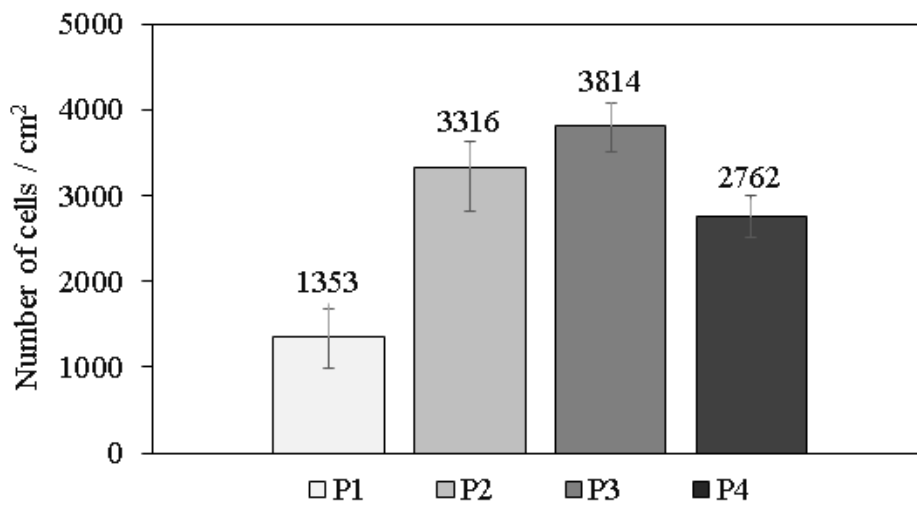


Figure 3:4 Number of cells captured on the surfaces functionalized with protocols P1-P4

This poor performance of P1 modified surfaces may be attributed to decrease in density and/or accessibility of active sites with random antibody immobilization. However, P2 gives a much higher cell capture efficiency despite involving random antibody immobilization. This efficiency difference between P1 and P2 is considered to be due to the hetero-bifunctional immobilization of the amino or carboxyl groups on antibodies. Antibody immobilization via amino groups can decrease the antigen detection due to the fact that amino groups are available at different sites of the antibody including the vicinity of antigen binding site, which leads to improper orientation. On the other hand, antibody immobilization via carboxyl groups provides favorable orientation as carboxyl groups are away from their antigen binding site [108]. Considering the fact that glutaraldehyde utilized in P1 reacts with the amino groups of antibodies [109,110] while EDC-NHS used in P2 first activates the carboxyl groups on the antibody which further reacts with the amine groups on the surface [111], it is seen that P2 yields significantly higher numbers of active sites on the surface as antibodies are immobilized from the regions away from their antigen binding sites. Furthermore, glutaraldehyde is known to form multiprotein complexes on the surface which may also hinder the antibody activity [40].

Cell capture efficiency of P3 and P4 were found be much higher than that of P1, which was expected as bioaffinity immobilization offers a high density of well-oriented antibodies on the surface spontaneously. Nevertheless, there was a significant difference ( $p < 0.0001$ ) between P3 and P4 as can also be seen from Figure 3:4. In both P3 and P4, streptavidin layer was used for bio affinity immobilization of antibodies where streptavidin was attached onto glutaraldehyde layer in P3 while P4 utilized NHS-biotin layer for streptavidin binding. As the chemistry of streptavidin–antibody binding is the same for both protocols, difference in cell capture efficiencies are considered to be due the difference between number densities of streptavidin molecules on the surfaces obtained with P3 and P4, which is directly related to number of linker molecules. Therefore, surface coverage of NHS-biotin molecules is speculated to be less than that of glutaraldehyde molecules within the experimental conditions presented. Besides, the number of theoretical binding sites of streptavidin is four, there are several studies demonstrate otherwise [112,113]. In fact, the available binding sites of streptavidin is changing between 0-4 [113,114]. In protocol P4 at least one binding sites of streptavidin

is occupied by NHS-Biotin molecule thus, there may no active sites left for antibody immobilization on the surface by utilizing streptavidin-biotin interaction.

Selectivity of functionalized surfaces with protocols P1-P4 is investigated by using non-target CCRF-CEM cells as described in Section 2.5.1. Representative images from the experiments after the washing step are presented in Figure 3:5. As can be seen from the figure, CCRF-CEM cells, which do not express EpCAM, cannot bind to the surface. Therefore, it is concluded that all protocols presented in this study are specific to CTCs with EpCAM expression, hence, does not suffer from selectivity losses in immunoaffinity based CTC isolation applications.

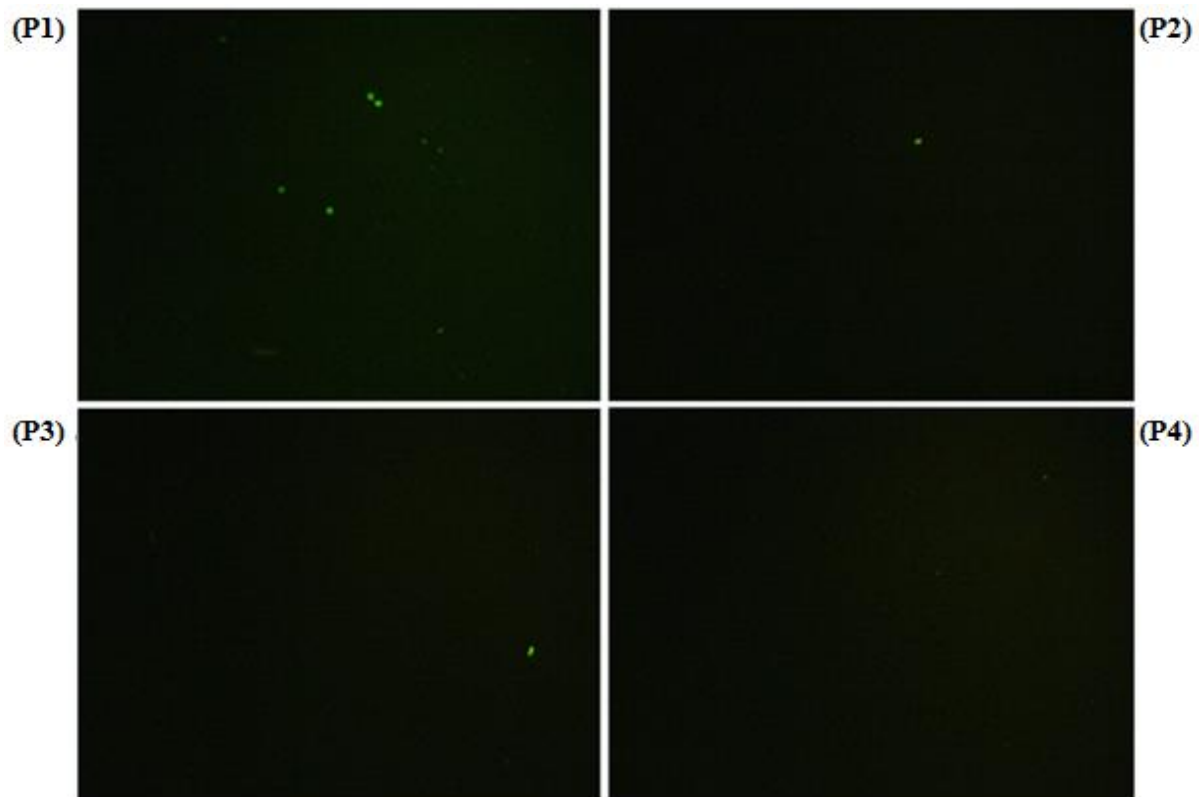


Figure 3:5 Fluorescent microscopy images of surfaces (5x) incubated in CCRF-CEM cell solution

Table 3.2 demonstrates cost and time spend for functionalization of 1 cm<sup>2</sup> oxide surface with 4 different coating strategy. It was observed that, P2 is the most cost and time effective protocol amongst others.

Table 3:2 Comparison of protocols with respect to cost and modification time

<b>Protocol</b>	<b>Chemicals used</b>	<b>Approximate cost per cm<sup>2</sup> (EUR)</b>	<b>Time spent for modification (minutes)</b>
<b>P1</b>	APTES GA Anti EpCAM (FITC) BSA	26.62	225
<b>P2</b>	APTES EDC NHS Anti EpCAM (FITC) BSA	27.14	105
<b>P3</b>	APTES GA Streptavidin Anti EpCAM (Biotin) BSA	31.18	285
<b>P4</b>	APTES NHS Biotin Streptavidin Anti EpCAM (Biotin) BSA	34.16	225

Following tables summarizes the comparison of all coating protocols in terms of cell capture efficiency, selectivity, cost of chemicals and coating time.

Table 3:3 Summary of protocol comparison

	<b>Efficiency</b>	<b>Selectivity</b>	<b>Cost</b>	<b>Time</b>
<b>P1</b>	+	++	+	++
<b>P2</b>	+++	+++	+	+
<b>P3</b>	+++	+++	++	+++
<b>P4</b>	++	+++	++	++
<b>+ Low; ++ High; +++ Very High</b>				

### 3.3 Cell Capture Efficiency in Microfluidic Channels

To determine the cell capture efficiency, MCF-7 cells were fed into the P2-functionalized microfluidic channel and incubated for 30 minutes to ensure sufficient cell-surface interaction. It should be noted that cell concentration was adjusted such that this interaction is held for each cell. Number of cells remained in the channel after a high flow rate washing step was counted and compared with that of before washing, to determine the cell capture efficiency. Example fluorescent microscopy images of cells inside the channel before and after washing step are shown in Figure 3:6. Similar capture efficiencies were obtained from eight different trials, with an average of 89.6%, which shows that the protocol (P2) can successfully be implemented in microfluidic channels (Table 3:4). It should be noted that in cell capture efficiency determination experiments, cell concentration was arranged such that maximum capture capacity of the channel was not reached; in other words, the cell concentration was not a limiting factor.

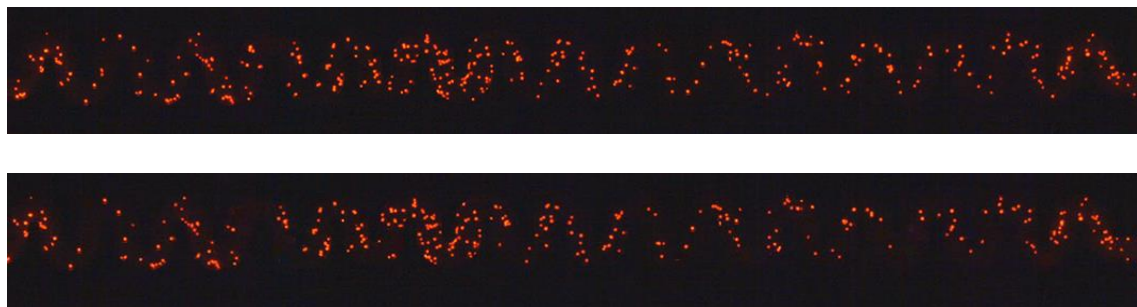


Figure 3:6 Images of whole channels showing the cells before (top) and after (bottom) high flow rate washing (5x)

Table 3:4 Cell Capture Efficiency Determination

	<i>Trial 1</i>	<i>Trial 2</i>	<i>Trial 3</i>	<i>Trial 4</i>
# of CTC before wash	64	188	190	64
# of CTC after wash	52	177	166	52
Capture efficiency (%)	<b>81</b>	<b>94</b>	<b>87</b>	<b>93</b>

	<i>Trial 5</i>	<i>Trial 6</i>	<i>Trial 7</i>	<i>Trial 8</i>
# of CTC before wash	107	111	210	415
# of CTC after wash	100	107	190	398
Capture efficiency (%)	<b>96</b>	<b>81</b>	<b>90</b>	<b>95</b>

### 3.4 Cell Capture Specificity in Microfluidic Channels

Selective CTC capture of P2 was demonstrated using breast cancer cells (MCF-7) spiked in buffer containing background leukocytes with a ratio of 1:10<sup>4</sup>. White blood cells and MCF-7 cells were pre-stained with fluorescein diacetate and cell tracker red fluorescence dye, respectively, and fed to the functionalized microchannel. Cells were incubated in the channel for 30 minutes to ensure target cell surface interaction. Numbers of WBCs and CTCs remained in the channel after the high flow rate washing step were counted and compared with those of before washing, to determine the cell capture specificity. It was seen that 90% (n=2) of MCF-7 cells were recovered while only 13% (n=2) of WBCs were nonspecifically captured in the channel (Table 3:5). The capture efficiency obtained here is found to be consistent with the ones determined by MCF-7-only samples. This comparison show that CTC capture efficiency is not affected by excess number of non-target background cells.

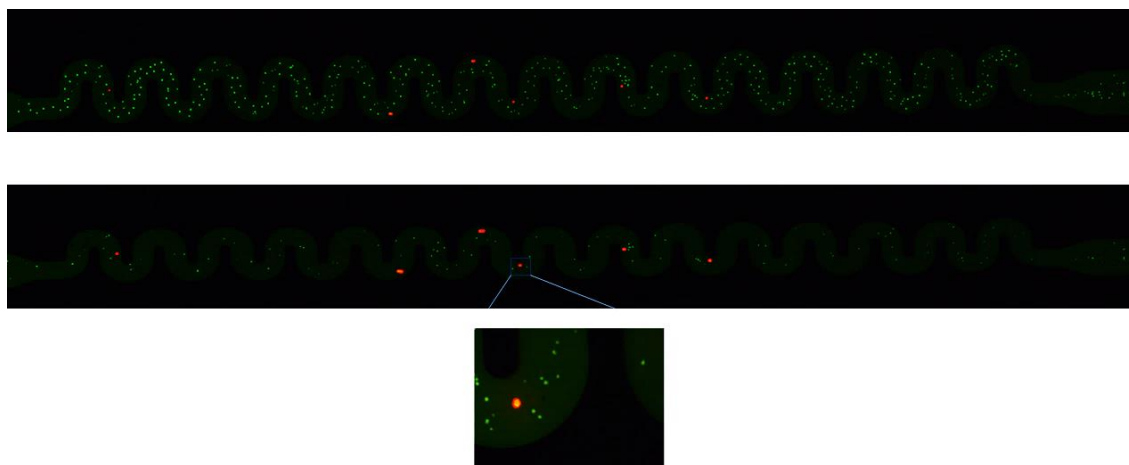


Figure 3:7 (a) WBC: CTC mixture in channel before (top) and after washing (bottom) step (5x), (b) CTC:WBC in channel (20x)

Table 3:5 Selective Cell Capture from Blood

	<i>Trial 1</i>		<i>Trial 2</i>	
	<b>MCF-7</b>	<b>WBCs</b>	<b>MCF-7</b>	<b>WBCs</b>
# of cells before wash	8	480	11	520
# of cells after wash	8	73	9	59

For on-chip detection of captured cells, another CTC: WBC cell suspension with a ratio of 1:100 was prepared and fed to the functionalized channel. After incubation and high flow rate washing, remaining cells were stained with immunofluorescence conjugated anti-pan cytokeratin antibody for epithelial cells and anti-CD45 antibody for hematologic cells and by DAPI for nuclear staining. panCK<sup>+</sup> and DAPI<sup>+</sup> cells were scored as CTCs, whereas CD45<sup>+</sup> and DAPI<sup>+</sup> cells were scored as leukocytes. Representative images of stained leukocytes and MCF-7 cells before washing step are demonstrated in Figure 3:8.

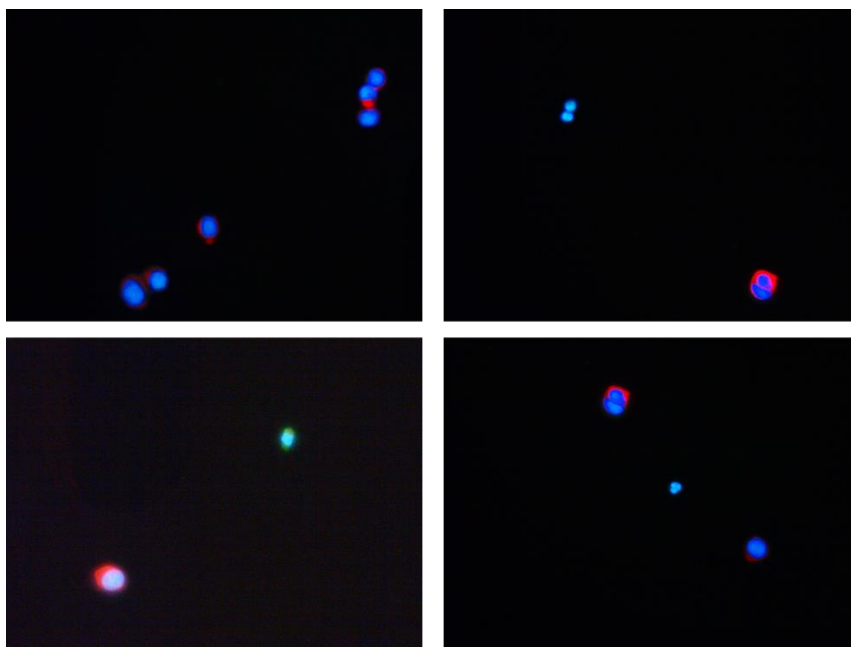


Figure 3:8 Fluorescent microscopy images of stained MCF-7 and leukocytes (40x)

### 3.5 Cell Capture Sensitivity

Up to this section, experiments were performed with MCF-7 cells, which is known to have high EpCAM expression. Nevertheless, in clinical samples, expression of EpCAM varies significantly, which is the main concern when affinity based isolation methods are used. Five different breast cancer cell lines with varying EpCAM expression levels, namely MDA-MB-231, MDA-MB-468, SKBR3, MCF-7 and CAMA-1 (Figure 3:9), were used to investigate the significance of EpCAM expression in cell capture. Expression levels for each cell line were measured with flow cytometry and measurements of both an unstained control and PE conjugated EpCAM were presented in Figure 3:10. The fluorescence intensity of unstained control was measured first and this value was used to determine a threshold of EpCAM expression for the cell line being measured. EpCAM tagged cells were analyzed and cells having fluorescent intensity above the threshold value were considered as EpCAM positive. As can be seen from the Figure 3:10, EpCAM is homogeneously expressed within the population in all cell lines.

Since binding efficiencies were normalized with respect to MCF-7 cells, EpCAM expression levels were plotted by taking MCF-7 cells as a reference. It was seen from the Figure 3:11 that expression levels of SKBR-3, CAMA-1 and MDA-MB-468 were high and quite similar to that of MCF-7 while MDA-MB-231 cells showed a low EpCAM expression.

The binding efficiencies of cell lines were investigated by standard cell capture experiments (Section 2.5.2). For each experiment, MCF-7 cells were fed together with the cell line being analyzed and binding efficiency was normalized with respect to that of MCF-7 cells, to eliminate any other factors that may affect binding efficiency such as differences occurred during the coating step. As can be seen in Figure 3:12, binding efficiency decreased with decreasing EpCAM expression and cells with similar surface protein expressions have similar binding efficiency.

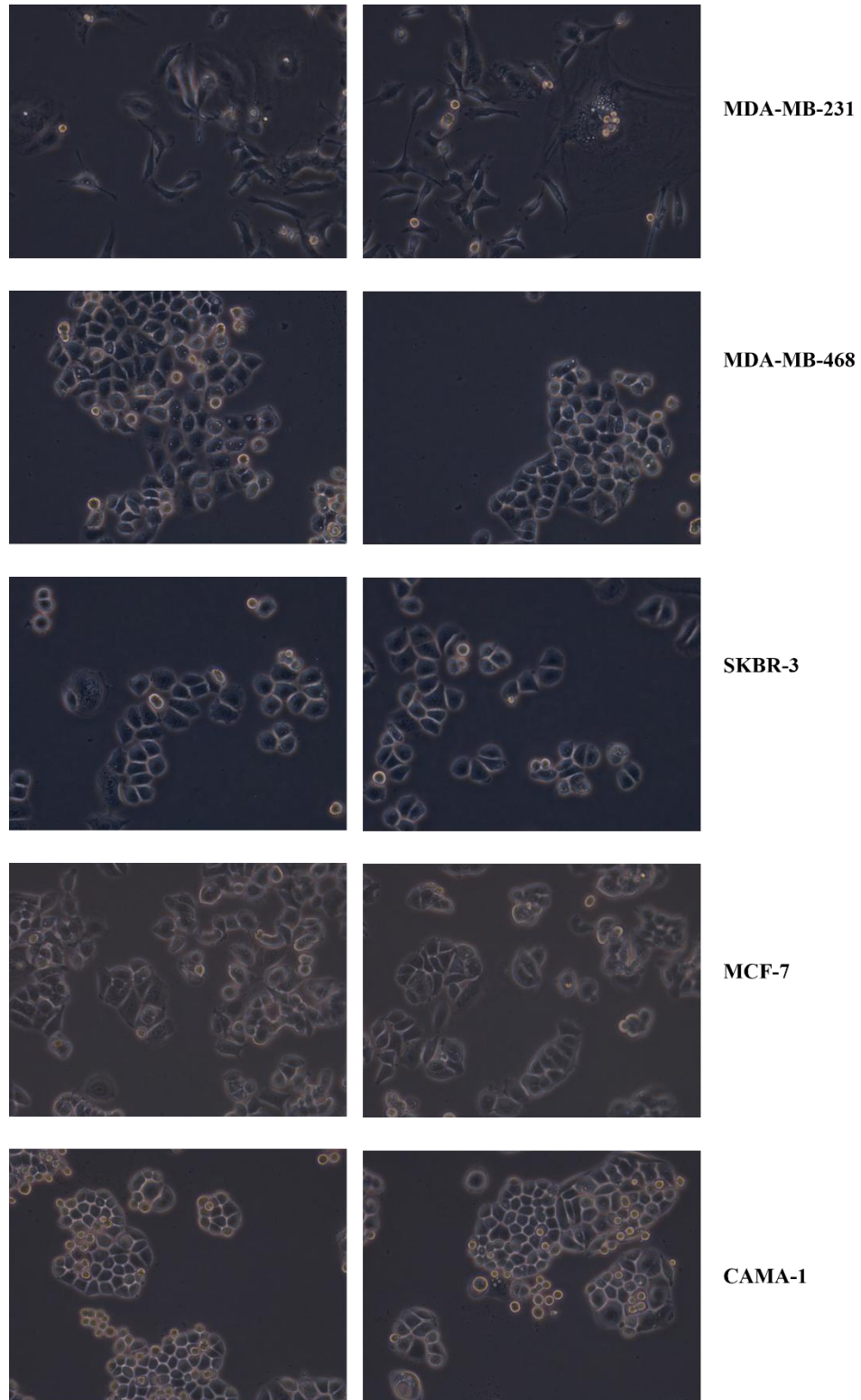


Figure 3:9 Morphology of breast cancer cell lines (20x)

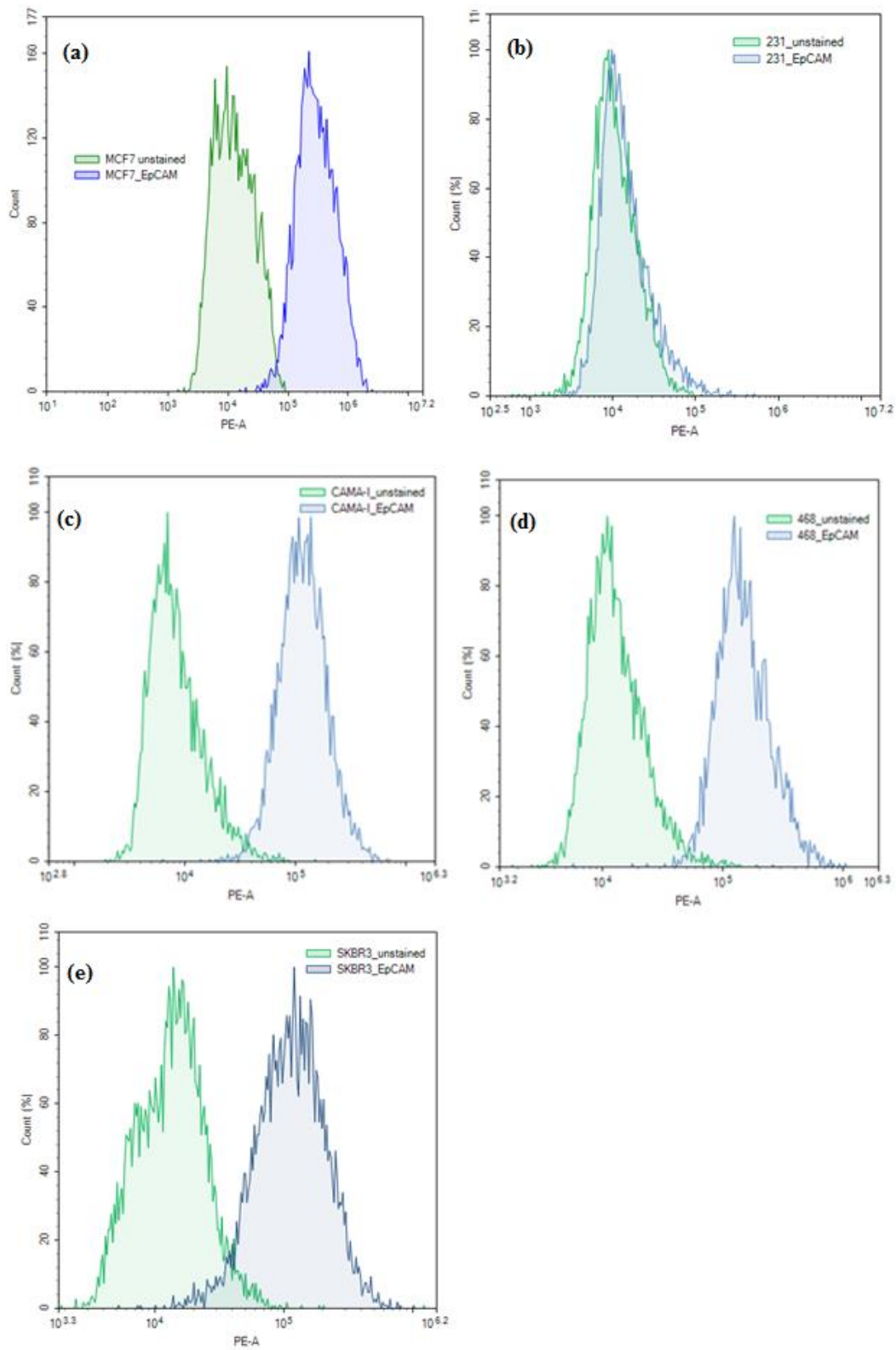


Figure 3:10 Flow cytometry measurements of unstained control and EpCAM (PE) for (a) MCF-7, (b) MDA-MB-231, (c) CAMA-1, (d) MDA-MB-468, (e) SKBR-3

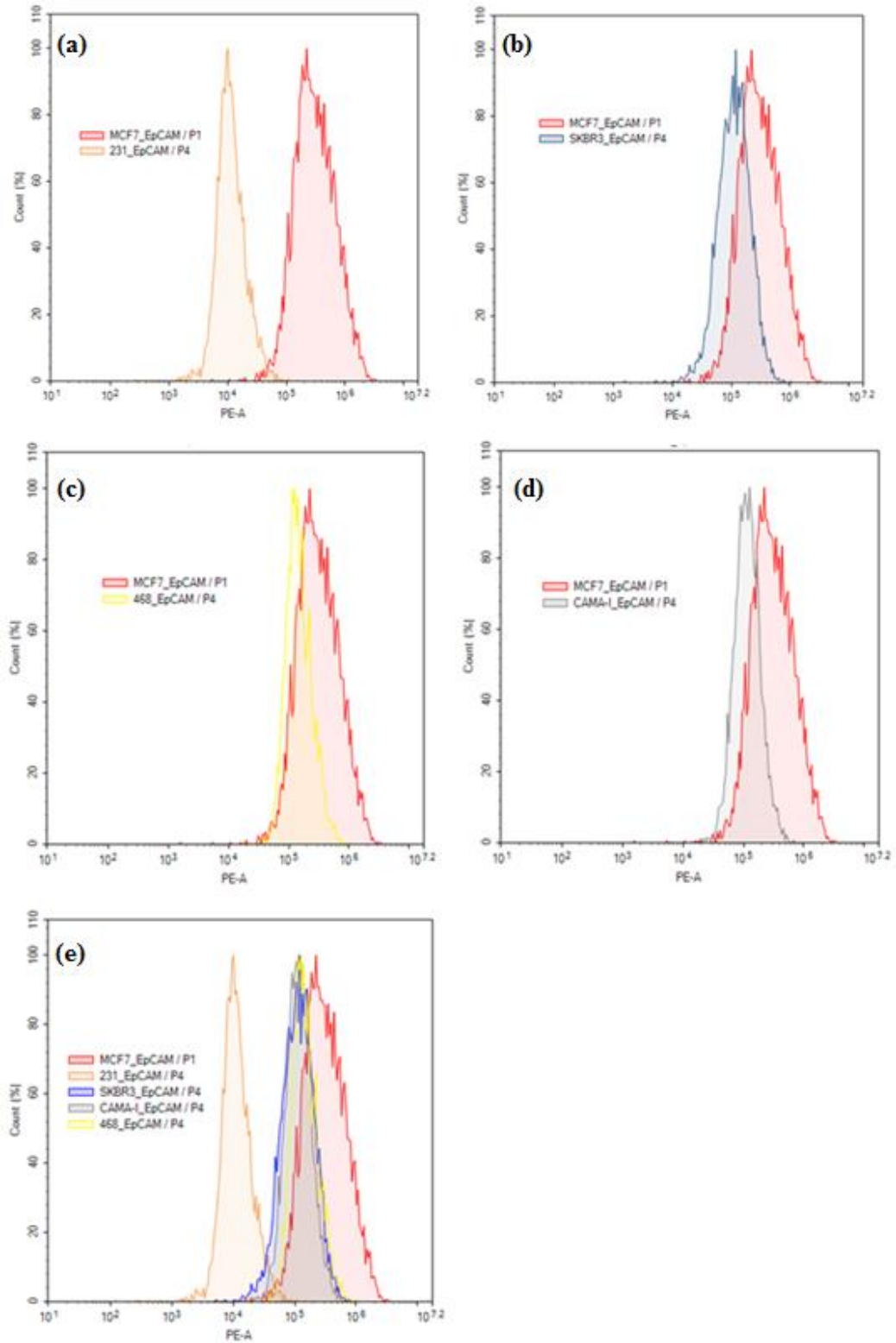


Figure 3:11 EpCAM expression of cell lines compared with MCF-7 (a) MDA-MB-231, (b) SKBR-3, (c) MDA-MB-468, (d) CAMA-1, (e) all cell lines

Table 3:6 Binding efficiency of CAMA-1 cells

<b>CAMA-1: MCF-7</b>				
	<i>Trial 1</i>		<i>Trial 2</i>	
	<b>CAMA-1</b>	<b>MCF-7</b>	<b>CAMA-1</b>	<b>MCF-7</b>
<b># of CTC before wash</b>	110	92	84	92
<b># of CTC after wash</b>	90	87	74	88
<b>Binding efficiency (%)</b>	82	95	88	96
<b>Normalized Efficiency (%)</b>	89%			

Table 3:7 Binding efficiency of MDA-MB-231 cells

<b>MDA-MB-231: MCF-7</b>				
	<i>Trial 1</i>		<i>Trial 2</i>	
	<b>MDA-MB-231</b>	<b>MCF-7</b>	<b>MDA-MB-231</b>	<b>MCF-7</b>
<b># of CTC before wash</b>	112	93	85	80
<b># of CTC after wash</b>	36	87	19	76
<b>Binding efficiency (%)</b>	32	94	22	95
<b>Normalized Efficiency (%)</b>	29%			

Table 3:8 Binding efficiency of MDA-MB-468 cells

<b>MDA-MB-468: MCF-7</b>				
	<i>Trial 1</i>		<i>Trial 2</i>	
	<b>MDA-MB-468</b>	<b>MCF-7</b>	<b>MDA-MB-468</b>	<b>MCF-7</b>
<b># of CTC before wash</b>	128	96	111	100
<b># of CTC after wash</b>	106	84	96	82
<b>Binding efficiency (%)</b>	83	88	87	82
<b>Normalized Efficiency (%)</b>	96%			

Table 3:9 Binding efficiency of SKBR-3 cells

<b>SKBR-3: MCF-7</b>				
	<i>Trial 1</i>		<i>Trial 2</i>	
	<b>SKBR-3</b>	<b>MCF-7</b>	<b>SKBR-3</b>	<b>MCF-7</b>
<b># of CTC before wash</b>	136	140	210	224
<b># of CTC after wash</b>	125	136	195	216
<b>Binding efficiency (%)</b>	92	97	93	96
<b>Normalized Efficiency (%)</b>	95%			

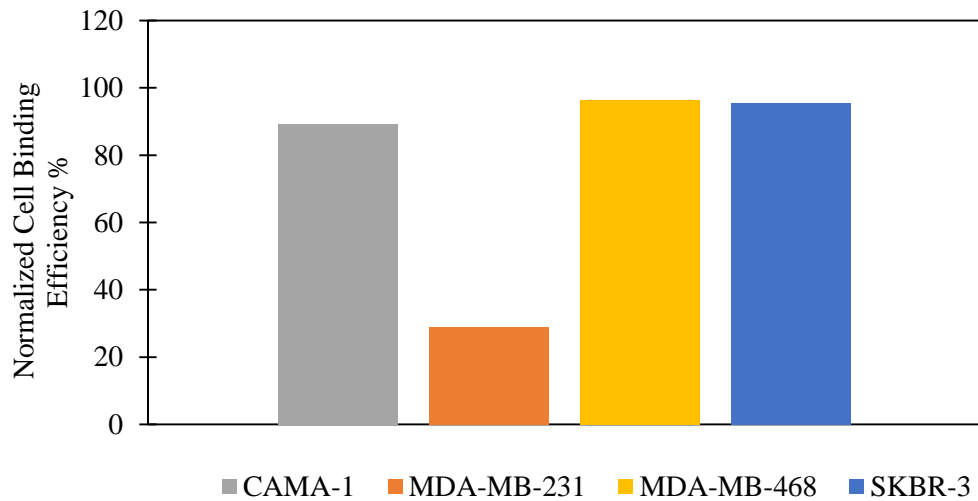


Figure 3:12 Normalized binding efficiencies of cell lines

Capture experiments performed with breast cancer cell lines with different EpCAM expression levels are the positive control of the hypothesis proposed in this study and prove that cell capture is proportional to the number of cell surface antigen that targeted by the antibodies on the surface. As a negative control, a microchannel was modified with P2, but no anti-EpCAM antibody was added to EDC/NHS activation solution. Bovine serum albumin solution was used to decrease non-specific binding of the cells. It was seen

that, number of MCF-7 cells in the channel before washing step was 403 while only 34 cells were remained in the channel. Non-specific binding of MCF-7 cells on the antibody free surfaces is found as 8 %, meaning that cells do not bind to surface when there is no antibody on it.

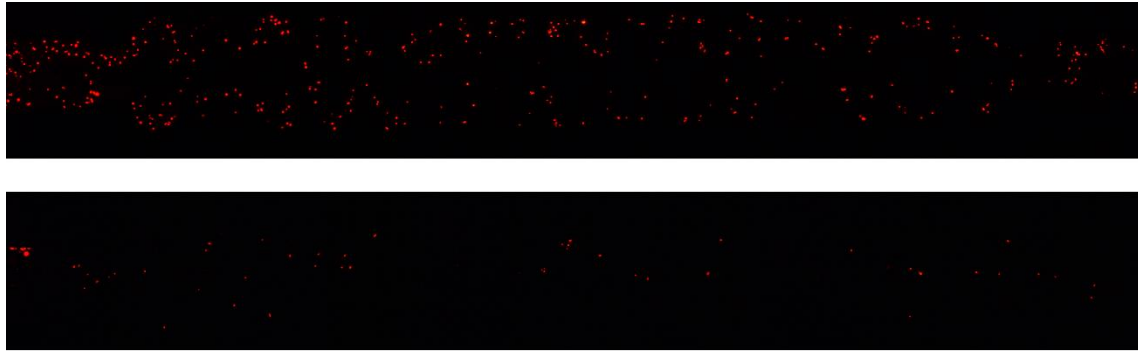


Figure 3:13 Fluorescence images of MCF-7 cells inside antibody-free microchannel before (top) and after (bottom) washing step (5x)

### 3.6 Viable Cell Release

In this section, cell release efficiency of the enzymatic treatment (described in Section 2.5.2.4) and viability of the released cells are demonstrated. Trypsinization was used to detach captured cells from the surface. Number of cells inside the channel were counted from the fluorescent microscopy images taken before and after the enzymatic treatment. Figure 3:14 illustrates an example of CTCs captured in the channel and the remaining cells after the enzymatic treatment.

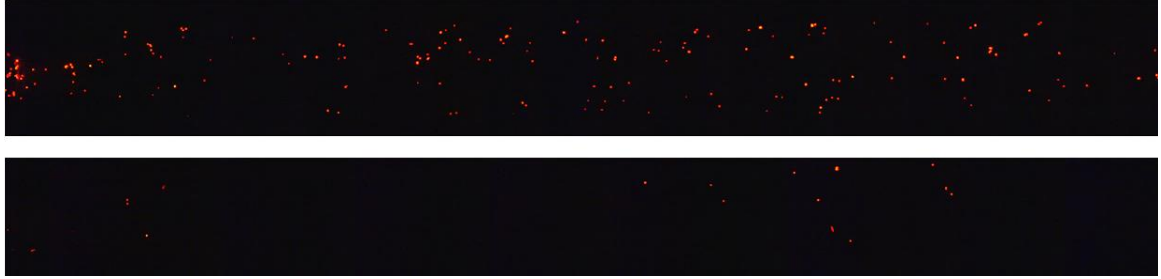


Figure 3:14 Fluorescence images of CTCs captured (top) and released (bottom) (5x)

Cell release efficiency was calculated by using:

$$\text{Efficiency (\%)} = \frac{\# \text{ of cells before treatment} - \# \text{ of cells after treatment}}{\# \text{ of cells after treatment}} \times 100$$

Calculated efficiencies for 5 different trials are tabulated in Table 3:10. As can be seen from the table, cell release efficiency changes between 89-92 % with an average efficiency of 90%, showing the success and repeatability of the applied method.

Table 3:10 Cell Release Efficiency

	<b>Trial 1</b>	<b>Trial 2</b>	<b>Trial 3</b>	<b>Trial 4</b>	<b>Trial 5</b>
<b># of CTC before wash</b>	64	188	427	210	415
<b># of CTC after wash</b>	58	177	329	190	398
<b># of CTC after release</b>	6	14	19	20	30
<b>Release efficiency (%)</b>	<b>90</b>	<b>92</b>	<b>88</b>	<b>89</b>	<b>92</b>

In order to determine the viability of the released cells, cells from the channel outlet were collected in a vial, containing cell growth media, and re-cultured to observe proliferation ability. Figure 3:15 and Figure 3:16 demonstrate microscopic images of the re-cultured cells, taken in Day 1-8. It was observed that released cells can adhere and proliferate on the culture plate by day 4 and form clusters and colonies by day 8. The morphologies were the same as intact control cells, although it took a little longer to reach confluence (proportion of the culture dish covered by the cells).

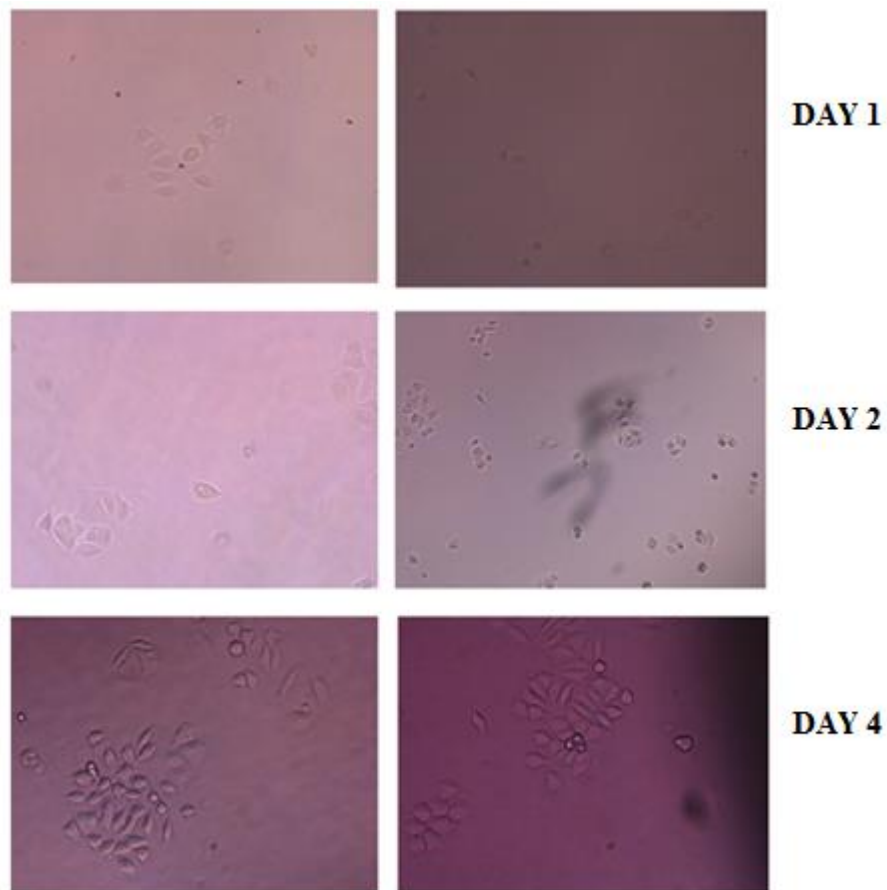


Figure 3:15 Observation of re-cultured cells (Day 1-4)

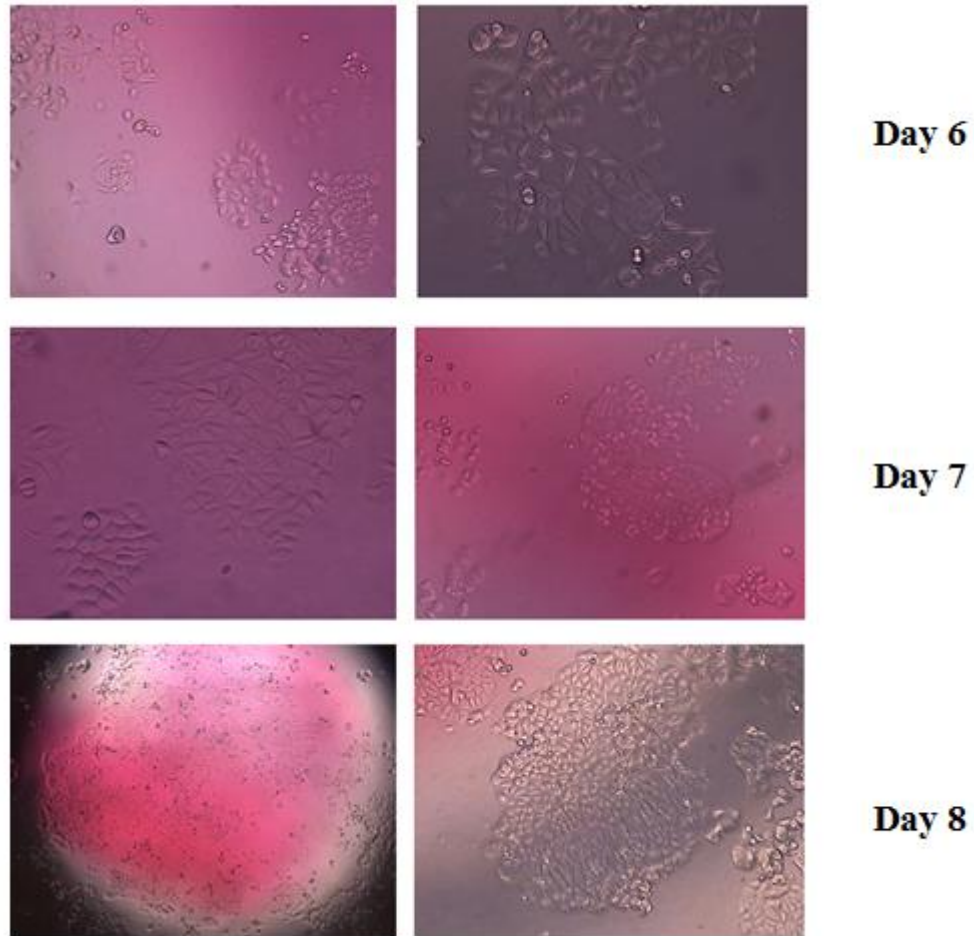


Figure 3:16 Observation of re-cultured cells (Day 6-8)

### 3.7 Shelf-Life of Bio-functionalized Surfaces

Optimized storage conditions that extend the shelf-life of bio-functionalized surfaces is needed to preserve multi-layer bio-functionalization, antibody activity and conformation. Considering the fact that complete functionalization process of one microchannel took 4 to 7 hours depending on the strategy chosen, effect of shelf-life on the functionality of the surface must be investigated as bio-functionalized channels have to be prepared in large quantities for a large set of controlled experiments. To fulfill this objective, six microchannels were functionalized with Protocol 2 and two of them were immediately

tested with respect to cell capture efficiency. The rest were kept in MES solution (50 mM pH: 6.4) at 4°C and were tested weekly. It was seen from the Table 3:11 that after two-weeks, there is a 50 % decrease in cell capture efficiency. Although one-week storage is enough for the present study, storage conditions should be optimized to extend this period. One solution could be changing the buffer solution [115] and/or adding some preservative chemicals like trehalose [116].

Table 3:11 Shelf-Life Determination

	Day 0		Day 7		Day 14	
	<i>Trial 1</i>	<i>Trial 2</i>	<i>Trial 3</i>	<i>Trial 4</i>	<i>Trial 5</i>	<i>Trial 6</i>
# of CTC before wash	107	111	254	212	72	50
# of CTC after wash	100	107	230	188	38	27
Capture efficiency (%)	<b>93</b>	<b>96</b>	<b>90</b>	<b>88</b>	<b>52</b>	<b>54</b>

## CHAPTER 4

### CONCLUSIONS

In this study, development and evaluation of four different surface modification approaches for anti-EpCAM immobilization on silicon oxide surfaces were presented and the selected modification method was successfully implemented in microfluidic channels.

The outcomes of the accomplished tasks can be summarized as follows:

- Physical and chemical characterization of bio-functionalized surfaces demonstrate that successful surface coverage was obtained at each step of functionalization.
- All methods provide very high selectivity for CTCs with EpCAM expression. Cell capture efficiency comparisons, on the other hand, reveal that bio-affinity based antibody immobilization involving streptavidin attachment with Glu linker (P3) gives the highest performance. Antibody immobilization via their carboxyl groups with EDC-NHS coupling reaction (P2) also gives a very high cell capture efficiency. However, considering the simplicity, time and cost efficiency of this covalent bonding method and its high cell capture efficiency, P2 appears to be the most feasible antibody immobilization method for efficient CTC capture.
- P2 was successfully implemented in microchannels, where the average cell capture efficiency was determined as 89.6% from eight different trials.

- Selective CTC capture of P2 modified microchannel was demonstrated using MCF-7 spiked lysed blood with a ratio of 1:10<sup>4</sup>. It was seen that non-specific capture is 13% and excess number of background cells does not affect the cell capture efficiency.
- Viable cell release from P2 modified microchannels was achieved with 90% efficiency and viability of released cells confirmed with 8-day cell culture, where the re-cultured cells formed clusters and proliferated.
- Five different breast cancer cell lines with different EpCAM expression levels, namely MDA-MB-231, MDA-MB-468, SKBR3, MCF-7 and CAMA-1, were used to investigate the significance of EpCAM expression level in cell capture. Results showed that binding efficiency of cells is proportional to EpCAM expression level on the cell surface.
- Finally, shelf-life of functionalized microchannels was found to be one-week under the proposed storage conditions.

Related future work and comments can be listed as:

- Microchannels utilized in this study was not specifically designed for rare cell isolation. Notably, the current design did not allow with-flow capture of cells from the mixture. In micro domain, flow is laminar and cells follow the streamlines when fed into channels. Considering the depth of the microchannels utilized in this study, varying between 50-120  $\mu\text{m}$ , there is almost no cell-surface interactions occurring in flow conditions. This is why cell capture studies were performed with incubation within this study. In fact, the aim of this study is to investigate cell capture behavior of activated surfaces when cell-surface interaction holds. Therefore, “with-incubation” is considered to be sufficient for this study. However, this “with-incubation” configuration is not feasible when working with clinical samples, where larger volumes must be processed to isolate rare cells. Hence there is a need for an “engineered microchannel design” to increase cell-surface collision probability for with-flow capture of rare cells.
- Flow velocity and shear force optimizations should be performed with the “engineered microchannel design” to determine optimum flow rate, which enables high target cell capture with low non-specific binding.

- By changing the immobilized antibody, different cell types can be targeted for a wide range of application such as different types of cancer cell detection or bacteria detection.
- Proposed surface functionalization methods can be implemented on different surfaces such as gold, parylene, glass, COC and PMMA.
- Storage conditions can be optimized to extent the shelf-life of functionalized surfaces.



## REFERENCES

- [1] Møller B, Fekjaer H, Hakulinen T, Sigvaldason H, Storm HH, Talback M, Haldorsen T (2003) Prediction of cancer incidence in the Nordic countries: empirical comparison of different approaches. *Stat Med* 22(17): 2751–2766.
- [2] S.I. Hajdu, M. Vadmal, P. Tang, A note from history: Landmarks in history of cancer, part 7, *Cancer*. 121 (2015) 2480–2513. doi:10.1002/cncr.29365.
- [3] C. Alix-Panabières, K. Pantel, Clinical prospects of liquid biopsies, *Nat. Biomed. Eng.* 1 (2017). doi:10.1038/s41551-017-0065.
- [4] C Ashworth, T.R. (1869) A Case of Cancer in Which Cells Similar to Those in the Tumors Were Seen in the Blood after Death. *Australasian Medical Journal*, 14, 146-149.
- [5] M.C. Miller, G. V. Doyle, L.W.M.M. Terstappen, Significance of Circulating Tumor Cells Detected by the CellSearch System in Patients with Metastatic Breast Colorectal and Prostate Cancer, *J. Oncol.* 2010 (2010) 1–8. doi:10.1155/2010/617421.
- [6] V. Murlidhar, L. Rivera-Báez, S. Nagrath, Affinity Versus Label-Free Isolation of Circulating Tumor Cells: Who Wins?, *Small*. (2016) 4450–4463. doi:10.1002/sml.201601394.
- [7] Y. Dong, A.M. Skelley, K.D. Merdek, K.M. Sprott, C. Jiang, W.E. Pierceall, J. Lin, M. Stocum, W.P. Carney, D.A. Smirnov, Microfluidics and circulating tumor cells, *J. Mol. Diagnostics*. 15 (2013) 149–157. doi:10.1016/j.jmoldx.2012.09.004.
- [8] Tosun, I. (2007). *Modelling in transport phenomena a conceptual approach*.

Oxford: Elsevier (2007).

- [9] J. Yue, G. Chen, Q. Yuan, L. Luo, Y. Gonthier, Hydrodynamics and mass transfer characteristics in gas-liquid flow through a rectangular microchannel, *Chem. Eng. Sci.* 62 (2007) 2096–2108. doi:10.1016/j.ces.2006.12.057.
- [10] W. Qian, Y. Zhang, W. Chen, Capturing Cancer: Emerging Microfluidic Technologies for the Capture and Characterization of Circulating Tumor Cells, *Small*. 11 (2015) 3850–3872. doi:10.1002/sml.201403658.
- [11] N.S. Ferreira, M.G.F. Sales, Biosensors and Bioelectronics Disposable immunosensor using a simple method for oriented antibody immobilization for label-free real-time detection of an oxidative stress biomarker implicated in cancer diseases, *Biosens. Bioelectron.* 53 (2014) 193–199. doi:10.1016/j.bios.2013.09.056.
- [12] K. Pu, C. Li, N. Zhang, H. Wang, W. Shen, Y. Zhu, Epithelial cell adhesion molecule independent capture of non-small lung carcinoma cells with peptide modified microfluidic chip, *Biosens. Bioelectron.* 89 (2016) 927–931. doi:10.1016/j.bios.2016.09.092.
- [13] S. Zheng, H. Lin, J.Q. Liu, M. Balic, R. Datar, R.J. Cote, Y.C. Tai, Membrane microfilter device for selective capture, electrolysis and genomic analysis of human circulating tumor cells, *J. Chromatogr. A.* 1162 (2007) 154–161. doi:10.1016/j.chroma.2007.05.064.
- [14] H.K. Lin, 3D microfilter device for viable circulating tumor cell (CTC) enrichment from blood, *Biomed Microdevices.* 13 (2011) 1–22. doi:10.1007/s10544-010-9485-3.3D.
- [15] X.J. Zheng, L.S.L. Cheung, J.A. Schroeder, L. Jiang, Y. Zohar, A high-performance microsystem for isolating viable circulating tumor cells, 2011 16th Int. Solid-State Sensors, Actuators Microsystems Conf. TRANSDUCERS'11. (2011) 226–229. doi:10.1109/TRANSDUCERS.2011.5969382.
- [16] M.E. Warkiani, B.L. Khoo, L. Wu, A.K.P. Tay, A.A.S. Bhagat, J. Han, C.T. Lim,

- Ultra-fast, label-free isolation of circulating tumor cells from blood using spiral microfluidics., *Nat. Protoc.* 11 (2016). doi:10.1038/nprot.2016.003.
- [17] D. Marrinucci, K. Bethel, R.H. Bruce, D.N. Curry, B. Hsieh, M. Humphrey, R.T. Krivacic, J. Kroener, L. Kroener, A. Ladanyi, N.H. Lazarus, J. Nieva, P. Kuhn, Case study of the morphologic variation of circulating tumor cells, *Hum. Pathol.* 38 (2007) 514–519. doi:10.1016/j.humphath.2006.08.027.
- [18] D.C. Lazar, E.H. Cho, M.S. Luttgen, T.J. Metzner, M.L. Uson, M. Torrey, M.E. Gross, P. Kuhn, Cytometric comparisons between circulating tumor cells from prostate cancer patients and the prostate-tumor-derived LNCaP cell line, *Phys. Biol.* 9 (2012) 1–16. doi:10.1088/1478-3975/9/1/016002.
- [19] F. Guilak, J.R. Tedrow, R. Burgkart, Viscoelastic properties of the cell nucleus, *Biochem. Biophys. Res. Commun.* 269 (2000) 781–786. doi:10.1006/bbrc.2000.2360.
- [20] A.J. Maniotis, C.S. Chen, D.E. Ingber, Demonstration of mechanical connections between integrins, cytoskeletal filaments, and nucleoplasm that stabilize nuclear structure., *Proc. Natl. Acad. Sci. U. S. A.* 94 (1997) 849–54. doi:10.1073/pnas.94.3.849.
- [21] S.M. McFaul, B.K. Lin, H. Ma, Cell separation based on size and deformability using microfluidic funnel ratchets, *Lab Chip.* 12 (2012) 2369. doi:10.1039/c2lc21045b.
- [22] M. Aghaamoo, Z. Zhang, X. Chen, J. Xu, Deformability-based circulating tumor cell separation with conical-shaped microfilters: Concept, optimization, and design criteria, *Biomicrofluidics.* 9 (2015) 1–17. doi:10.1063/1.4922081.
- [23] S.H. Au, B.D. Storey, J.C. Moore, Q. Tang, Y.-L. Chen, S. Javaid, A.F. Sarioglu, R. Sullivan, M.W. Madden, R. O’Keefe, D.A. Haber, S. Maheswaran, D.M. Langenau, S.L. Stott, M. Toner, Clusters of circulating tumor cells traverse capillary-sized vessels, *Proc. Natl. Acad. Sci.* 113 (2016) 4947–4952. doi:10.1073/pnas.1524448113.

- [24] J. Zhou, P.V. Giridhar, S. Kasper, I. Papautsky, Modulation of aspect ratio for complete separation in an inertial microfluidic channel, *Lab Chip*. 13 (2013) 1919. doi:10.1039/c3lc50101a.
- [25] J. Zhou, P.V. Giridhar, S. Kasper, I. Papautsky, Modulation of rotation-induced lift force for cell filtration in a low aspect ratio microchannel, *Biomicrofluidics*. 8 (2014) 44112. doi:10.1063/1.4891599.
- [26] H.W. Hou, M.E. Warkiani, B.L. Khoo, Z.R. Li, R.A. Soo, D.S.W. Tan, W.T. Lim, J. Han, A.A.S. Bhagat, C.T. Lim, Isolation and retrieval of circulating tumor cells using centrifugal forces, *Sci. Rep.* 3 (2013) 1–8. doi:10.1038/srep01259.
- [27] L.R. Huang, E.C. Cox, R.H. Austin, J.C. Sturm, Continuous particle separation through deterministic lateral displacement, *Science* (80-. ). 304 (2004) 987–991.
- [28] K. Louthback, J.D. Silva, L. Liu, A. Wu, R.H. Austin, J.C. Sturm, Deterministic separation of cancer cells from blood at 10 mL / min Deterministic separation of cancer cells from blood at 10 mL / min, *AIP Adv.* 42107 (2012) 1–8. doi:10.1063/1.4758131.
- [29] T.B. Jones, Basic Theory of Dielectrophoresis and Electrorotation, *IEEE Eng. Med. Biol. Mag.* 22 (2003) 33–42. doi:10.1109/MEMB.2003.1304999.
- [30] M. Ignatiadis, M. Lee, S.S. Jeffrey, Circulating tumor cells and circulating tumor DNA: Challenges and opportunities on the path to clinical utility, *Clin. Cancer Res.* 21 (2015) 4786–4800. doi:10.1158/1078-0432.CCR-14-1190.
- [31] Y. Demircan, E. Ozgur, H. Kulah, Dielectrophoresis: Applications and future outlook in point of care, (2013) 1008–1027. doi:10.1002/elps.201200446.
- [32] H.A. Pohl, The motion and precipitation of suspensoids in divergent electric fields, *J. Appl. Phys.* 22 (1951) 869–871. doi:10.1063/1.1700065.
- [33] F.F. Becker, X.B. Wang, Y. Huang, R. Pethig, J. Vykoukal, P.R. Gascoyne, Separation of human breast cancer cells from blood by differential dielectric affinity., *Proc. Natl. Acad. Sci.* 92 (1995) 860–864. doi:10.1073/pnas.92.3.860.

- [34] J. Park, B. Kim, S.K. Choi, S. Hong, S.H. Lee, K.-I. Lee, An efficient cell separation system using 3D-asymmetric microelectrodes, *Lab Chip*. 5 (2005) 1264. doi:10.1039/b506803g.
- [35] A. Alazzam, I. Stiharu, R. Bhat, A.N. Meguerditchian, Interdigitated comb-like electrodes for continuous separation of malignant cells from blood using dielectrophoresis, *Electrophoresis*. 32 (2011) 1327–1336. doi:10.1002/elps.201000625.
- [36] V. Gupta, I. Jafferji, M. Garza, V.O. Melnikova, D.K. Hasegawa, R. Pethig, D.W. Davis, ApoStream???, a new dielectrophoretic device for antibody independent isolation and recovery of viable cancer cells from blood, *Biomicrofluidics*. 6 (2012) 1–14. doi:10.1063/1.4731647.
- [37] J.J. Hawkes, W.T. Coakley, Force @eld particle @lter, combining ultrasound standing waves and laminar ¯ow, *Methods*. 75 (2001) 213–222.
- [38] C. Grenvall, C. Magnusson, H. Lilja, T. Laurell, Concurrent isolation of lymphocytes and granulocytes using prefocused free flow acoustophoresis, *Anal. Chem*. 87 (2015) 5596–5604. doi:10.1021/acs.analchem.5b00370.
- [39] M. Antfolk, S.H. Kim, S. Koizumi, T. Fujii, T. Laurell, Label-free single-cell separation and imaging of cancer cells using an integrated microfluidic system, *Sci. Rep*. 7 (2017) 46507. doi:10.1038/srep46507.
- [40] M. Antfolk, C. Magnusson, P. Augustsson, H. Lilja, T. Laurell, Acoustofluidic, Label-Free Separation and Simultaneous Concentration of Rare Tumor Cells from White Blood Cells, *Anal. Chem*. 87 (2015) 9322–9328. doi:10.1021/acs.analchem.5b02023.
- [41] P. Li, Z. Mao, Z. Peng, L. Zhou, Y. Chen, P.-H. Huang, C.I. Truica, J.J. Drabick, W.S. El-Deiry, M. Dao, S. Suresh, T.J. Huang, Acoustic separation of circulating tumor cells, *Proc. Natl. Acad. Sci*. 112 (2015) 4970–4975. doi:10.1073/pnas.1504484112.
- [42] A.H.J. Yang, H.T. Soh, Acoustophoretic sorting of viable mammalian cells in a

- microfluidic device, *Anal. Chem.* 84 (2012) 10756–10762. doi:10.1021/ac3026674.
- [43] K. Pu, C. Li, N. Zhang, H. Wang, W. Shen, Y. Zhu, Epithelial cell adhesion molecule independent capture of non-small lung carcinoma cells with peptide modified microfluidic chip, *Biosens. Bioelectron.* 89 (2017) 927–931. doi:10.1016/j.bios.2016.09.092.
- [44] H.K. Lin, S. Zheng, A.J. Williams, M. Balic, S. Groshen, H.I. Scher, M. Fleisher, W. Stadler, R.H. Datar, Y.C. Tai, R.J. Cote, Portable filter-based microdevice for detection and characterization of circulating tumor cells, *Clin. Cancer Res.* 16 (2010) 5011–5018. doi:10.1158/1078-0432.CCR-10-1105.
- [45] L.S. Lim, M. Hu, M.C. Huang, W.C. Cheong, A.T.L. Gan, X.L. Looi, S.M. Leong, E.S.-C. Koay, M.-H. Li, Microsieve lab-chip device for rapid enumeration and fluorescence in situ hybridization of circulating tumor cells, *Lab Chip.* 12 (2012) 4388. doi:10.1039/c2lc20750h.
- [46] K.A. Hyun, K. Kwon, H. Han, S. Il Kim, H. Il Jung, Microfluidic flow fractionation device for label-free isolation of circulating tumor cells (CTCs) from breast cancer patients, *Biosens. Bioelectron.* 40 (2013) 206–212. doi:10.1016/j.bios.2012.07.021.
- [47] H.S. Moon, K. Kwon, K.A. Hyun, T. Seok Sim, J. Chan Park, J.G. Lee, H. Il Jung, Continual collection and re-separation of circulating tumor cells from blood using multi-stage multi-orifice flow fractionation, *Biomicrofluidics.* 7 (2013). doi:10.1063/1.4788914.
- [48] and F.F.B. Peter R. C. Gascoyne, Xiao-Bo Wang [Member, IEEE], Ying Huang [Member, IEEE], Dielectrophoretic Separation of Cancer Cells from Blood, *IEEE Trans Ind Appl.* 33 (1997) 670–678. doi:10.1109/28.585856.Dielectrophoretic.
- [49] X.B. Wang, J. Yang, Y. Huang, J. Vykoukal, F.F. Becker, P.R.C. Gascoyne, Cell separation by dielectrophoretic field-flow-fractionation, *Anal. Chem.* 72 (2000) 832–839. doi:10.1021/ac990922o.

- [50] P. Massoner, T. Thomm, B. Mack, G. Untergasser, A. Martowicz, K. Bobowski, H. Klocker, O. Gires, M. Puhr, EpCAM is overexpressed in local and metastatic prostate cancer, suppressed by chemotherapy and modulated by MET-associated miRNA-200c/205, *Br. J. Cancer*. 111 (2014) 955–964. doi:10.1038/bjc.2014.366.
- [51] B.T.F. van der Gun, L.J. Melchers, M.H.J. Ruiters, L.F.M.H. de Leij, P.M.J. McLaughlin, M.G. Rots, EpCAM in carcinogenesis: The good, the bad or the ugly, *Carcinogenesis*. 31 (2010) 1913–1921. doi:10.1093/carcin/bgq187.
- [52] E. Racila, D. Euhus, a J. Weiss, C. Rao, J. McConnell, L.W. Terstappen, J.W. Uhr, Detection and characterization of carcinoma cells in the blood., *Proc. Natl. Acad. Sci. U. S. A.* 95 (1998) 4589–94. doi:10.1073/pnas.95.8.4589.
- [53] S. Negrath, L. V Sequist, S. Maheswaran, D.W. Bell, D. Irimia, L. Ulkus, M.R. Smith, E.L. Kwak, S. Digumarthy, A. Muzikansky, P. Ryan, U.J. Balis, R.G. Tompkins, D. a Haber, M. Toner, Isolation of rare circulating tumour cells in cancer patients by microchip technology., *Nature*. 450 (2007) 1235–9. doi:10.1038/nature06385.
- [54] B.J. Kirby, M. Jodari, M.S. Loftus, G. Gakhar, E.D. Pratt, C. Chanel-Vos, J.P. Gleghorn, S.M. Santana, H. Liu, J.P. Smith, V.N. Navarro, S.T. Tagawa, N.H. Bander, D.M. Nanus, P. Giannakakou, Functional characterization of circulating tumor cells with a prostate-cancer-specific microfluidic device, *PLoS One*. 7 (2012) 1–10. doi:10.1371/journal.pone.0035976.
- [55] S.L. Stott, C.-H.C.-H. Hsu, D.I. Tsukrov, M. Yu, D.T. Miyamoto, B. a. Waltman, S.M. Rothenberg, A.M. Shah, M.E. Smas, G.K. Korir, F.P. Floyd, A.J. Gilman, J.B. Lord, D. Winokur, S. Springer, D. Irimia, S. Negrath, L. V. Sequist, R.J. Lee, K.J. Isselbacher, S. Maheswaran, D. a. Haber, M. Toner, Isolation of circulating tumor cells using a, *October*. 107 (2010) 18392–7. doi:10.1073/pnas.1012539107/-/DCSupplemental.www.pnas.org/cgi/doi/10.1073/pnas.1012539107.
- [56] W. Sheng, O.O. Ogunwobi, T. Chen, J. Zhang, T.J. George, C. Liu, Z.H. Fan, Capture, release and culture of circulating tumor cells from pancreatic cancer patients using an enhanced mixing chip, *Lab Chip*. 14 (2014) 89–98.

doi:10.1039/C3LC51017D.

- [57] Y. Yoon, S. Kim, J. Lee, J. Choi, R.K. Kim, S.J. Lee, O. Sul, S.B. Lee, Clogging-free microfluidics for continuous size-based separation of microparticles, *Sci. Rep.* 6 (2016) 1–8. doi:10.1038/srep26531.
- [58] J.W. Kamande, M.L. Hupert, M.A. Witek, H. Wang, R.J. Torphy, U. Dharmasiri, S.K. Njoroge, J.M. Jackson, R.D. Aufforth, A. Snavelly, J.J. Yeh, S.A. Soper, Modular microsystem for the isolation, enumeration, and phenotyping of circulating tumor cells in patients with pancreatic cancer, *Anal. Chem.* 85 (2013) 9092–9100. doi:10.1021/ac401720k.
- [59] J. Autebert, B. Coudert, J. Champ, L. Saias, E.T. Guneri, R. Lebofsky, F.-C. Bidard, J.-Y. Pierga, F. Farace, S. Descroix, L. Malaquin, J.-L. Viovy, High purity microfluidic sorting and analysis of circulating tumor cells: towards routine mutation detection, *Lab Chip.* 15 (2015) 2090–2101. doi:10.1039/C5LC00104H.
- [60] C.M. Earhart, C.E. Hughes, R.S. Gaster, C.C. Ooi, R.J. Wilson, L.Y. Zhou, E.W. Humke, L. Xu, D.J. Wong, S.B. Willingham, E.J. Schwartz, I.L. Weissman, S.S. Jeffrey, J.W. Neal, R. Rohatgi, H.A. Wakelee, S.X. Wang, Isolation and mutational analysis of circulating tumor cells from lung cancer patients with magnetic sifters and biochips, *Lab Chip.* 14 (2014) 78–88. doi:10.1039/C3LC50580D.
- [61] J.P. Winer-Jones, B. Vahidi, N. Arquilevich, C. Fang, S. Ferguson, D. Harkins, C. Hill, E. Klem, P.C. Pagano, C. Peasley, J. Romero, R. Shartle, R.C. Vasko, W.M. Strauss, P.W. Dempsey, Circulating tumor cells: Clinically relevant molecular access based on a novel CTC flow cell, *PLoS One.* 9 (2014) 1–10. doi:10.1371/journal.pone.0086717.
- [62] E. Ozkumur, A.M. Shah, J.C. Ciciliano, B.L. Emmink, T. David, E. Brachtel, M. Yu, P. Chen, B. Morgan, J. Trautwein, A. Kimura, S. Sengupta, S.L. Stott, N.M. Karabacak, T.A. Barber, J.R. Walsh, K. Smith, P.S. Spuhler, J.P. Sullivan, R.J. Lee, D.T. Ting, X. Luo, A.T. Shaw, A. Bardia, V. Lecia, D.N. Louis, S. Maheswaran, R. Kapur, D.A. Haber, Inertial focusing for tumor antigen-dependent and -independent sorting of rare circulating tumor cells, *Sci Transl Med.*

5 (2013) 1–20. doi:10.1126/scitranslmed.3005616.Inertial.

- [63] N.M. Karabacak, P.S. Spuhler, F. Fachin, E.J. Lim, V. Pai, E. Ozkumur, J.M. Martel, N. Kojic, K. Smith, P. Chen, J. Yang, H. Hwang, B. Morgan, J. Trautwein, T. a Barber, S.L. Stott, S. Maheswaran, R. Kapur, D. a Haber, M. Toner, Microfluidic, marker-free isolation of circulating tumor cells from blood samples., *Nat. Protoc.* 9 (2014). doi:10.1038/nprot.2014.044.
- [64] Z. Liu, A. Fusi, E. Klopocki, A. Schmittl, I. Tinhofer, A. Nonnenmacher, U. Keilholz, Negative enrichment by immunomagnetic nanobeads for unbiased characterization of circulating tumor cells from peripheral blood of cancer patients, *J. Transl. Med.* 9 (2011) 70. doi:10.1186/1479-5876-9-70.
- [65] O. Lara, X. Tong, M. Zborowski, J.J. Chalmers, O. Lara, X. Tong, X. Tong, M. Zborowski, M. Zborowski, J.J. Chalmers, J.J. Chalmers, Enrichment of rare cancer cells through depletion of normal cells using density and flow-through, immunomagnetic cell separation, *Exp. Hematol.* 32 (2004) 891–904. doi:10.1016/j.exphem.2004.07.007.
- [66] Y. Wu, C.J. Deighan, B.L. Miller, P. Balasubramanian, M.B. Lustberg, M. Zborowski, J.J. Chalmers, Isolation and analysis of rare cells in the blood of cancer patients using a negative depletion methodology, *Methods.* 64 (2013) 169–182. doi:10.1016/j.ymeth.2013.09.006.
- [67] A. Giordano, H. Gao, S. Anfossi, E. Cohen, M. Mego, B.-N. Lee, S. Tin, M. De Laurentiis, C.A. Parker, R.H. Alvarez, V. Valero, N.T. Ueno, S. De Placido, S.A. Mani, F.J. Esteva, M. Cristofanilli, J.M. Reuben, Epithelial-Mesenchymal Transition and Stem Cell Markers in Patients with HER2-Positive Metastatic Breast Cancer, *Mol. Cancer Ther.* 11 (2012) 2526–2534. doi:10.1158/1535-7163.MCT-12-0460.
- [68] H.J. Yoon, T.H. Kim, Z. Zhang, E. Azizi, T.M. Pham, C. Paoletti, J. Lin, N. Ramnath, M.S. Wicha, D.F. Hayes, Sensitive capture of circulating tumour cells by functionalised graphene oxide nanosheets, *Nat Nanotechnol.* 8 (2013) 735–741. doi:10.1038/nnano.2013.194.Sensitive.

- [69] A.A. Adams, P.I. Okagbare, J. Feng, M.L. Hupert, D. Patterson, J. Götten, R.L. McCarley, D. Nikitopoulos, M.C. Murphy, S.A. Soper, Highly efficient circulating tumor cell isolation from whole blood and label-free enumeration using polymer-based microfluidics with an integrated conductivity sensor, *J. Am. Chem. Soc.* 130 (2008) 8633–8641. doi:10.1021/ja8015022.
- [70] K. Hoshino, Y.-Y. Huang, N. Lane, M. Huebschman, J.W. Uhr, E.P. Frenkel, X. Zhang, Microchip-based immunomagnetic detection of circulating tumor cells, *Lab Chip*. 11 (2011) 3449. doi:10.1039/c1lc20270g.
- [71] A.-E. Saliba, L. Saias, E. Psychari, N. Minc, D. Simon, F.-C. Bidard, C. Mathiot, J.-Y. Pierga, V. Fraissier, J. Salamero, V. Saada, F. Farace, P. Vielh, L. Malaquin, J.-L. Viovy, Microfluidic sorting and multimodal typing of cancer cells in self-assembled magnetic arrays, *Proc. Natl. Acad. Sci.* 107 (2010) 14524–14529. doi:10.1073/pnas.1001515107.
- [72] X. Yu, R. He, S. Li, B. Cai, L. Zhao, L. Liao, W. Liu, Q. Zeng, H. Wang, S.S. Guo, X.Z. Zhao, Magneto-controllable capture and release of cancer cells by using a micropillar device decorated with graphite oxide-coated magnetic nanoparticles, *Small*. 9 (2013) 3895–3901. doi:10.1002/sml.201300169.
- [73] J.P. Gleghorn, E.D. Pratt, D. Denning, H. Liu, N.H. Bander, S.T. Tagawa, D.M. Nanus, P.A. Giannakakou, B.J. Kirby, Capture of circulating tumor cells from whole blood of prostate cancer patients using geometrically enhanced differential immunocapture (GEDI) and a prostate-specific antibody, *Lab Chip*. 10 (2010) 27–29. doi:10.1039/B917959C.
- [74] J.A. Phillips, Y. Xu, Z. Xia, Z.H. Fan, W. Tan, J.A. Phillips, Y. Xu, Z. Xia, Z.H. Fan, W. Tan, Enrichment of Cancer Cells Using Aptamers Immobilized on a Microfluidic Channel Enrichment of Cancer Cells Using Aptamers Immobilized on a Microfluidic Channel, 81 (2009) 1033–1039. doi:10.1021/ac802092j.
- [75] Q. Shen, L. Xu, L. Zhao, D. Wu, Y. Fan, Y. Zhou, W.H. Ouyang, X. Xu, Z. Zhang, M. Song, T. Lee, M.A. Garcia, B. Xiong, S. Hou, H.R. Tseng, X. Fang, Specific capture and release of circulating tumor cells using aptamer-modified

- nanosubstrates, *Adv. Mater.* 25 (2013) 2368–2373. doi:10.1002/adma.201300082.
- [76] J. Sekine, S.C. Luo, S. Wang, B. Zhu, H.R. Tseng, H.H. Yu, Functionalized conducting polymer nanodots for enhanced cell capturing: The synergistic effect of capture agents and nanostructures, *Adv. Mater.* 23 (2011) 4788–4792. doi:10.1002/adma.201102151.
- [77] D.J. Kim, G. Lee, G.S. Kim, S.K. Lee, Statistical analysis of immuno-functionalized tumor-cell behaviors on nanopatterned substrates, *Nanoscale Res. Lett.* 7 (2012) 1–8. doi:10.1186/1556-276X-7-637.
- [78] L. Yang, J.C. Lang, P. Balasubramanian, K.R. Jatana, D. Schuller, A. Agrawal, M. Zborowski, J.J. Chalmers, Optimization of an enrichment process for circulating tumor cells from the blood of head and neck cancer patients through depletion of normal cells, *Biotechnol. Bioeng.* 102 (2009) 521–534. doi:10.1002/bit.22066.
- [79] A. Makaraviciute, A. Ramanaviciene, Site-directed antibody immobilization techniques for immunosensors, *Biosens. Bioelectron.* 50 (2013) 460–471. doi:10.1016/j.bios.2013.06.060.
- [80] A.K. Trilling, J. Beekwilder, H. Zuilhof, Antibody orientation on biosensor surfaces: a minireview, *Analyst.* 138 (2013) 1619. doi:10.1039/c2an36787d.
- [81] Q. Yu, Q. Wang, B. Li, Q. Lin, Y. Duan, Technological Development of Antibody Immobilization for Optical Immunoassays: Progress and Prospects, *Crit. Rev. Anal. Chem.* 45 (2014) 62–75. doi:10.1080/10408347.2014.881249.
- [82] A. Chiad??, G. Palmara, S. Ricciardi, F. Frascella, M. Castellino, M. Tortello, C. Ricciardi, P. Rivolo, Optimization and characterization of a homogeneous carboxylic surface functionalization for silicon-based biosensing, *Colloids Surfaces B Biointerfaces.* 143 (2016) 252–259. doi:10.1016/j.colsurfb.2016.03.048.
- [83] Y. Liu, J. Yu, Oriented immobilization of proteins on solid supports for use in biosensors and biochips: a review, *Microchim. Acta.* 183 (2016) 1–19. doi:10.1007/s00604-015-1623-4.

- [84] S.K. Vashist, E. Lam, S. Hrapovic, K.B. Male, J.H.T. Luong, Immobilization of antibodies and enzymes on 3-aminopropyltriethoxysilane-functionalized bioanalytical platforms for biosensors and diagnostics, *Chem. Rev.* 114 (2014) 11083–11130. doi:10.1021/cr5000943.
- [85] K.C. Andree, A.M.C. Barradas, A.T. Nguyen, A. Mentink, I. Stojanovic, J. Baggerman, J. Van Dalum, C.J.M. Van Rijn, L.W.M.M. Terstappen, Capture of Tumor Cells on Anti-EpCAM-Functionalized Poly(acrylic acid)-Coated Surfaces, *ACS Appl. Mater. Interfaces.* 8 (2016) 14349–14356. doi:10.1021/acsami.6b01241.
- [86] S.K. Arya, K.C. Lee, D. Bin Dah'alan, Daniel, A.R.A. Rahman, Breast tumor cell detection at single cell resolution using an electrochemical impedance technique, *Lab Chip.* 12 (2012) 2362. doi:10.1039/c2lc21174b.
- [87] F. Breton, B. Bennetau, R. Lidereau, L. Thomas, G. Regnier, J.C. Ehrhart, P. Tauc, P.L. Tran, A mesofluidic multiplex immunosensor for detection of circulating cytokeratin-positive cells in the blood of breast cancer patients, *Biomed. Microdevices.* 13 (2011) 1–9. doi:10.1007/s10544-010-9465-7.
- [88] U. Dharmasiri, S.K. Njoroge, M.A. Witek, M.G. Adebisi, J.W. Kamande, M.L. Hupert, F. Barany, High-Throughput Selection , Enumeration , Electrokinetic Manipulation , and Molecular Profiling of Low-Abundance Circulating Tumor Cells Using a Microfluidic System ( 1 ) Center for Bio-Modular Multi-Scale Systems , Louisiana State University , 8000 G . S, *Anal. Chem.* 83 (2011) 2301–2309. doi:Doi 10.1021/Ac103172y.
- [89] F.G. Ortega, M.A. Fernandez-Baldo, M.J. Serrano, G.A. Messina, J.A. Lorente, J. Raba, Epithelial cancer biomarker EpCAM determination in peripheral blood samples using a microfluidic immunosensor based in silver nanoparticles as platform, *Sensors and Actuators B-Chemical.* 221 (2015) 248–256. doi:10.1016/j.snb.2015.06.066.
- [90] S.B. Nimse, K. Song, M.D. Sonawane, D.R. Sayyed, T. Kim, Immobilization Techniques for Microarray: Challenges and Applications, (2014) 22208–22229.

doi:10.3390/s141222208.

- [91] A. Ansari, F.T. Lee-Montiel, J.R. Amos, P.I. Imoukhuede, Secondary anchor targeted cell release, *Biotechnol. Bioeng.* 112 (2015) 2214–2227. doi:10.1002/bit.25648.
- [92] L.S.L. Cheung, X. Zheng, L. Wang, R. Guzman, J.A. Schroeder, R.L. Heimark, J.C. Baygents, Y. Zohar, Kinematics of specifically captured circulating tumor cells in bio-functionalized microchannels, *J. Microelectromechanical Syst.* 19 (2010) 752–763. doi:10.1109/JMEMS.2010.2052021.
- [93] K.A. Hyun, T.Y. Lee, S.H. Lee, H. Il Jung, Two-stage microfluidic chip for selective isolation of circulating tumor cells (CTCs), *Biosens. Bioelectron.* 67 (2015) 86–92. doi:10.1016/j.bios.2014.07.019.
- [94] S. Jeon, J.M. Moon, E.S. Lee, Y.H. Kim, Y. Cho, An electroactive biotin-doped polypyrrole substrate that immobilizes and releases EpCAM-positive cancer cells, *Angew. Chemie - Int. Ed.* 53 (2014) 4597–4602. doi:10.1002/anie.201309998.
- [95] Z. Liu, W. Zhang, F. Huang, H. Feng, W. Shu, Biosensors and Bioelectronics High throughput capture of circulating tumor cells using an integrated microfluidic system, *Biosens. Bioelectron.* 47 (2013) 113–119. doi:10.1016/j.bios.2013.03.017.
- [96] U. Dharmasiri, S. Balamurugan, A.A. Adams, P.I. Okagbare, A. Obubuafo, S.A. Soper, Highly efficient capture and enumeration of low abundance prostate cancer cells using prostate-specific membrane antigen aptamers immobilized to a polymeric microfluidic device, *Electrophoresis.* 30 (2009) 3289–3300. doi:10.1002/elps.200900141.
- [97] J.M. Jackson, M.A. Witek, J.W. Kamande, S.A. Soper, Materials and microfluidics: enabling the efficient isolation and analysis of circulating tumour cells, *Chem. Soc. Rev.* 46 (2017) 4245–4280. doi:10.1039/C7CS00016B.
- [98] S. V. Nair, M.A. Witek, J.M. Jackson, M.A.M. Lindell, S.A. Hunsucker, T. Sapp, C.E. Perry, M.L. Hupert, V. Bae-Jump, P.A. Gehrig, W.Z. Wysham, P.M. Armistead, P. Voorhees, S.A. Soper, Enzymatic cleavage of uracil-containing

- single-stranded DNA linkers for the efficient release of affinity-selected circulating tumor cells, *Chem. Commun.* 51 (2015) 3266–3269. doi:10.1039/C4CC09765C.
- [99] S. Hou, H. Zhao, L. Zhao, Q. Shen, K.S. Wei, D.Y. Suh, A. Nakao, M.A. Garcia, M. Song, T. Lee, B. Xiong, S.C. Luo, H.R. Tseng, H.H. Yu, Capture and stimulated release of circulating tumor cells on polymer-grafted silicon nanostructures, *Adv. Mater.* 25 (2013) 1547–1551. doi:10.1002/adma.201203185.
- [100] A. Martowicz, G. Spizzo, G. Gastl, G. Untergasser, Phenotype-dependent effects of EpCAM expression on growth and invasion of human breast cancer cell lines, *BMC Cancer.* 12 (2012) 501. doi:10.1186/1471-2407-12-501.
- [101] J. Zhang, Z.H. Fan, A universal tumor cell isolation method enabled by fibrin-coated microchannels, *Analyst.* 141 (2016) 563–566. doi:10.1039/C5AN01783A.
- [102] N.S.K. Gunda, M. Singh, L. Norman, K. Kaur, S.K. Mitra, Optimization and characterization of biomolecule immobilization on silicon substrates using (3-aminopropyl)triethoxysilane (APTES) and glutaraldehyde linker, *Appl. Surf. Sci.* 305 (2014) 522–530. doi:10.1016/j.apsusc.2014.03.130.
- [103] S. Libertino, F. Giannazzo, V. Aiello, A. Scandurra, F. Sinatra, M. Renis, M. Fichera, XPS and AFM characterization of the enzyme glucose oxidase immobilized on SiO<sub>2</sub> surfaces, *Langmuir.* 24 (2008) 1965–1972. doi:10.1021/la7029664.
- [104] J. Diao, D. Ren, J.R. Engstrom, K.H. Lee, A surface modification strategy on silicon nitride for developing biosensors, *Anal. Biochem.* 343 (2005) 322–328. doi:10.1016/j.ab.2005.05.010.
- [105] E.H. Williams, A. V. Davydov, A. Motayed, S.G. Sundaresan, P. Bocchini, L.J. Richter, G. Stan, K. Steffens, R. Zangmeister, J.A. Schreifels, M. V. Rao, Immobilization of streptavidin on 4H-SiC for biosensor development, *Appl. Surf. Sci.* 258 (2012) 6056–6063. doi:10.1016/j.apsusc.2012.02.137.
- [106] B.J. Nehilla, K.C. Papat, T.Q. Vu, S. Chowdhury, R.F. Standaert, D.R. Pepperberg, T.A. Desai, Neurotransmitter analog tethered to a silicon platform for neuro-

- BioMEMS applications, *Biotechnol. Bioeng.* 87 (2004) 669–674. doi:10.1002/bit.20171.
- [107] J. Spinke, M. Liley, F. -J. Schmitt, H. -J. Guder, L. Angermaier, W. Knoll, Molecular recognition at self-assembled monolayers: Optimization of surface functionalization, *J. Chem. Phys.* 99 (1993) 7012–7019. doi:10.1063/1.465447.
- [108] S.K. Vashist, Comparison of 1-Ethyl-3-(3-Dimethylaminopropyl) Carbodiimide Based Strategies to Crosslink Antibodies on Amine-Functionalized Platforms for Immunodiagnostic Applications, *Diagnostics.* 2 (2012) 23–33. doi:10.3390/diagnostics2030023.
- [109] P. Batalla, M. Fuentes, C. Mateo, V. Grazu, R. Fernandez-lafuente, J.M. Guisan, Covalent Immobilization of Antibodies on Finally Inert Support Surfaces through their Surface Regions Having the Highest Densities in Carboxyl Groups, (2008) 2230–2236.
- [110] O. Barbosa, C. Ortiz, Á. Berenguer-Murcia, R. Torres, R.C. Rodrigues, R. Fernandez-Lafuente, Glutaraldehyde in bio-catalysts design: a useful crosslinker and a versatile tool in enzyme immobilization, *RSC Adv.* 4 (2014) 1583–1600. doi:10.1039/C3RA45991H.
- [111] N.G. Welch, J.A. Scoble, B.W. Muir, P.J. Pigram, Orientation and characterization of immobilized antibodies for improved immunoassays (Review), *Biointerphases.* 12 (2017) 02D301. doi:10.1116/1.4978435.
- [112] C.S. Neish, I.L. Martin, R.M. Henderson, J.M. Edwardson, Direct visualization of ligand-protein interactions using atomic force microscopy, *Br. J. Pharmacol.* 135 (2002) 1943–1950. doi:10.1038/sj.bjp.0704660.
- [113] C.E. Chivers, A.L. Koner, E.D. Lowe, M. Howarth, How the biotin–streptavidin interaction was made even stronger: investigation via crystallography and a chimaeric tetramer, *Biochem. J.* 435 (2011) 55–63. doi:10.1042/BJ20101593.
- [114] Y.J. Yuan, R. Jia, Study on pivot-point vibration of molecular bond-rupture events by quartz crystal microbalance for biomedical diagnostics, *Int. J. Nanomedicine.* 7

(2012) 381–391. doi:10.2147/IJN.S26808.

- [115] K. Bravo, F.G. Ortega, G.A. Messina, M.I. Sanz, M.A. Fernández-Baldo, J. Raba, Integrated bio-affinity nano-platform into a microfluidic immunosensor based on monoclonal bispecific trifunctional antibodies for the electrochemical determination of epithelial cancer biomarker, *Clin. Chim. Acta.* 464 (2017) 64–71. doi:10.1016/j.cca.2016.11.012.
- [116] T. Lin, M. Chung, Using Monoclonal Antibody to Determine Lead Ions with a Localized Surface Plasmon Resonance Fiber-optic Biosensor, *Sensors.* 8 (2008) 582–593. doi:10.3390/s8010582.

## APPENDIX A

Change in the atomic composition of surfaces after each successive functionalization step was determined by XPS analysis. Full XPS spectra with Si2p, C1s, N1s and O1s atomic orbital peaks for the silane, glutaraldehyde, NHS-Biotin, streptavidin and antibody layers are given in the Figure S1-S9.

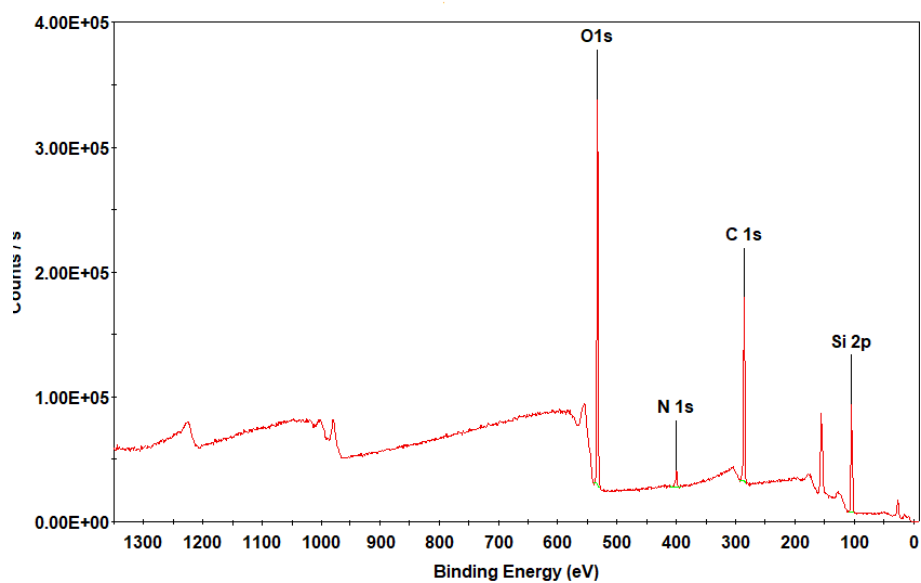


Figure S1: XPS survey scan of APTES layer

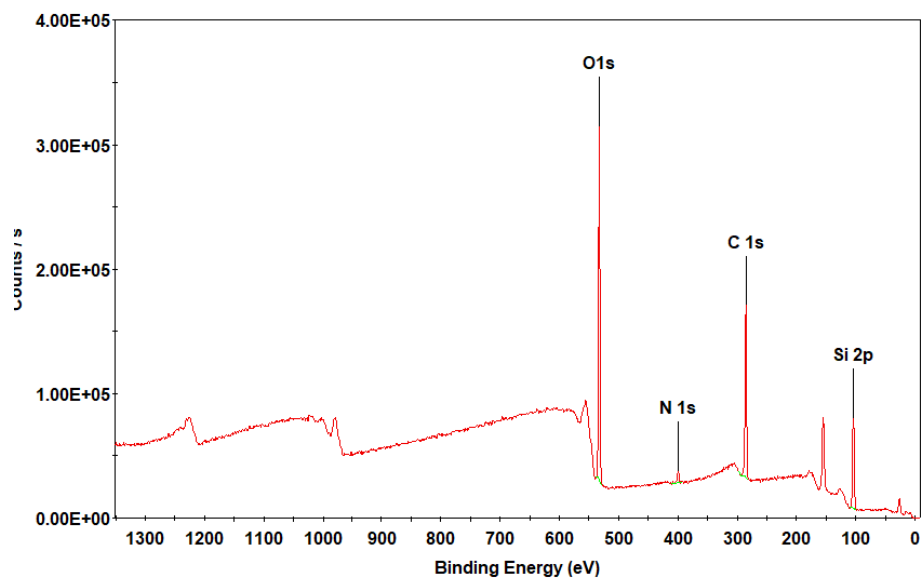


Figure S2: XPS survey scan of Glutaraldehyde layer on APTES

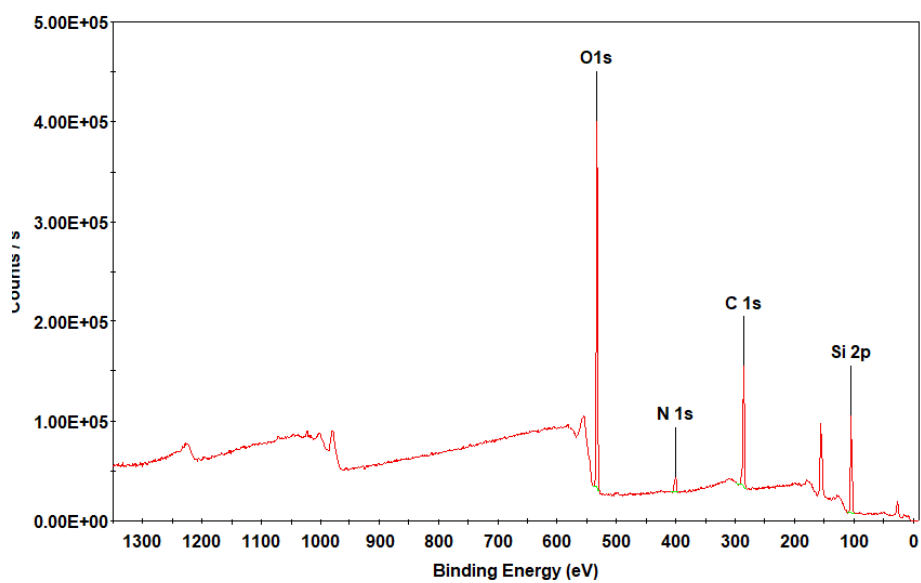


Figure S3: XPS survey scan of NHS-Biotin layer on APTES

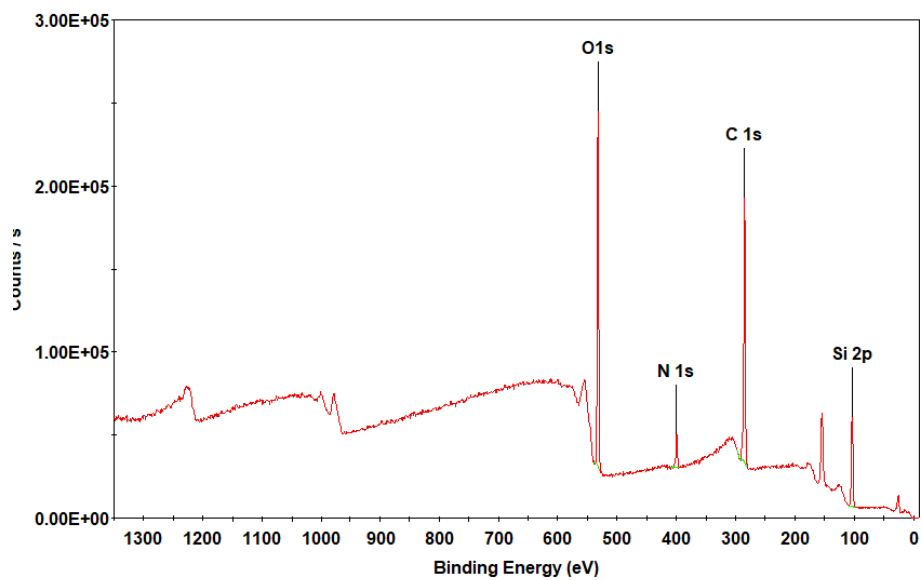


Figure S4: XPS survey scan of Streptavidin layer on Glutaraldehyde

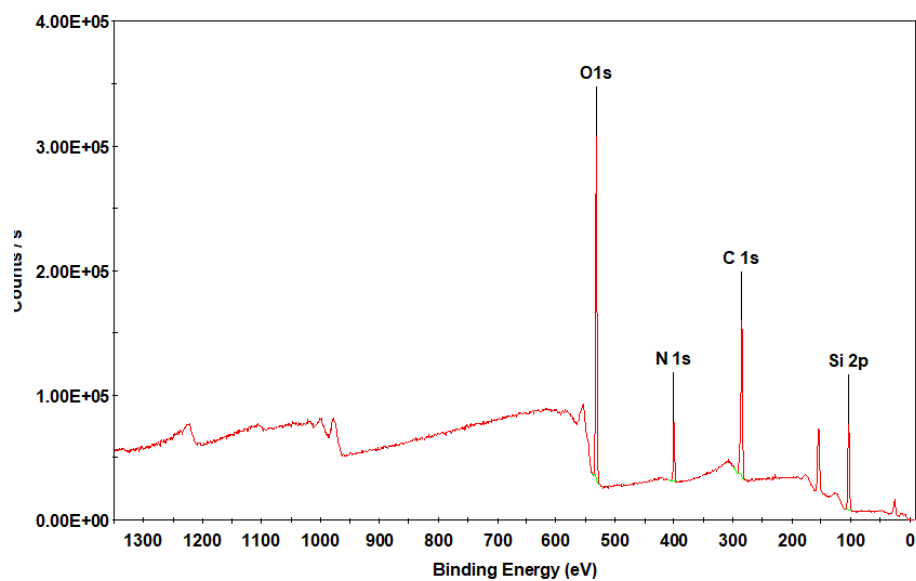


Figure S5: XPS survey scan of Streptavidin layer on NHS-Biotin

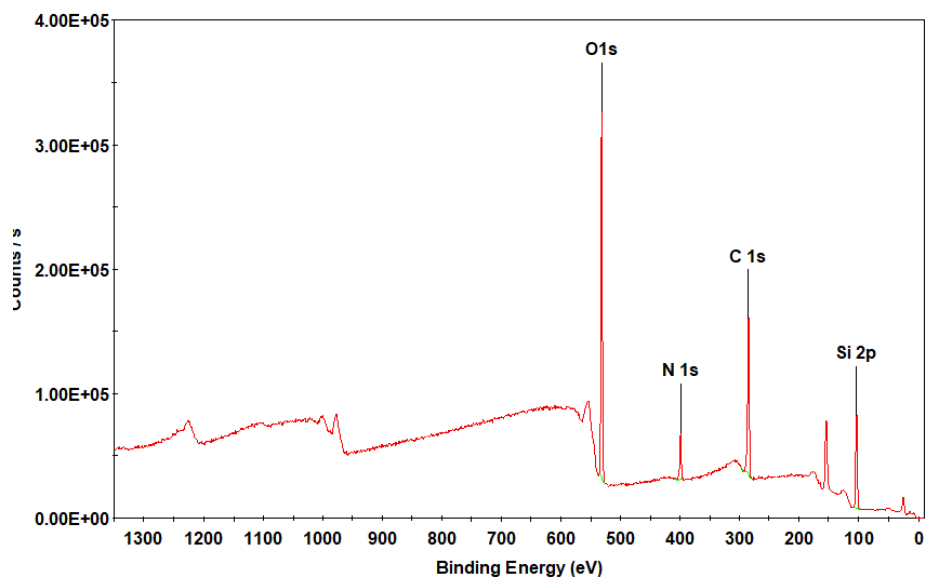


Figure S6: XPS survey scan of Antibody layer on Glutaraldehyde (P1)

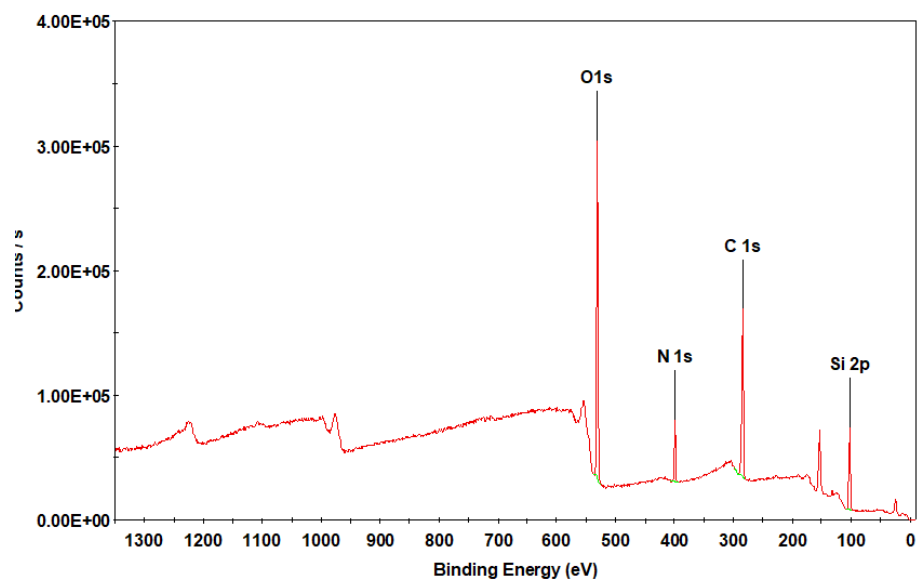


Figure S7: XPS survey scan of EDC/NHS activated Antibody layer on APTES (P2)

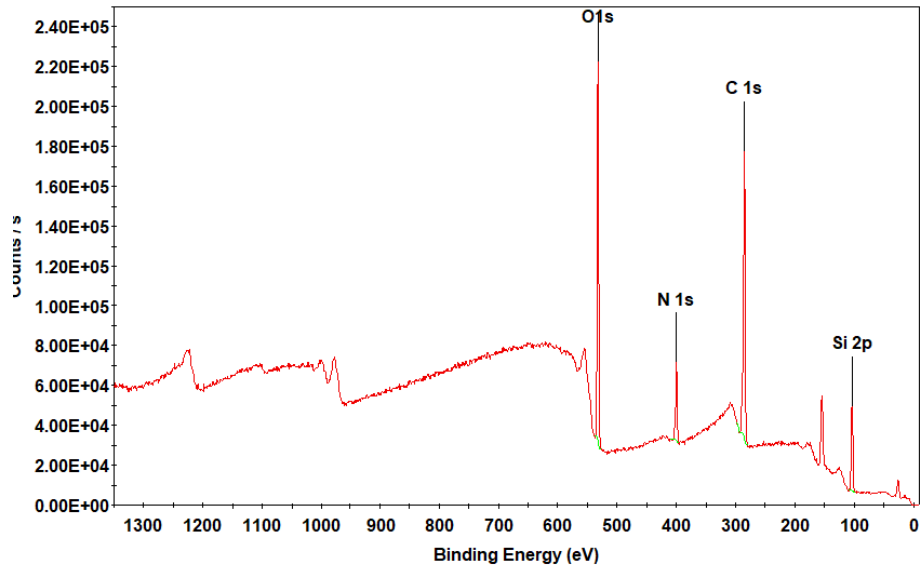


Figure S8: XPS survey scan of Antibody layer on Streptavidin (P3)

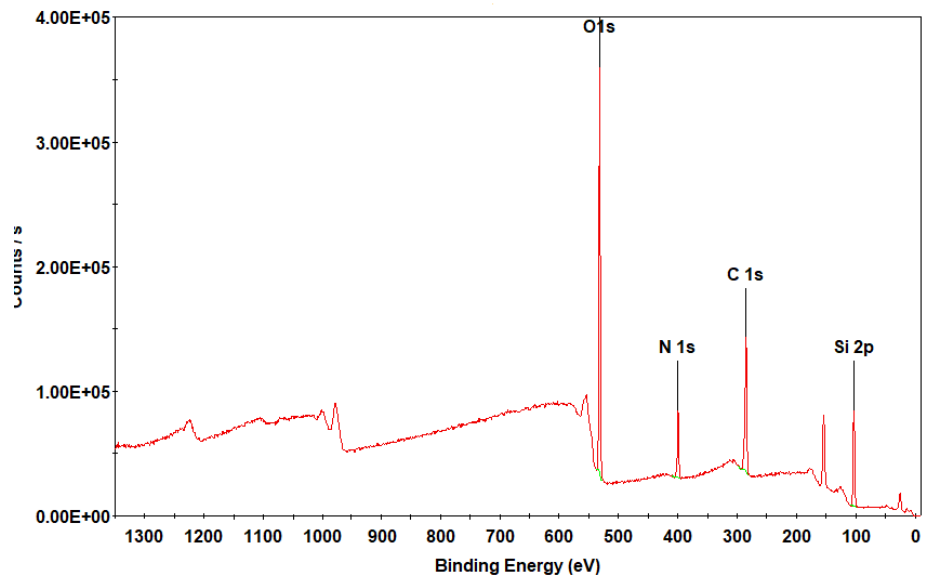


Figure S9: XPS Survey Scan Antibody layer on Streptavidin (P4)